pennsylvania
DEPARTMENT OF TRANSPORTATION

Superpave In-Situ Stress/Strain Investigation – Phase II

FINAL REPORT
Vol. I: Summary Report

May 2009

By Mansour Solaimanian, Shelley M. Stoffels, Hao Yin, and Laxmikanth Premkumar

The Thomas D. Larson
Pennsylvania Transportation Institute

PENNSTATE
1855

COMMONWEALTH OF PENNSYLVANIA
DEPARTMENT OF TRANSPORTATION

CONTRACT No. 999012
PROJECT No. HA2006-02

Technical Report Documentation Page

1. Report No. FHWA-PA-2009-009-999012 HA 2006-02	**2. Government Accession No.**	**3. Recipient's Catalog No.**
4. Title and Subtitle SuperPave In-Situ Stress/Strain Investigation, Phase II Volume II: Characterization of Materials		**5. Report Date** May 2009 **6. Performing Organization Code**
7. Author(s) Mansour Solaimanian, Laxmikanth Premkumar, Hao Yin, Ghassan Chehab, and Shelley M. Stoffels		**8. Performing Organization Report No.** PTI 2009-17
9. Performing Organization Name and Address The Thomas D. Larson Pennsylvania Transportation Institute Transportation Research Building The Pennsylvania State University University Park, PA 16802-4710		**10. Work Unit No. (TRAIS)** **11. Contract or Grant No. 999012** Project HA2006-02
12. Sponsoring Agency Name and Address The Pennsylvania Department of Transportation Bureau of Planning and Research Commonwealth Keystone Building 400 North Street, 6th Floor Harrisburg, PA 17120-0064		**13. Type of Report and Period Covered** Final Report 6/23/2006 – 11/30/2008 **14. Sponsoring Agency Code**
15. Supplementary Notes COTR: Mr. Michael Long, johlong@state.pa.us		

16. Abstract

The characterization of materials is an integral part of the overall effort to validate the Superpave system and to calibrate the performance prediction models for the environmental conditions observed in the Commonwealth of Pennsylvania. Material properties are among the most important input parameters to the models of the *Mechanistic Empirical Pavement Design Guide* for flexible pavements. An extensive laboratory testing program was followed during Phases I and II of the Superpave In-situ Stress Strain Investigation (SISSI) project to determine binder properties, mix volumetric properties, and mix engineering properties. Testing of SISSI binders during Phase II with the bending beam rheometer at various temperatures and loading times showed that the equivalence principle of testing at low temperature is not satisfied. The indirect tensile creep and strength tests on wearing layers of SISSI provided a ranking of these mixtures based on their low-temperature material properties. Fracture analysis of SISSI mixtures indicated that the maximum tensile stress is independent of the type of asphalt concrete mixtures. Considerable deviations were observed between the calculated fracture energy from linear elastic and linear viscoelastic solutions. Results of repeated shear testing at maximum pavement temperature indicate performance of SISSI mixtures to be in the range of good to excellent since no excessive permanent deformation was observed from these laboratory tests. The present report is one of four volumes, Volume I: Summary Report; Volume II, Materials Characterization; Volume III: Field Data Collection and Summary; Volume IV: Mechanistic Analysis and Implementation.

17. Key Words Pavement materials, characterization, asphalt concrete, binder, modulus, creep compliance, shear deformation, mechanistic empirical pavement design guide models	**18. Distribution Statement** No restrictions. This document is available from the National Technical Information Service, Springfield, VA 22161

19. Security Classif. (of this report)	**20. Security Classif. (of this page)**	**21. No. of Pages**	**22. Price**
Unclassified	Unclassified	149	

Form DOT F 1700.7 (8-72) **Reproduction of completed page authorized**

This work was sponsored by the Pennsylvania Department of Transportation and the U.S. Department of Transportation, Federal Highway Administration. The contents of this report reflect the views of the authors, who are responsible for the facts and the accuracy of the data presented herein. The contents do not necessarily reflect the official views or policies of either the Federal Highway Administration, the U.S. Department of Transportation, or the Commonwealth of Pennsylvania at the time of publication. This report does not constitute a standard, specification, or regulation.

ACKNOWLEDGEMENTS

The work described in this report was the result of the foresight of the original Superpave In-Situ Stress-Strain Instrumentation (SISSI) Task Force, led by Mr. James Moretz and later by Mr. Dan Dawood and Mr. Mike Long. The other members of the task force are duly recognized, especially Ronald Cominsky, Carlos Rosenberger, and Zahur Siddiqui for their invaluable guidance. Our most sincere thanks goes to Dr. David Anderson for his vision in formulating the plan for the original SISSI contract and moving the project forward with his leadership during the first two years of the project. We are also thankful to Dr. Ghassan Chehab, who oversaw the low temperature testing during Phase II. The kind counsel and perseverance of Mr. Michael Bonini and Ms. Michelle Tarquino, project contract managers, are greatly appreciated.

Preparation of this final summary report for Phase II of the Superpave In-Situ Stress/Strain Investigation was possible because of the financial support of the Pennsylvania Department of Transportation (PennDOT). This financial support is greatly appreciated.

Thanks are also extended to Scott Milander of LTI for his assistance with laboratory testing.

TABLE OF CONTENTS

LIST OF FIGURES

LIST OF TABLES

EXECUTIVE SUMMARY

The Superpave mix design system was one of the major products of the Strategic Highway Research Program (SHRP). Implementation of this new technology began in the mid-1990s, soon after introduction to state highway agencies and industry. After several years of using this new system, a major question that remained to be addressed in regard to the Superpave system was whether constructed Superpave pavements would meet design expectations. Furthermore, with the emergence of improved mechanistic-empirical performance prediction models, actual pavement response and performance data were needed to calibrate and validate such models.

To address these concerns, the Pennsylvania Department of Transportation (PennDOT) initiated a major 5-year research program with Penn State titled "Superpave In-Situ Stress/Strain Investigation" (SISSI). The project began in May 2001 and was completed in May 2006. The project was then extended, under Phase II, for an additional two and a half years and ended in November 2008. The main objectives achieved under the SISSI project included instrumentation of pavement sections, direct measurement of the response of Superpave asphalt pavement sections to vehicle loading and environment, direct evaluation of distresses developed in pavements using Superpave mixes, and collection of the data for validation of mechanistic-empirical pavement design guide (MEPDG) and validation of the integrated climatic models for pavement design. The major objective achieved during Phase II of the program was utilization of SISSI data with the MEPDG and comparison of predicted performance to observed field measurements.

Considering the project objectives, Phase I included an extensive effort to complete instrumentation of eight pavement sites throughout the Commonwealth of Pennsylvania. Instrumentation took place during pavement construction with care taken to minimize interference to common and normal paving operations. Four of the selected sites were full-depth new construction or reconstruction. These included sites in Tioga, Mercer (East), Somerset, and Blair counties. The remaining sites, in Mercer (West), Warren, Perry, and Delaware counties, were included as overlay structures. Instrumentation included dynamic (load-associated) sensors and environmental (non-load) sensors. Upon completion of the instrumentation, a great deal of effort was made in testing, measurements, and data collection. In general, these efforts fell into two major categories: field activities and laboratory activities.

The field activities during Phase I included measurement of traffic, pavement performance, and pavement responses to both load and environmental factors. Dynamic data were collected during several visits to the sites at different times to capture seasonal effects on pavement response. Environmental data were collected remotely every half an hour for temperature and moisture content and every hour for frost.

Laboratory activities during Phase I were conducted with the goal of characterizing all asphalt binders and mixtures used in the pavements of the SISSI project and determining the required engineering properties for use with performance prediction models. Characterization of materials is an integral part of the overall effort to validate the Superpave system and to calibrate the performance prediction models for the environmental conditions observed in the

Commonwealth of Pennsylvania. The major laboratory tests conducted on the procured binders during Phase I included the Superpave grading tests: short- and long-term aging, rotational viscometer, dynamic shear rheometer (DSR), and bending beam rheometer (BBR). The mixture testing included the tests required for verification of mix design, as well as dynamic modulus testing at a range of temperatures and frequencies to capture properties required for input to performance prediction models. The results of Phase I laboratory testing and the significance of those results were provided in a SISSI Phase I Materials Characterization report (Solaimanian et al. 2006).

Part of the Phase II work included all field data collection activities as was conducted during Phase I, with the exceptions that pavement condition surveys and dynamic data collection were conducted at a significantly lower frequency. A major challenge during Phase II was the need for an extensive level of effort to maintain sensors and data acquisition systems in functional condition. We were not able to maintain continuity of environmental data collection at all times, which resulted in gaps and discontinuity in the collected data. Some of the sensors did not provide reasonable responses because of malfunction or damage, specifically multi-depth deflectometers, frost gages, and moisture content gages. In spite of all data collection problems, we believe the data collected at SISSI sites are extremely valuable, considering that multiple sites were available and collection of data was continued for such an extended time period.

One major attempt during Phase II of the SISSI project was to utilize data with the highest analysis level in MEPDG, i.e., Level 1. One general conclusion from Level 1 analysis was that no significant amount of fatigue or thermal cracking was predicted by the MEPDG models; this is consistent with field observations for most of the sites, except the sites at Delaware and Warren counties, where transverse cracking was dominant. At the Warren site, the pavement is built on a cracked and seated old rigid pavement. It cannot be determined with any certainty whether the observed cracks were caused by underlying concrete, fatigue behavior, thermally induced, or some combination of causes. For the Delaware site, the pavement is built over old concrete in some sections and on old flexible pavements in others. As for the Warren site, it cannot be determined with certainty that the observed transverse cracking at this site was thermally induced. In regard to pavement permanent deformation, overall MEPDG under-predicted rutting compared to field measurements. The magnitude of this under-prediction varied significantly in the range of 5 to 90 percent depending on the site. Average under-prediction was approximately 40 percent. The discrepancy observed between the predictions and field conditions was perhaps due to the national calibration coefficients in the empirical performance models. It is believed that with the availability of large amounts of field condition data, the MEPDG models could be more accurately calibrated locally.

Laboratory testing during Phase II included indirect tensile creep and strength tests at three temperatures to capture low temperature properties of SISSI mixtures, constant height repeated test at maximum pavement temperature to capture rutting resistance properties, and constant height strain-controlled frequency sweep tests to characterize the variation of shear modulus of SISSI mixtures with temperature and loading time. The testing also included characterizing the behavior of SISSI binders at low temperatures under extended loading times to validate the Superpave low temperature binder specification. Detailed results of the Phase II

laboratory study are documented in a separate report titled "Material Characterization, SISSI-Phase II" (Solaimanian et al. 2008).

The validity of the Superpave binder specification in regard to the equivalence principle for the binder flexural creep stiffness was evaluated during Phase II. Based on this principle, the binder creep stiffness at a specified temperature under two hours of loading [S(7200)] is approximately equal to its creep stiffness at a temperature 10ºC warmer under 60 seconds of loading [S(60)]. This principle also assumes that all asphalt binders can be characterized by similar shift factors. Our testing and analysis indicated that the S(60) at T_1+10 is significantly different from S(7200) at T_1. The S(60) values are significantly higher than the S(7200) values, and the differences range between 40 and 52 percent. Alternate testing times and temperatures to satisfy the equivalence principle for the SISSI binders were developed and introduced as part of this work.

The SISSI sites were ranked based on their low temperature material properties obtained from indirect tensile creep and strength tests. Based on measured properties, it seems that the SISSI mixture used at the wearing course of the Delaware site is probably the most susceptible to thermal cracking. This is consistent with field observations; the wearing course used at this site was the most cracked among all SISSI sites even though it cannot be concluded with certainty that observed cracking is thermally induced.

Results of repeated shear testing at maximum pavement temperature indicates performance of SISSI mixtures in the range of good to excellent, with no excessive permanent deformation observed from these laboratory tests. For the wearing layer, the permanent shear strain ranged between 0.3 and 1.7 percent, indicating excellent to good rutting resistance. For the binder layer, the range was between 0.4 to 1.7 percent, indicating good rutting resistance. The exception was the binder layer of the Perry site, for which a permanent strain of 2.4 percent was obtained, indicating fair rutting resistance; no excessive rutting was observed in the field for this site. Overall, the field measured rutting, after 5 to 8 years of service, ranged between 2.5 and 8.5 millimeters, indicating excellent rut resistance of SISSI mixtures at all sites. This is, in general, consistent with laboratory measured shear strains as discussed above.

An additional field activity during Phase II included determination of in-situ modulus using Portable Seismic Pavement Analyzer (PSPA). In summary, field-focused efforts during Phase II consisted of collection of pavement condition data, dynamic data, falling weight deflectometer (FWD) data, traffic data, in-situ modulus data, and environmental data.

All SISSI sites appeared to be in good shape except for the two overlaid pavement sections, which were at the Warren and Delaware sites. At these two sites, a significant amount of the longitudinal cracking at the lane-lane and lane-shoulder joints are probably due to poor construction. Transverse cracks on the pavement surface may be induced by underlying concrete slabs or may be thermally induced. Durability of Superpave mixes was of concern at two of these sites, Warren and Mercer, based on field observations. The Warren site was finally milled and overlaid during the spring of 2007. For the Mercer site, only a small section of the road prior to the SISSI site was milled and overlaid. Our last pavement condition survey at this site, during November 2007, indicated no cracking of the pavement mat at the site even though minor to

moderate raveling and loss of fines was evident at the vicinity of the longitudinal joint. The pavement had also experienced longitudinal cracking both at the joint between two lanes and the joint between the travel lane and the shoulder. These cracks appear to be construction related rather than mix related. However, the minor to moderate raveling observed at the Mercer site is probably an indication of insufficient binder content at this site. In general, some Superpave mixes have demonstrated that they are highly resistant to rutting, and this excellent rut resistance has come at the cost of lower durability in some cases. In general, the field-measured rutting, after 5 to 8 years of service, ranged between 2.5 and 8.5 millimeters, indicating excellent rut resistance of SISSI mixtures at all sites.

Collection of dynamic data during Phase II was conducted at a significantly lower frequency than during Phase I. During Phase II, dynamic data collection was conducted at specific sites to complement data collected during Phase I. More repeated measurements were conducted at the same speed, and lower speeds were included in Phase II. At a few sites, collection of such data did not become possible because of loss or corrosion of gages. Dynamic data collected during Phase II indicated significantly larger strain levels induced in the pavement during warmer times and lower speeds as compared to those during colder seasons and higher speeds. Backcalculated moduli of asphalt concrete from FWD measurements were compared to the laboratory-obtained elastic moduli. The comparisons indicated that the backcalculated moduli were always higher than the laboratory-determined values. This observation is in general agreement with the suggestion by the 1993 AASHTO design guide that the FWD backcalculated moduli are typically higher than the laboratory-determined moduli.

The moduli of asphalt concrete determined from laboratory complex modulus tests were also compared with the moduli from in-situ nondestructive tests using PSPA. Statistical analysis indicated an excellent PSPA measurement repeatability. Comparison between seismic and dynamic moduli indicated about 30 percent difference in these two moduli. When making such comparisons, it is important to consider the impact of air void content because the in-situ seismic modulus is very sensitive to the air void of the asphalt concrete. For the SISSI project, pavement cores obtained one to two years after construction revealed air voids very similar to those of the laboratory specimens tested for dynamic modulus. The second important point in making such comparison is in regard to the aging of the asphalt binders. Aging increases binder stiffness and therefore results in a higher mixture modulus. In this study, no attempts were made to determine the aging level of binder and base layers. However, it is expected that since these layers are not exposed to solar radiation and experience moderate temperatures, considering the Pennsylvania climate, there is not a significant aging level for the binder and base layers. Significant aging is expected for the wearing course binder, but modulus of this layer is not measured by PSPA.

Most of the successful environmental data during Phase II consist of pavement temperature and solar radiation. Frost and moisture content data were limited because of gage malfunction. Environmental data from Phase I and the first year of Phase II were analyzed in regard to frost depth and freezing index. Different approaches were used in determination of the freezing index, and the effects of the freezing index on the computed frost depth were evaluated as part of the Phase-II SISSI research. Freezing index was calculated based on a major freeze cycle, as well as based upon multiple freeze-thaw cycles. It was observed that there is rarely a freeze-thaw cycle that is over 40 days in Pennsylvania. Most freeze-thaw cycles have periods

less than 10 days. For freezing index differences less than 150 °C-days, variation of computed frost depth, in most cases, does not exceed 0.20 meters. However, for freezing index differences of approximately 200 °C-days, computed values vary from 0.15 to 0.25 meters. Frost data from the Blair site was analyzed to determine the depth and rate of frost penetration. Data indicate that as freezing period lasts longer, frost severity increases at various depths. Overall, at deeper pavement layers, more time is required to reach a specific freezing condition.

In summary, a considerable amount of valuable data was collected from SISSI sites during Phases I and II of this project. The data were extensively used with the AASHTO mechanistic empirical pavement design guide (MEPDG) to predict pavement performance. The collected SISSI data was also very valuable when used in conjunction with an independent mechanistic analysis of pavement response under load. The results of such analyses are documented in a separate report. The data were also analyzed to provide overall assessment of the condition of SISSI pavements and Superpave mixtures and to provide freezing condition of Pennsylvania pavements. These data provide a very useful source for local calibration of the MEPDG and of the Enhanced Integrated Climatic Models (EICM) used in the MEPDG.

There are three other volumes in the series of SISSI-II reports. Volume 2 deals with material characterization and covers laboratory testing of SISSI mixtures and binders. Field data collection efforts and corresponding data are covered in Volume 3. Implementation of SISSI data with the mechanistic empirical pavement design guide is discussed in Volume 4.

CHAPTER 1
INTRODUCTION

An outcome of the Strategic Highway Research Program (SHRP), conducted from 1987 through 1993, was the introduction of a new volumetric design procedure for asphalt concrete, known as Superpave. This new design methodology brought the promise of providing superior performing hot-mix asphalt (HMA) pavements to the motoring public. Immediately after introduction of this new system, various technology-transfer means were used to implement the new mix design procedure. The Pennsylvania Department of Transportation (PennDOT) began using the new design system in the mid-1990's, and after several years of using this new system, a major question that remained was whether constructed Superpave pavements would meet design expectations. Furthermore, with the emergence of improved mechanistic-empirical performance prediction models, actual pavement response and performance data were needed to calibrate and validate such models.

There have been numerous studies on the properties of Superpave design from the perspectives of how the component materials perform in the laboratory and how various construction methods yield different in-place results. However, the question "How does Superpave perform when compared to design expectations?" had not been adequately answered. It was in the year 2000 that PennDOT decided to invest in a research study to answer this important question.

To address these concerns, PennDOT sponsored a comprehensive 5-year project called Superpave In-Situ Stress/Strain Investigation (SISSI). At the time this project was initiated, PennDOT had been piloting Superpave construction for 3 years and had future plans to implement a policy of 100 percent Superpave design for all of its structurally designed HMA work within a few years. The first phase of the SISSI project began in May 2001 and was completed in May 2006. The project was extended through a second phase, which was completed on November 30, 2008. This project was a unique, state-of-the-art instrumentation, validation, and analysis project that encompassed eight different pavement sections in the northern and southern parts of the Commonwealth. The pavement sections were instrumented as designed and as constructed, with no special modifications for this research and with minimal interruption to the construction process.

Phase I of this project focused on completion of instrumentation and collection of various types of data required for validation of the Superpave mix design system, as well as pavement performance prediction models. In general, SISSI testing, measurements, and data collection efforts fell into two major categories: 1) field activities and 2) laboratory activities. The field activities during Phase I included measurement of traffic, pavement performance, and pavement response to both load and environmental factors (Figure 1). Laboratory activities were conducted with the goal of characterizing all asphalt binders and mixtures used in the SISSI project and determining the required engineering properties for performance prediction models (Figure 2).

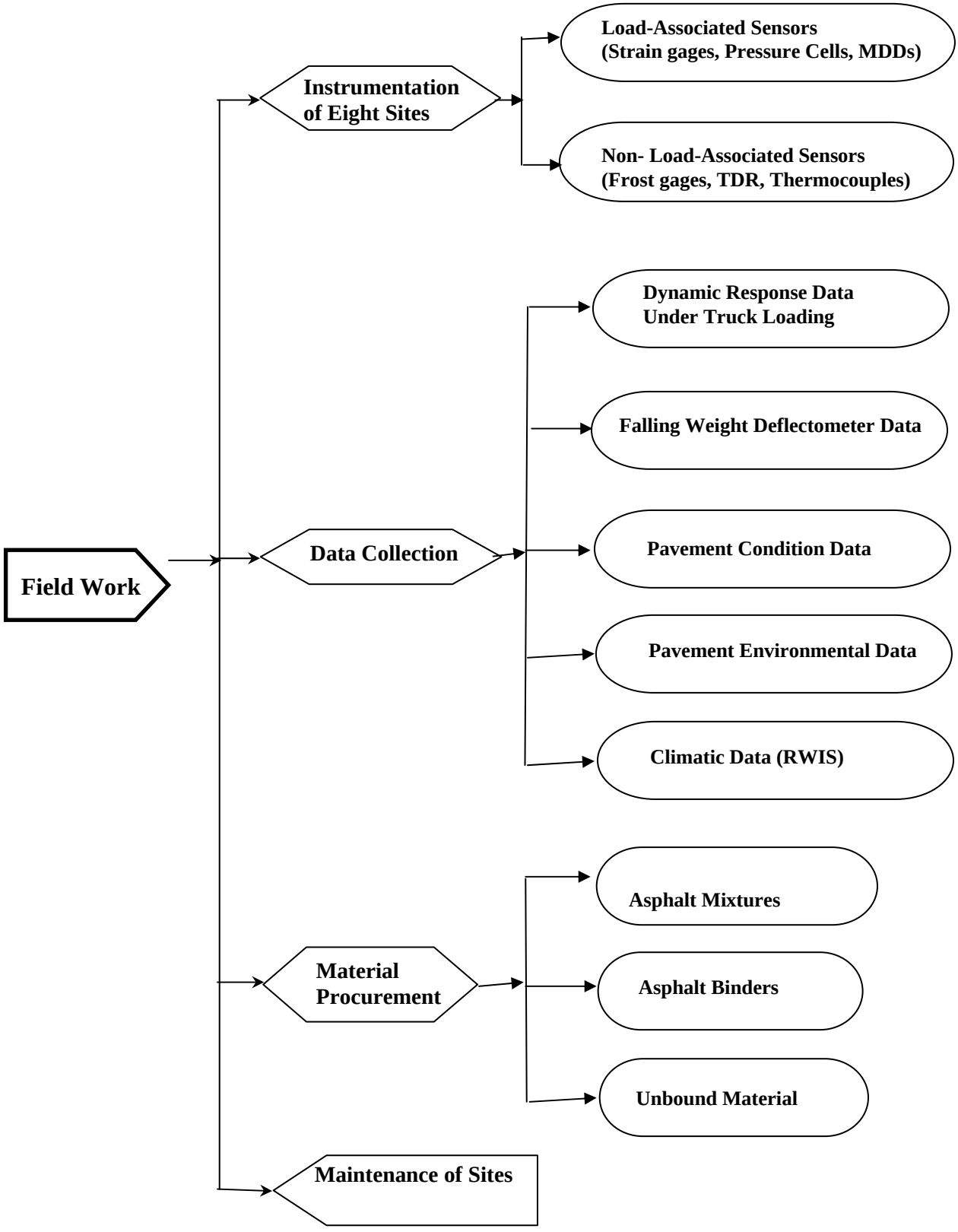

Figure 1. Field activities during Phase I of the SISSI project.

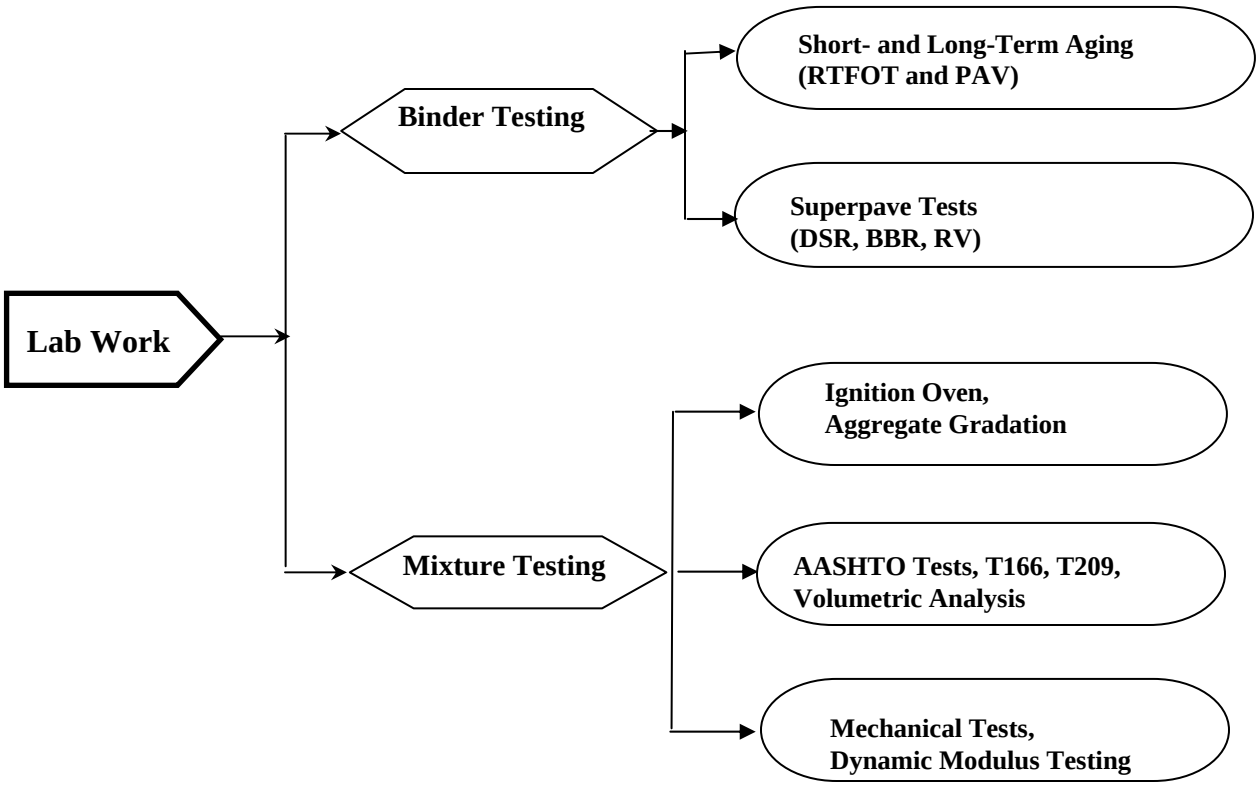

Figure 2. Lab activities during Phase I of the SISSI project.

OBJECTIVES OF SISSI PHASE II PROJECT

With the very extensive amount of data collected during Phase I of this project, it was decided that Phase II would focus on extensive analysis of the collected data and implementation of results from Phase I. One purpose of Phase II of the SISSI instrumentation project was to continue the data collection and laboratory characterization efforts of Phase I as appropriate. However, the major goal of Phase II was to use SISSI data with the AASHTO newly developed mechanistic design guide (MEPDG). Furthermore, final assessment of the condition of SISSI sites and conduct of an independent mechanistic analysis were among the objectives pursued during Phase II.

WORK PLAN AND RESEARCH APPROACH IN PHASE II

Phase II of the project was conducted by carrying out several tasks. General field and laboratory activities under this phase are presented in Figures 3 and 4, respectively.

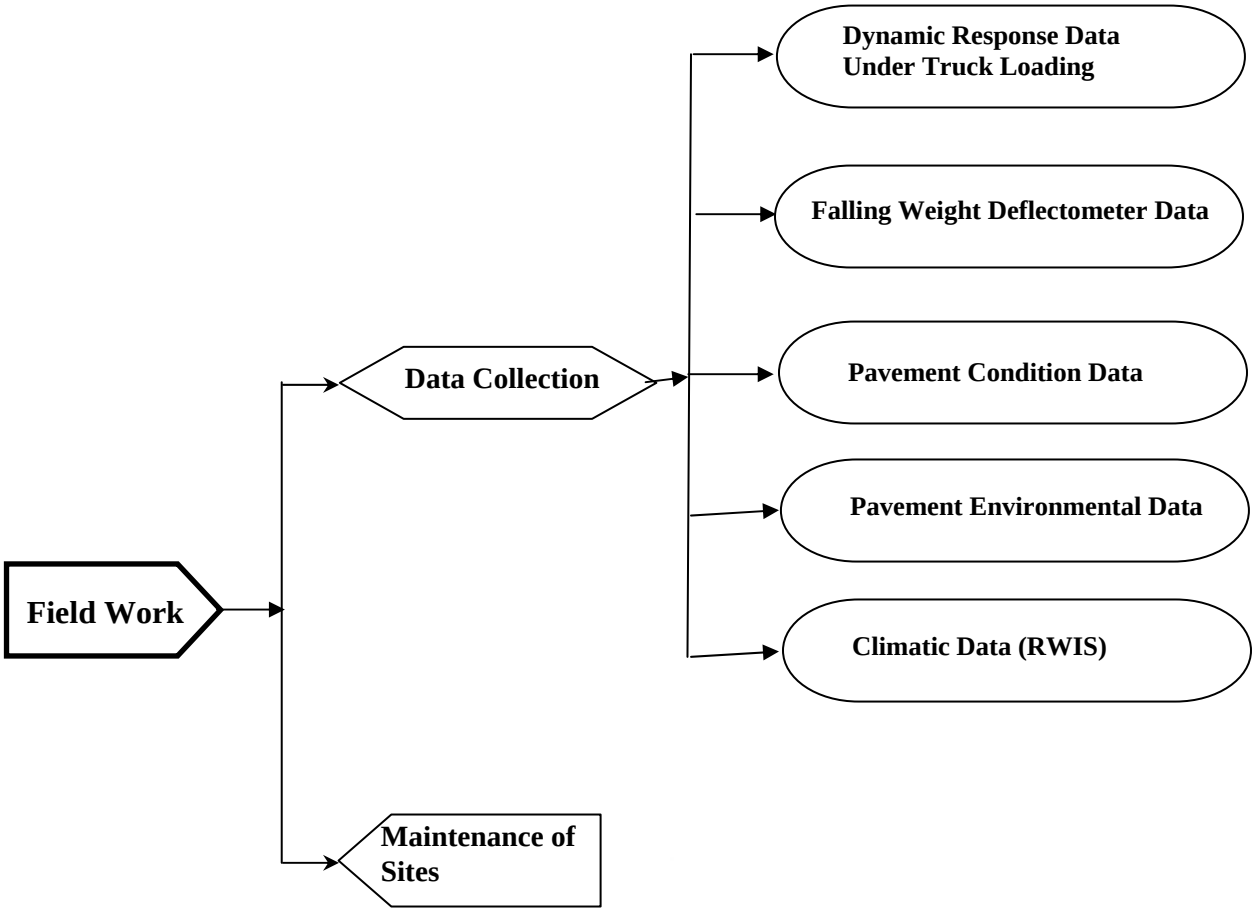

Figure 3. Field activities during Phase II of the SISSI project.

Continuation of Field Data Collection Efforts

Data collection efforts continued during Phase II even though such efforts were more limited than the level exercised during Phase I. The following activities were conducted as part of the field work.

Initial Evaluation of Instrumentation

One major factor affecting the extent of data collection during Phase II was the functioning of the sensors. During Phase I, continuous problems with instrumentation and data collection were faced, and the research team made the best effort possible, within limited time,

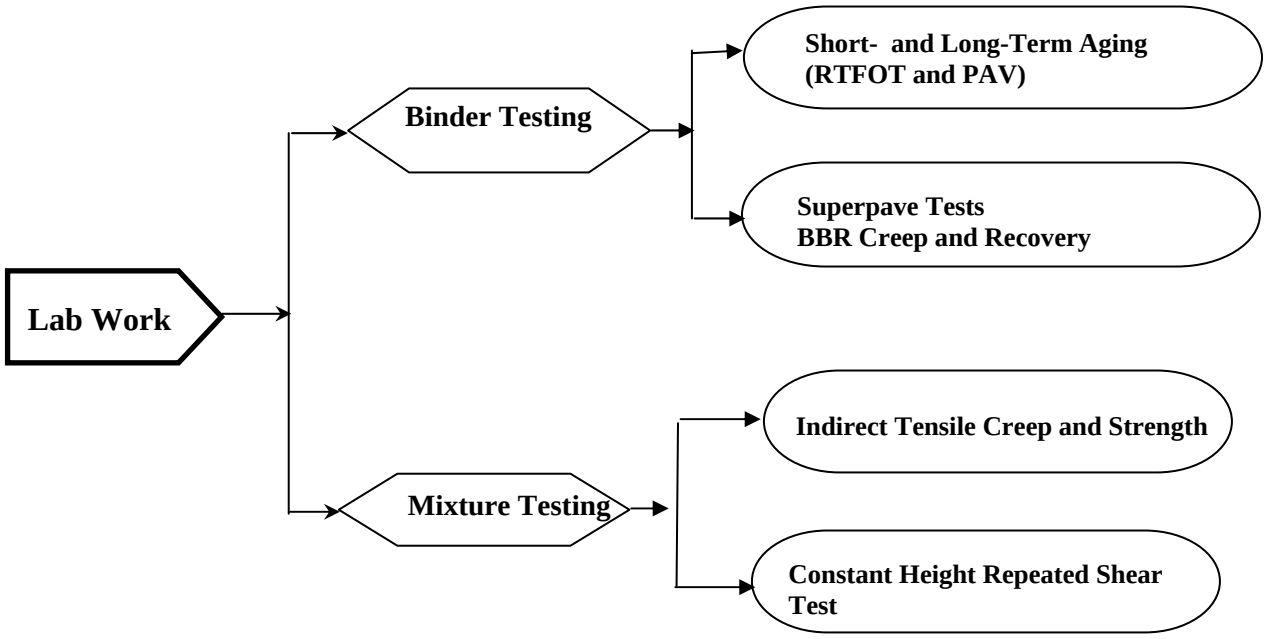

Figure 4. Lab activities during Phase II of the SISSI project.

budget, and resources, to maintain the functioning of gages and data collection efforts; however, a concentrated effort was needed for an initial evaluation of the data collection system and sensors at the beginning of Phase II. Therefore, all sites were visited for comprehensive evaluation of all the sensors (both dynamic and environmental). The results of that assessment were provided to PennDOT in a report in October 2006 that included information regarding the condition of the sensors.

Site Maintenance

On certain occasions, trips to the site were required to conduct necessary repairs to maintain a successful data collection effort. At times, a specific piece of equipment had to be removed and replaced with a new piece in order to maintain the integrity of the data collection system.

Collection of Pavement Dynamic and Environmental Data

Dynamic data were collected at a limited level. The data collection effort was a selective process to complement the data collected during Phase I.

Collection of WIM, RWIS, Pavement Condition, and FWD Data

A final effort was conducted to evaluate the condition of the SISSI pavements during Phase II. The pavement condition data were essential for comparing the long-term performance of the pavement sections with the performance predictions from the design guide models and other mechanistic analyses.

FWD measurements were limited to the Blair site during Phase II. FWD testing at this site enhanced the analysis of the Phase I FWD testing. Archived RWIS climatic data were obtained from Penn State Climatologist (PASC) Department through October 2007. Afterwards, PASC maintained climatic data from four other sources: Citizen Weather Observation Program

(CWOP), Cooperative Observer Program (COOP), Federal Aviation Administration (FAA), and Department of Environmental Protection (DEP). The major source for SISSI climatic data was FAA after RWIS data were no longer available. The traffic and weather data obtained from SISSI sites were processed to prepare the input for the MEPDG software.

Implementation of Results from Phase I

This task was a major portion of the work accomplished under Phase II; it focused on using the results from SISSI data. The SISSI project is nationally considered as a significant endeavor toward validation and calibration of performance prediction models, specifically the newly developed AASHTO mechanistic empirical pavement design guide (MEPDG).

Implementing the SISSI Data with MEPDG

The MEPDG models were used with the SISSI data for SISSI sites constructed under Phase I of the project. The data from field and laboratory measurements were used as input in the models, and the predicted results were compared with field measurements.

Evaluating Sensitivity of the MEPDG to SISSI Data

There is always some variability associated with any type of measurement, and the data collected for the SISSI project were no exception. Furthermore, numerous pieces of data were required as input for the MEPDG models. So, to the extent that SISSI data are concerned, a limited level of sensitivity analysis was conducted for better evaluation of predicted results for the range of uncertainty for some variables. There was no intention of a thorough sensitivity analysis of the design guide under this subtask. Rather, the intention was to evaluate how output and results were affected for specific types of SISSI input data that could be variable.

Characterization of Materials

Extensive work was conducted during Phase I in regard to characterization of materials. All the asphalt binders were characterized, and all asphalt mixtures were tested at a range of temperatures and frequencies to determine dynamic modulus, an important input to the MEPDG models. However, low-temperature properties of the asphalt mixtures were not determined during Phase I; therefore, Phase II laboratory work focused on such testing.

Analysis of Results

Comparison of Predicted Results from MEPDG with Measured Results

The computed distresses from MEPDG models were directly compared to the measured distresses for SISSI sites. The comparison was conducted for rutting, fatigue cracking, low-temperature cracking, and roughness.

Conducting Independent Mechanistic Analysis using Dynamic Data

Because most of the SISSI sites are still early in their performance life, it was determined that additional analysis would be needed beyond direct application of MEPDG with SISSI data. One of the key aspects of the SISSI project, which has gained national attention, is the

combination of dynamic response from the instrumentation and the distribution of real sites with extensive data sets for MEPDG and performance model validation. To employ the power of this data set, additional analysis was conducted.

Finite element analysis using ABAQUS was conducted for each pavement site. This analysis was three-dimensional, permitting the comparison of the measured dynamic pavement responses from the instrumentation to those predicted using the measured material properties at different temperatures and speeds. These responses were also compared to the stress and strain responses predicted by the MEPDG performance models. This analysis is essential to using the instrumentation data to permit the preliminary validation of Superpave and of the MEPDG for these sites, without waiting for the full pavement life and deterioration, and is a key component of the SISSI goals.

REPORT ORGANIZATION

This is the summary report for Phase II of the Superpave In-Situ Stress Strain Investigation. Chapter 2 of the report includes a historical overview of the SISSI project. This is followed by interpretation and analysis in Chapter 3. Finally, the last chapter provides a summary and conclusions.

There are three other volumes in the series of SISSI-II reports. Volume 2 deals with material characterization and covers laboratory testing of SISSI mixtures and binders. Field data collection efforts and corresponding data are covered in Volume 3. Implementation of SISSI data with the mechanistic empirical pavement design guide is discussed in Volume 4.

CHAPTER 2
SISSI PROJECT - A HISTORICAL OVERVIEW

At the time of writing this report, it was over 7 years since the SISSI project had been initiated. The project was born as a result of inspiration from PennDOT to improve the quality of pavements constructed within the Commonwealth of Pennsylvania. A great deal of effort has been put into the project since its inception, as explained in Phase I final report (Solaimanian et al. 2006). There was also tremendous effort exercised prior to the beginning of the project during the period that the research framework was under preparation. Today, the outcome of those extensive efforts is reflected in the data generated from eight instrumented sites and the associated field and laboratory investigation. This chapter provides an overview of the SISSI project development and associated tasks.

INSTRUMENTATION SITES AND PAVEMENT MATERIALS

At the heart of the SISSI project was instrumentation of several Superpave projects. Sites were selected based on specific criteria (sufficient length, tangent section, power access, etc.) at both the northern and southern parts of the Commonwealth to represent the temperature difference and the difference in the freeze-thaw cycles the pavement undergoes during the winter-spring period. Two types of pavements were considered: (1) full-depth structures including subbase, base, and Superpave-designed hot-mix asphalt layers constructed over subgrade and (2) structural overlays including only Superpave-designed hot-mix asphalt layers. Figure 5 shows the counties in which the Superpave pavements were instrumented for the SISSI project, and Table 1 provides details of each location. Construction and instrumentation of the projects occurred at various dates as shown in Table 2. Tables 3 and 4 present the pavement design information and binder grade for SISSI sites. The asphalt binders are mostly PG 64-22, but for four of the sites, the binder used at the upper layers was a PG 76-22.

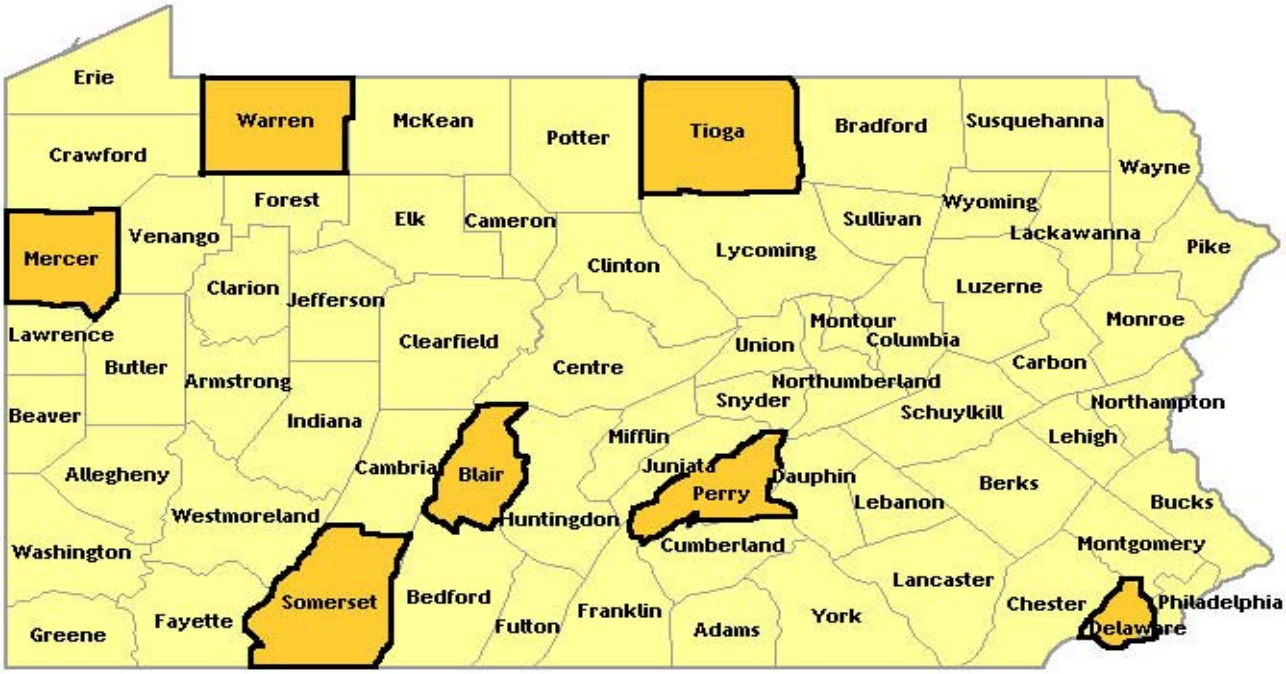

Figure 5. Counties where SISSI instrumentation sites are located.

Table 1. Highways selected for instrumentation.

Site No.	District & County	Route No.	Instrumentation Location 1		Instrumentation Location 2	
			Latitude	Longitude	Latitude	Longitude
1	3-Tioga	6015	N/A	N/A	N41° 37.523’	W077° 07.110’
2	1-Mercer	0080 (E)	N41° 12.066’	W080° 03.825’	N/A	N/A
3	1-Mercer	0080 (W)	N41° 11.941’	W080° 05.836’	N/A	N/A
4	1-Warren	0006	N41° 50.880’	W079° 18.371’	N41° 50.873’	W079° 18.348’
5	8-Perry	0022	N40° 29.660’	W077° 05.779’	N40° 29.659’	W077° 05.822’
6	6-Delaware	0202	N39° 53.518’	W075°33.351’	N39° 53.485’	W075°33.324’
7	9-Somerset	I-76	N/A	N/A	N39° 59.650’	W079° 01.382’
8	9-Blair	1001	N40° 26.414’	W78° 24.756	N40° 26.382	W78° 24.749’

Table 2. Type of pavement structure and season of construction for SISSI sites.

County	Route No.	Pavement Type	Traffic Level	Location	Construction Period
Tioga	SR 0015	New HMA	High	North	Summer 2000
Mercer	SR 0080	New HMA	High	North	Summer/Fall 2000
Mercer	SR 0080	Overlay	High	North	Summer/Fall 2000
Warren	SR 0006	Overlay	Low	North	Summer/Fall 2001
Perry	SR 0022	Overlay	High	South	Summer/Fall 2001
Delaware	SR 0202	Overlay	Low	South	Summer 2002
Somerset	I-76	New HMA	High	South	Summer/Fall 2002
Blair	SR 1001	New HMA	Low	South	Summer/Fall 2003

Table 3. Construction information for SISSI sites.

Site 1. Tioga County, SR-0015, Full Depth, < 30 million ESALs 11.5" CSSB[a], 37.5 mm AC[b] @ 9", 19 mm AC @ 2", 12.5 mm AC wearing @ 1.5",
Site 2. Mercer County, I-80, Full Depth, > 30 million ESALs 8" CSSB, 37.5 mm AC @ 15", 25 mm AC @ 3", 12.5 mm AC wearing @ 1.5",
Site 3. Mercer County, I-80, Structural Overlay, > 30 million ESALs 12" Cracked PCC, 37.5 mm AC @ 9", 25 mm AC @ 3", 12.5 mm AC wearing @ 1.5"
Site 4. Warren County, SR -0006, Structural Overlay, < 30 million ESALs 25 mm AC @ 4", 37.5 mm AC @ 5.5", 25 mm AC @ 2", 9.5 mm AC @ 1.5"
Site 5. Perry County, SR-0022, Structural Overlay, < 30 million ESALs 19 mm AC @ 2", 12.5 mm AC @ 1.5"
Site 6. Delaware County, SR-0202, Structural Overlay, < 30 million ESALs 19 mm AC @ 2.5", 12.5 mm AC @ 2.0"
Site 7. Somerset County, I-76, Full Depth, > 30 million ESALs 300 mm Lime Stabilization, 150 mm CSSB, 100 mm ATPM[c], 37.5 mm AC @ 7", 25 mm AC @ 3.0", 19 mm AC @ 2.0"
Site 8. Blair County, SR 1001, Full Depth, < 30 million ESALs 180 mm CSSB, 25 mm AC @ 8", 19 mm AC @ 2.0", 12.5 mm AC @ 1.5"

[a]CSSB indicates crushed stone subbase.

[b]AC indicates asphalt concrete designed according to Superpave system. Value in mm indicates mix designation, value in inches indicates layer thickness.

[c] ATPM indicates Asphalt Treated Permeable base.

Table 4 Performance grade asphalt binders at SISSI Sites

Site	Route	Layer	PG
Tioga	SR 0015	Wearing	64-28
		Binder	64-22
		BCBC	64-22
Mercer New (East)	SR 0080	Wearing	76-22
		Binder	76-22
		BCBC	64-22
Mercer Overlay (West)	SR 0080	Wearing	76-22
		Binder	76-22
		BCBC	64-22
Perry	SR 0022	Wearing	76-22
		Binder	64-22
		Leveling	64-22
Warren	SR 006	Wearing	64-22
		BCBC	64-22
		Leveling	64-22
Delaware	SR 202	Wearing	76-22
		Binder	76-22
Somerset	Turnpike	Wearing	64-22
		Binder	64-22
		BCBC	64-22
Blair	Plank Road	Wearing	64-22
		Binder	64-22
		BCBC	64-22

Pavement Instrumentation

Instrumentation of the pavement layers, details of which are reported elsewhere (Anderson et al., 2003), was an integral part of this project. Both load-associated and environmental transducers were installed at different layers. Two replicate locations were instrumented at each of the eight SISSI sites. The number and location of the transducers varied according to the pavement structure at each site. Cables buried in the pavement connected the transducers to an instrumentation cabinet at the edge of the shoulder. The instrumentation cabinet contained the data logger used for the environmental measurements and a modem for transmitting data. A typical schematic showing the positioning of the transducers and the instrumentation cabinet is given in Figure 6.

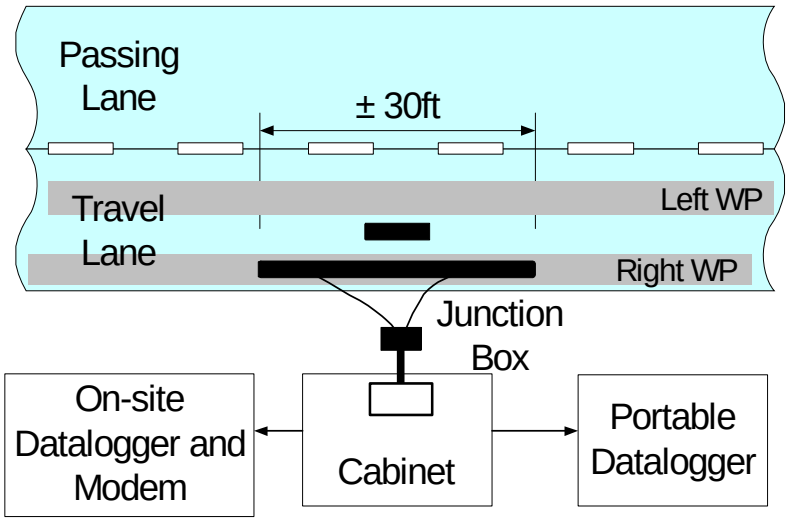

Figure 6. Typical instrumentation layout.

The load-associated and environmental transducers were installed in the travel lane. The load-associated transducers were either in or immediately adjacent to the right wheel path, and the environmental transducers were placed at the center of the travel lane between the wheelpaths, where they would be least affected by the wheel loads.

Transducers installed to capture the pavement response under truck loading included pressure cells and strain gages in the unbound layers, H-type strain gages in the asphalt layers, and multi-depth deflectometers (MDD) throughout all the pavement layers.

The principal sources of in-situ environmental data at the test sites were thermocouples for temperature measurement, time-domain reflectometers for moisture content measurement, resistivity probes for frost depth measurements, and pyranometers for solar flux.

Material Sampling

The magnitude of material procurement required an organized approach to ensure that a sufficient and representative sample was obtained for each material. Table 5 provides details of sampling, which included the following materials: asphalt binder, hot-mix asphalt/aggregate mixture, aggregates, and subgrade material.

Table 5. Material sampling for SISSI sites.

Site Name	Site #	Layer	Nominal Maximum Aggregate Size	Binder Grade	Sampling Status
Tioga County SR 6015-A53	1	Wearing	12.5mm	64-28	*S*
		Binder	19mm	64-22	*S*
		BCBC	37.5mm	64-22	*S*
		Sub-base	na	na	*S*
		Sub-grade	na	na	*S*
Mercer County East SR80-A04 Seg. 205	2	Wearing	12.5mm	76-22	*S*
		Binder	25mm	76-22	*S*
		BCBC	37.5mm	64-22	*S*
		Sub-base	*(rubble-ized concrete)*	na	*N*
		Sub-grade	*	*	*
Mercer County West SR80-A04 Seg. 205	3	Wearing	12.5mm	76-22	*S*
		Binder	25mm	76-22	*S*
		BCBC	37.5mm	64-22	*S*
		Sub-base	*	*	*
		Sub-grade	*	*	*
Warren County SR0006-A01 Seg. 420	4	Wearing	9.5mm	64-22	*S*
		Binder	19mm	64-22	*S*
		BCBC	37.5mm	64-22	*S*
		Sub-base	*(rubble-ized concrete)*	na	*N*
		Sub-grade	*	*	*
Perry County SR0022-020 Seg. 161	5	Wearing	12.5mm	76-22	*S*
		Binder	19mm	64-22	*S*
		BCBC	*	*	*
		Sub-base	*	*	*
		Sub-grade	*	*	*
Delaware County SR202 M10	6	Wearing	12.5mm	76-22	*S*
		Binder	19mm	76-22	*S*
		BCBC	*	*	*
		Sub-base	*	*	*
		Sub-grade	*	*	*
Somerset County PA Turnpike Mille post 115	7	Wearing	19mm	64-22	*S*
		Binder	25mm	64-22	*S*
		BCBC	37.5mm	64-22	*S*
		ATPB	na	na	*S*
		Sub-base	na	na	*S*
		Sub-grade	na	na	*S*
Blair County SR1001-012	8	Wearing	12.5mm	64-22	*S*
		Binder	19mm	64-22	*S*
		BCBC	25mm	64-22	*S*
		Sub-base	na	na	*S*
		Sub-grade	na	na	*S*

S : sampled for testing
N : not sampled

∗ : layer was not part of construction of this site
na: not applicable or not available

DATA COLLECTION

The SISSI project required collection of a great amount of data. The following categories of data were collected during the course of the project:

- Pavement dynamic (load-associated) data
- Pavement environmental (non-load-associated) data
- Materials data

- Traffic data
- Falling weight deflectometer data
- Climatic data
- Pavement condition data (performance data)

Pavement Dynamic (Load-associated) Data

Load-associated pavement response was captured through application of controlled loads at certain speeds using a specially mounted truck (Figure 7). Different speeds and load configurations were used for this purpose. The tractor-trailer was equipped with moveable concrete blocks so that the distribution of load on different axles could be controlled.

Figure 7. Truck with moveable weights for pavement loading.

The load-associated measurements were obtained by closing the sites to traffic. Portable data loggers were used to condition the transducers and acquire the data. Load-associated measurements were not obtained during normal trafficking. Loading the pavement was conducted by both the front and rear load configurations at speeds of 20, 40, and 60 mph. At a later time during the project, a 5-mph speed was added to capture pavement response at creep-inducing loading rates.

Pavement Environmental (non-Load-Associated) Data

Measurement of environmental data was conducted on a continuous basis, and the resulting data were acquired by permanently installed data loggers that were connected to the server at Penn State via land lines or wireless service.

Materials Characterization Data

During phases I and II of the SISSI project, significant effort was made to characterize the binders and mixtures used at all instrumented sites.

Binder Testing

The following tests were the primary tests conducted for the binder characterization during Phase I:

- Rotational viscometer (RV)
- Dynamic shear rheometer (DSR)
- Bending beam rheometer (BBR)

Short-term and long-term aging were applied to the binders as needed throughout the course of the project.

Phase II binder testing was focused on validation of the Superpave binder specification at low temperature using BBR.

Mixture Testing

The tests on HMA during phases I and II included tests on the loose mixture and tests on the compacted specimens. The tests on the loose mixture included determination of the maximum theoretical specific gravity and determination of binder content and aggregate gradation. AASHTO procedures were followed for this purpose. The tests on the compacted specimens included determination of the bulk specific gravity, dynamic modulus tests, constant height repeated shear test, and indirect tensile test.

Traffic Data

Consideration of traffic loading information is one of the most important elements of a successful pavement design process. Mechanistic design procedures consider the response of pavement materials to applied loads; for highways, these are wheel loads. Therefore, it is important to accurately consider the effect of wheel loads of individual size and account for cumulative damage resulting from repeated loading. The design procedure used in MEPDG does this in the form of load spectra, a catalog of each wheel load, including size and weight. Load repetitions are estimated by extrapolating historical trends or applying other growth projections.

The SISSI project undertook the collection of traffic data at each individual pavement test location as a part of the information-gathering process. Weigh-in-motion (WIM) equipment was installed by PennDOT adjacent to each pavement test location to collect traffic information on site.

Data Collection Process

The data collected at each site were downloaded remotely from the field data collection device and posted to an FTP site by the PennDOT Bureau of Planning and Statistics. Once downloaded, the raw data, which were in binary format, were converted into ASCII format for further analysis. The conversion was performed using a proprietary software program called "Reporter," which was developed by PAT America Traffic Control Corporation. The PAT

Reporter generates truck records from raw data. It splits raw data into classification and weight data as two separate files. It also generates monthly classification reports that contain daily traffic counts for each vehicle class.

The following files are generated using the PAT Reporter software:

1. ASCII truck record files (with "A" prefix) that include vehicle class, gross weight, vehicle length, speed, axle weight and spacing, and number of axles for each truck record.
2. ASCII classification record files (with "B" prefix) that include records of hourly traffic counts for each vehicle class.
3. Monthly classification report (with "MC" prefix) that documents daily traffic counts for each vehicle class.
4. Monthly weight report (with "MW" prefix)

These records were then processed using a series of programs written in MATLAB to check the quality of data, check monthly trends, and collect summaries. These summaries were used to prepare the necessary input for the NCHRP 1-37 software.

Data Processing

The traffic files were examined for any missing data, bad quality of data, and number of erroneous records. The quality of traffic data was checked every month as the data were collected. In addition, the monthly trends of key elements such as number of trucks and gross weight of vehicles were examined to observe seasonal variations. Quality check procedures adopted in this study include:

1. Document all missing raw data files ("D" files).
2. Document the ASCII truck files ("A" files) with an unreasonably small number of truck records.
3. Detect the truck records with abnormal axle weights and/or axle spacing in ASCII truck files.
4. Document the ASCII classification files ("B" files) that do not have 24 records (one record summarizes 1 hour of traffic information).
5. Detect the ASCII classification files having zero hourly traffic records, which are determined to be unreasonable after the traffic trends are checked.
6. Average the truck gross weight, length, and speed monthly. The averaged values are plotted against time, and any deviation from normal traffic variation patterns is investigated to identify the causes.

The vehicle and classification records were then used to develop data summaries and prepare input for the NCHRP 1-37 software. The necessary input parameters included axle load distribution for each vehicle class, vehicle class distribution, monthly adjustment factors, number of axles per truck, vehicle speed, and axle and wheelbase spacing. Some sites had a higher percentage of missing data than other sites since data collection began. The data collection sites at Tioga, Mercer, and Somerset had 30 percent to 40 percent missing data. The other sites had minimal proportions of missing data. The missing data could be either due to bad quality of data

or the data were not recorded on a particular day. The sites with a significant occurrence of missing data had operational problems. In several instances, the data collection equipment was not functional. PennDOT initiated a maintenance and calibration contract with PAT America, which ultimately resulted in the correction of these equipment problems.

Falling Weight Deflectometer Data

Falling weight deflectometer (FWD) testing was conducted at each of the SISSI locations on a periodic basis during Phase I. During Phase II, falling weight deflectometer testing was conducted at the Blair site only. The Blair site was selected for a number of reasons, including its age and condition. The primary reason was that backcalculation efforts using the Phase I data were only marginally successful. Therefore, it was desirable to collect data at additional load levels and to collect the load-deflection history data during testing. Finally, it provided an opportunity to collect simultaneous data from the embedded instrumentation and the FWD.

Climatic Data

The climatic data came from a number of sources. The primary sources of site-specific data were the PennDOT RWIS sites. These data have been supplemented by data from the Department of Environmental Protection and national weather data. The Penn State Department of Meteorology Mesonet was the direct source for all climatic data, with the data downloaded from their Web site. The collection and processing of the SISSI climatic data is described in detail in the SISSI Seasonal Variations Report.

Performance Data

Performance data are essential to the long-term use of the SISSI data for calibration and validation of performance and design models. Manual distress surveys were conducted on field visits in conjunction with other testing. Longitudinal profile and videologging distress summaries were provided by PennDOT for the affected segments during Phase I. The performance data are described in detail in the SISSI Phase I Pavement Condition Report (Stoffels and Solaimanian, 2006) and SISSI Phase II Field Data Collection and Summary Report (Solaimanian et al., 2008).

PROBLEMS AND ISSUES WITH DATA COLLECTION

The research team made every effort during the project to make the data collection as smooth as possible. However, there were many occasions of interruption in collection of data during the course of both Phases I and II of the project. These interruptions resulted in discontinuity in the collected data, specifically in the dynamic, environmental, and traffic (weigh-in-motion) data. Several sources contributed to the problems encountered during the data collection phase of the project. These sources are discussed below for various types of data.

Problems with Collection of Environmental Data

In general, the following factors contributed to discontinuity in the environmental data:

- Random power outages at the site
- Malfunctioning of datalogger
- Problems with wires and connectors
- Damaged installed gage
- Disconnected phone service

Random Power Outage at the Site

The loss of power to the site was, in most cases, the result of a tripped GFCI (ground fault circuit interrupter) due to thunderstorms and lightning. This resulted in the loss of power to the on-site datalogger. The datalogger was equipped with two 12-volt deep cycle batteries, arranged in parallel, to maintain power to the datalogger for extended periods of time in case of power outage. The PTI technician would monitor the battery voltage from the central office at PTI every time data were downloaded. This monitoring was done to ensure that sufficient power was available to the datalogger. In case of a battery voltage drop below acceptable levels, the technician would visit the site to fix the problem. Sometimes, the problem would be resolved through restoring the power to the site (resetting GFCI), and sometimes the problem was with a damaged battery that needed to be replaced by a new one. The batteries were replaced frequently when problems were noticed; however, they also were replaced after one year in service regardless of the situation. On occasion, limited resources made it difficult to travel to the site immediately after such problems had occurred.

On one occasion for one of the sites, power was lost because of common circuits with three light poles at the vicinity of the site. The wires to one of these lights had to be disconnected to restore power to the site.

Malfunctioning of Datalogger

The second type of problem with collection of environmental data was related to the datalogger. Occasionally, the datalogger was damaged for various reasons after some time in service. This prevented collection of any data. Once such a problem was identified, the datalogger was removed from the site, and a new datalogger was installed if available. The damaged datalogger was shipped back to the manufacturer for repair.

Problems with Wires and Connectors

On rare occasions, loose wires or damaged connectors were the reasons preventing data collection. These were fixable, and the research team made an effort to keep such problems to a minimum; however, such repairs, though simple, always required a physical presence at the site. Having resources available for such activities was always a challenge considering the vast number of activities.

Damaged Installed Gage

The most serious problem associated with collection of environmental data occurred when a gage or sensor installed inside the pavement was damaged. Under such circumstances, the gage would be considered permanently lost, and no data could be collected from that gage. The most prevalent problem of this nature occurred to the time domain reflectometers, which were installed for determination of moisture content. It appears that some of these gages were damaged by lightning.

Problems with Collection of Dynamic Data

It was discussed in Chapter 2 that load-associated pavement response data (i.e., dynamic data) were collected at the sites by running a truck with known weight and speed on the instrumented pavement. While considerable data of this type were captured through many trips to the sites, various problems prevented having a complete set of data from various sensors, as was originally perceived. Several factors contributed to the collected data being of smaller quantity than was originally planned. These included:

- Delayed construction and instrumentation of several sites
- Limited time and resources
- Inclement weather conditions
- Problems with data acquisition system
- Problems with installed gages
- Co-occurrence of measurements with other construction activities

Inclement Weather Conditions

When required to visit the sites for dynamic measurement and transverse profiling, attempts were made to conduct such measurements on days when weather conditions would not be a hindrance; however, there were many occasions when a scheduled trip had to be canceled or postponed because of weather. There were also times when during measurements, a significant change in weather conditions was encountered and measurements had to be abandoned. To the extent possible, such measurements were rescheduled. Sometimes, rescheduling would move the measurement late enough to close the window for conducting the measurement within a specific season. In such a case, no measurement set would be available for a particular site for that season.

Problems with Data Acquisition System

The data acquisition system was functional for most of the time during the project. There were a few cases, however, when system problems prevented timely trips to the site. In some cases, the dataloggers had to be sent back to the manufacturer for repair or calibration.

Problems with Installed Gages

It was discussed earlier that different pavement layers were instrumented with four types of gages: strain gages for bound layers, strain gages for unbound layers, multi-depth deflectometers, and pressure cells. These gages are continuously exposed to traffic and the environment, and therefore it is reasonable to expect that their functional life span is limited. The service life of the gages and their survival depend on the type of gage as well as the intensity

of influencing factors (traffic level and harshness of environment). Of the gages, the multi-depth deflectometers seemed to be the most susceptible and exhibited the shortest service life.

The dynamic data collected from the site located on the Somerset County Turnpike are very limited because of the loss of some of the sensors during construction of the site as well as difficulties in establishing the traffic control needed to conduct pavement response measurements. However, the environmental, traffic, and materials characterization data from this site are, in terms of quantity, comparable with the data from other sites.

Simultaneous Occurrence of Measurements with other Construction Activities

On rare occasions, measurements could not be scheduled for a specific period of time at a site because other construction activities were taking place at the same time, preventing lane closure for the instrumented section.

Frequent inoperability of the RWIS Climatic Data Stations

The RWIS sites are used principally for winter-weather maintenance and are operated and have their data managed by the counties. Unfortunately, the sites were not able to operate year-round as planned, even for the sites installed adjacent to the SISSI sites for that purpose. In addition, some sites had extended periods of inoperability even in the winter. Therefore, the RWIS data need to be supplemented with quality data from other sources. Beyond October 2007, Penn State Meteorological Department stopped archiving RWIS data. After this time, the SISSI research team began using Federal Aviation Administration Data (FAA) archived by Penn State.

MAINTENANCE OF SITES

Maintaining smooth collection of environmental data and minimizing delays in the collection of dynamic data required frequent maintenance visits to the instrumented sites. These visits were required for various reasons: restoring power to the dataloggers, replacing batteries, and replacing or repairing modems, dataloggers, multiplexers, or cables. Sometimes the trips were needed to mend broken wires and damaged or corroded connectors. This was a very challenging and time-consuming effort considering the number of locations requiring maintenance.

THE IMPACT OF AN INCOMPLETE DATA SET ON THE GOALS OF THE SISSI PROJECT

Despite the shortcomings and problems discussed earlier, a vast and unique set of valuable data of various types was collected from the SISSI sites. Undoubtedly, the collected information has provided a very useful database for implementation and model calibration validation efforts. It is, however, true that at some places, the existence of missing data will require taking logical steps and making reasonable assumptions to fill the gaps in the data. The best available or closest data, or accepted quality models, should be used to fill those gaps.

SISSI STEERING COMMITTEE

Prior to initiation of the SISSI project, a steering committee was established to oversee and guide this investigation. This committee included experts and individuals from PennDOT, Federal Highway Administration, and industry. The initial organizing meeting of the steering committee was held in January 2000. The SISSI research team met with the steering committee every month to discuss the research progress, problems, and needs during Phase I. The meetings were conducted on a quarterly basis during Phase II.

PROJECT PEER REVIEW

An external peer review panel was established to seek the opinions of experts in regard to the direction of the SISSI research project and the possible actions needed to improve the quality of data collection. Members of the external peer review/advisory panel were selected to represent a number of projects and agencies with specific expertise related to various areas of the project, such as the instrumentation, materials characterization, or modeling. The meeting was held in Harrisburg, PA, on October 3, 2002. The meeting was attended by four members of the peer review panel, as well as by some members of the SISSI steering committee. The panel members later provided written feedback to PennDOT about the research project and its activities. Several of the comments were about instrumentation and data collection. Installation of solar radiation sensors, installation of thermocouples closer to the surface of the pavement, and increasing sampling rate for pavement temperature were among the suggestions that were implemented.

CHAPTER 3
RESULTS, ANALYSIS, AND INTERPRETATION

GENERAL SCOPE OF ANALYSIS FOR SISSI PHASE II

Chapter 1 of this report presented the scope of activities pursued during SISSI Phase II. Field measurements and laboratory testing during Phase II generated a sizeable amount of data. Basically, Phase II analysis included results from material characterization, final assessment of condition of SISSI pavements, implementation with MEPD, and independent mechanistic analysis. Detailed analysis of such data is provided in three separate reports referred to as volumes 2 through 4 reports of SISSI-II. Volume 2 covers material characterization, and volumes 3 and 4 present analysis of field data and MEPDG implementation, respectively. In this chapter, a summary of analysis covered in those three volumes is presented.

ANALYSIS OF FIELD DATA

Pavement Condition Evaluation

Manual distress surveys were conducted in accordance with Long-Term Pavement Performance protocols. The distress definitions used for this project were detailed in the *Performance, Traffic and Weather Data Collection and Reporting Manual*; some of the distress definitions have changed over time. Distress surveys were conducted over one-thousand-foot sections, including both instrumentation sections. Detailed crack maps were prepared for each instrumentation section, and photographs were taken in conjunction with the manual distress surveys.

All SISSI sites appeared to be in good shape except for the two overlaid pavement sections at the Warren and Delaware sites. At these two sites, a significant amount of the longitudinal cracks at the lane-lane and lane-shoulder joints were probably due to poor construction. Transverse cracks on the pavement surface may have been induced by underlying concrete slabs or may have been thermally induced.

Durability of Superpave mixes was of concern at two of these sites, Warren and Mercer, based on observations of PennDOT personnel. The Warren site was finally milled and overlaid during spring 2007. For the Mercer site, only a small section of the road prior to the SISSI site was milled and overlaid. Our last pavement condition survey at this site, during November 2007, indicated no cracking of the pavement mat at the site even though minor to moderate raveling and loss of fines was evident at the vicinity of the longitudinal joint. The pavement had also experienced longitudinal cracking both at the joint between two lanes and the joint between the travel lane and the shoulder. These cracks appeared to be construction related rather than mix related; however, the minor to moderate raveling observed at the Mercer site is probably an indication of insufficient binder content at this site. In general, some Superpave mixes have demonstrated that they are highly resistant to rutting, and this rut resistance has come at the cost

of lower durability in some cases. In general, the field-measured rutting, after 5 to 8 years of service, ranged between 2.5 and 8.5 millimeters, indicating excellent rut resistance of SISSI mixtures at all the sites.

The rut depths were determined by the differences between the maximum peak and minimum valley measurements from the profiles (Figure 8). As rut depths progressed, transverse profiles were plotted and shapes evaluated as appropriate. A summary of average rut-depth measurements is included in Table 6. It can be seen that the rut depths in the left wheelpath are smaller than those in the right wheelpath at some SISSI sites and vice versa at other sites. In general, the field-measured rutting after 5 to 8 years of service ranged between 2.5 and 8.5 millimeters, indicating excellent rut resistance of SISSI mixtures at all the sites.

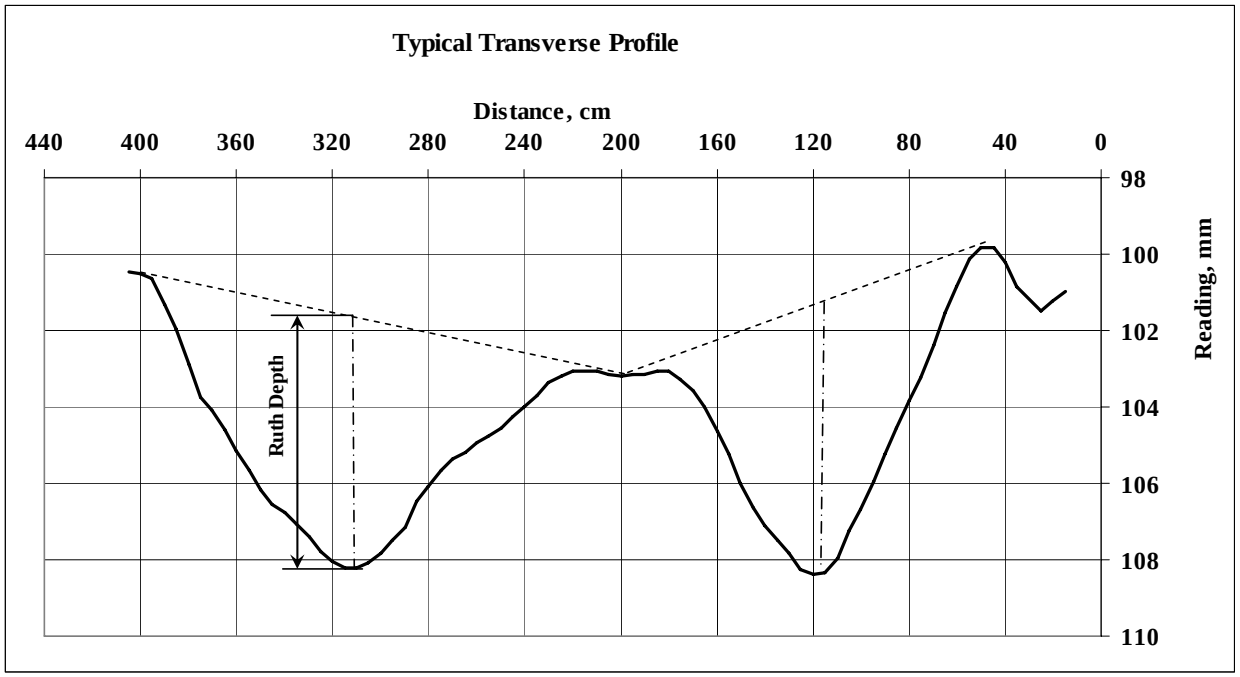

Figure 8. Schematics of the approach taken in determination of rut depth.

Table 6. Summary of transverse profile data.

SISSI Site	Loc.	Date	Rut Depth, mm		Loc.	Date	Rut Depth, mm	
			LWP	RWP			LWP	RWP
Tioga	1	11/6/2007	3.7	6.0	2	11/6/2007	5.7	6.9
		8/25/2005	3.3	5.7		8/25/2005	4.5	6.6
		10/26/2004	2.8	5.0		10/26/2004	-	-
		8/17/2004	2.3	5.2		8/17/2004	-	-
Mercer East	1	10/30/2007	3.4	3.1	2	10/30/2007	5.0	4.2
		3/22/2005	3.1	3.4		3/22/2005	3.8	2.7
		8/3/2004	3.1	3.4		8/3/2004	3.8	3.5
		4/6/2004	2.7	3.0		4/6/2004	3.1	3.2
Mercer West	1	10/30/2007	4.3	3.0	2	10/30/2007	4.0	3.3
		12/1/2005	5.0	2.5		12/1/2005	-	-
		8/4/2004	3.2	3.0		8/4/2004	2.8	3.0
		4/7/2004	-	-		4/7/2004	2.7	2.9
Warren	1	3/26/2007	5.6	2.4	2	3/26/2007	4.8	4.5
		3/17/2005	4.3	1.7		3/17/2005	4.3	2.4
		11/5/2004	4.5	2.1		11/5/2004	4.2	2.4
		8/24/2004	4.5	1.8		8/24/2004	3.9	2.0
Delaware	1	10/7/2008	2.4	8.6	2	10/7/2008	-	-
		3/15/2007	4.8	9.1		3/15/2007	5.2	4.4
		3/30/2005	4.1	6.7		3/30/2005	4.9	4.1
		11/10/2004	4.1	4.4		11/10/2004	4.7	3.7
		3/22/2004	3.3	6.5		3/22/2004	-	-
Perry	1	7/17/2008	-	-	2	7/17/2008	5.5	2.9
		2/23/2005	3.3	2.5		2/23/2005	3.8	2.1
		10/28/2004	4.0	2.6		10/28/2004	-	-
		7/27/2004	3.6	2.5		7/27/2004	3.2	2.1
Blair	1	4/29/2008	3.5	5.2	2	4/29/2008	3.8	5.6
		8/23/2005	2.8	3.5		8/23/2005	2.8	4.3
		10/22/2004	1.9	3.2		10/22/2004	2.0	3.0
		7/20/2004	1.6	2.2		7/20/2004	1.6	2.3

Dynamic Data

The first stage toward analysis of Phase II dynamic data was to compare these data to the data collected under Phase I of the project under similar loading and environmental conditions. In general, such comparison, as reported in volume 4, indicates good agreement between the dynamic data collected from both phases. The difference is usually smaller than 20 percent.

Results from Phase II dynamic measurements at the Blair SR 1001 site are presented in Figures 9 through 13. As expected, it was noticed that the magnitude of tensile strain was decreased at deeper pavement layers. It was also observed that strain decreased as the speed increased from 5 to 10 and then to 20 mph. However, there was not a significant change in response observed when the speed increased beyond this level. Measurements at lower speeds such as 5 mph resulted in considerably higher strain levels compared to the values at 20 mph. The data indicate the significance of loading at lower speeds, since the deformations in pavement layers increase with reduced speed, thus increasing the potential for developing permanent deformation. Regarding vertical pressures, it was observed that the induced vertical stress is considerably higher at the top of the subbase than that at the top of subgrade; however, the speed effect on stress responses is not as pronounced as strain responses.

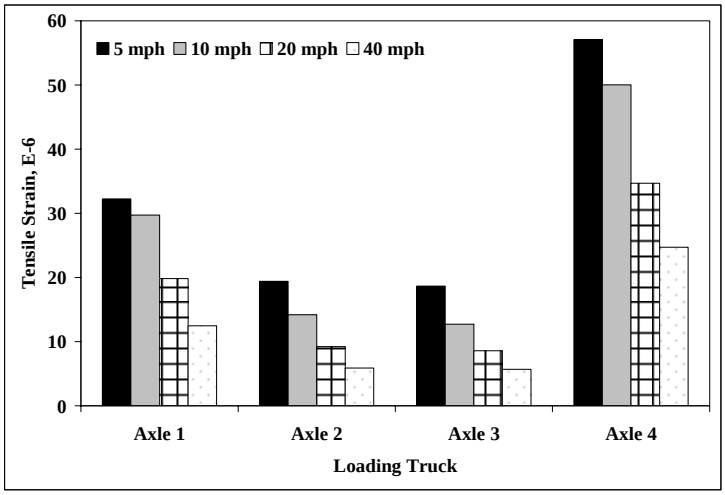

(a) tensile strain at the bottom of wearing layer

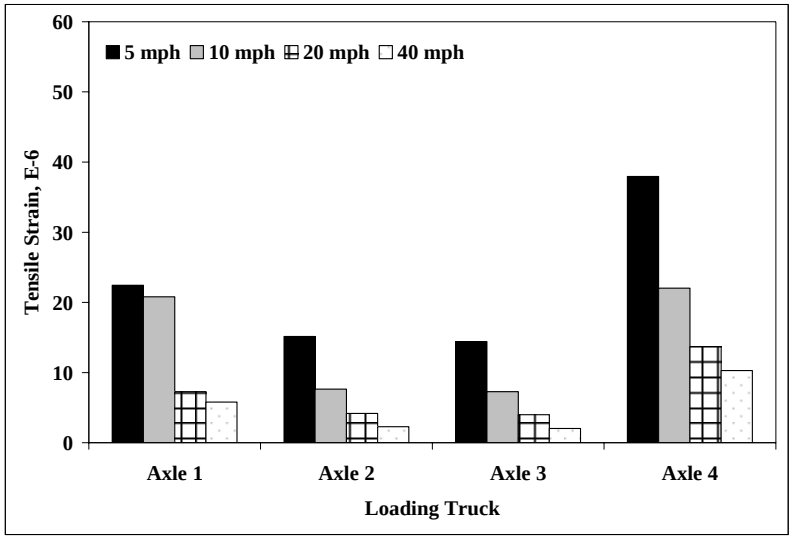

(b) tensile strain at the bottom of binder layer

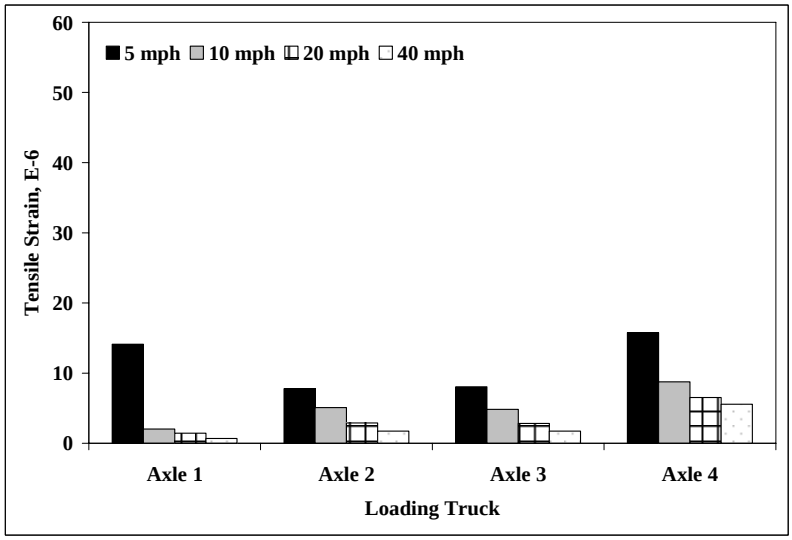

(c) tensile strain at the bottom of BCBC layer

Figure 9. Strain response of pavement layers at Blair location 1 (measured on 03/27/2008, back load configuration).

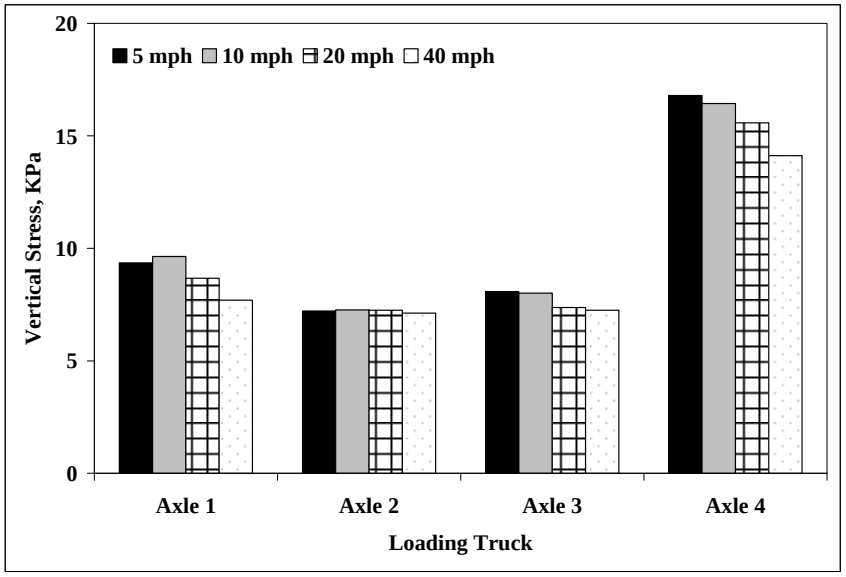

(a) vertical stress at the top of subbase layer

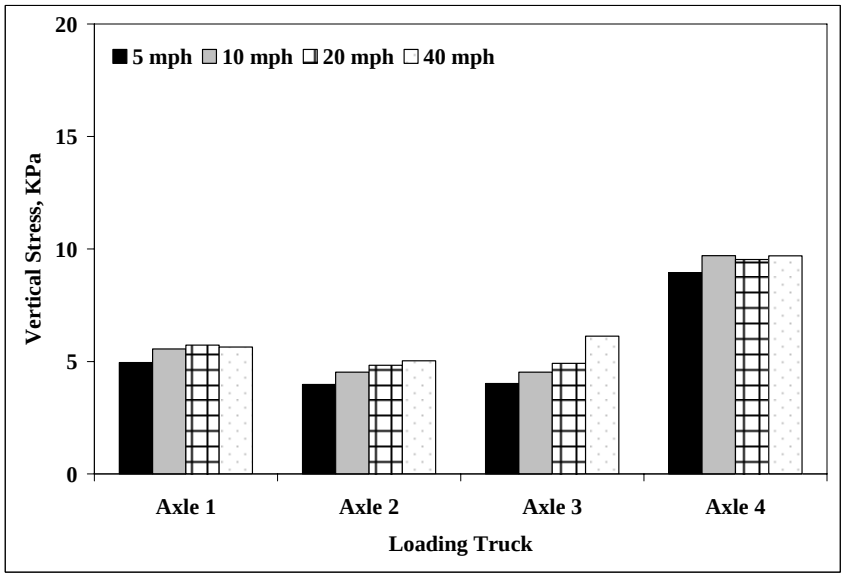

(b) vertical stress at the top of subgrade layer

Figure 10. Stress response of pavement layers at Blair location 1 (measured on 03/27/2008, back load configuration).

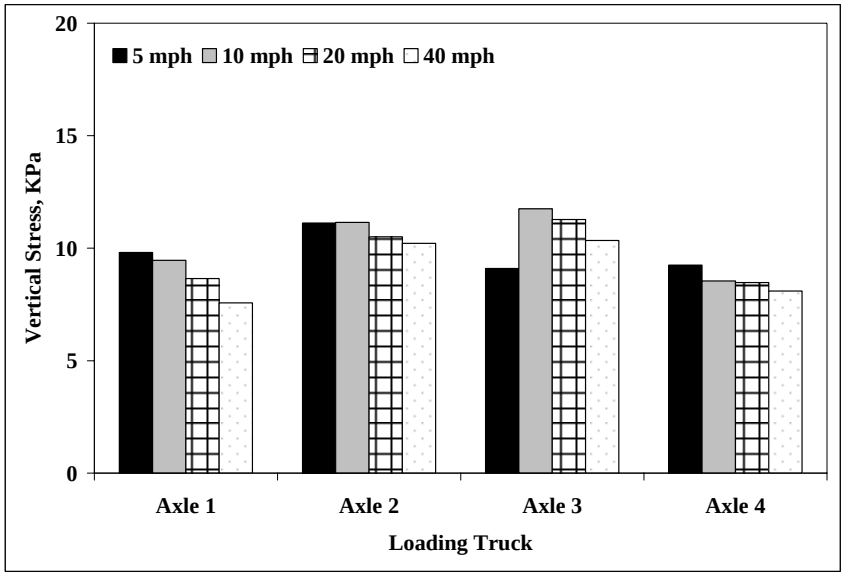

(a) vertical stress at the top of subbase layer

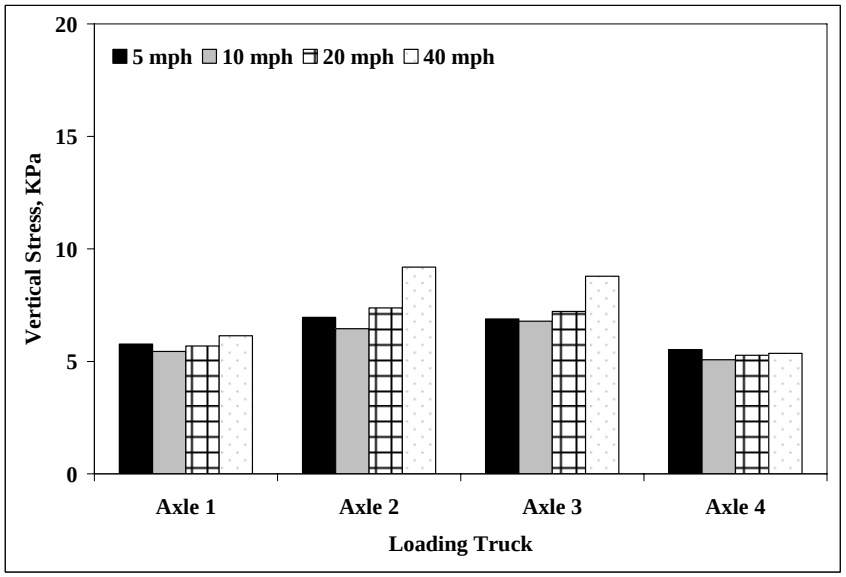

(b) vertical stress at the top of subgrade layer

Figure 11. Stress response of pavement layers at Blair location 1 (measured on 03/27/2008, front load configuration).

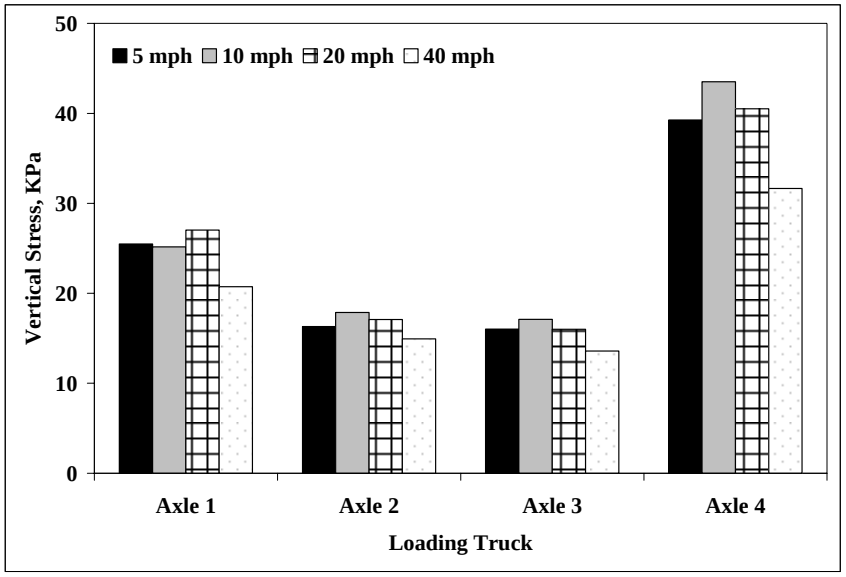

(a) vertical stress at the top of subbase layer

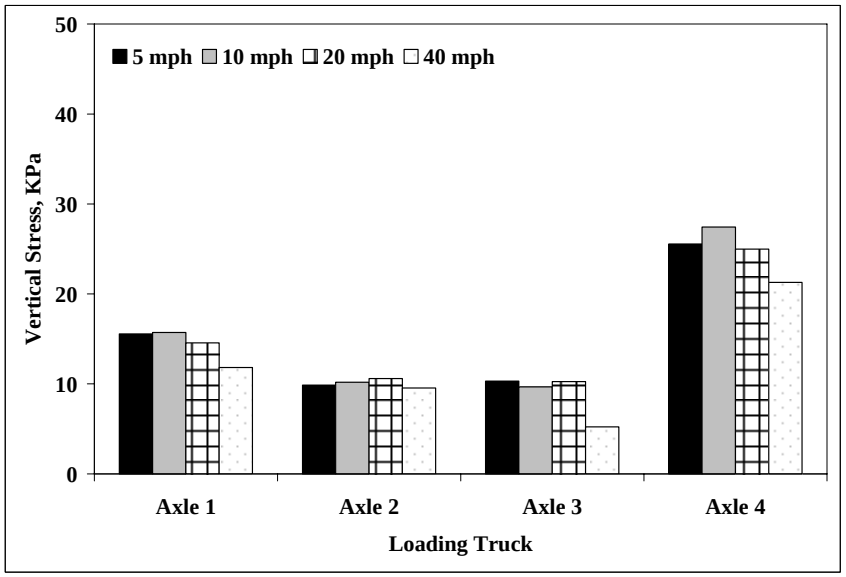

(b) vertical stress at the top of subgrade layer

Figure 12. Stress response of pavement layers at Blair location 2 (measured on 06/24/2008, back load configuration).

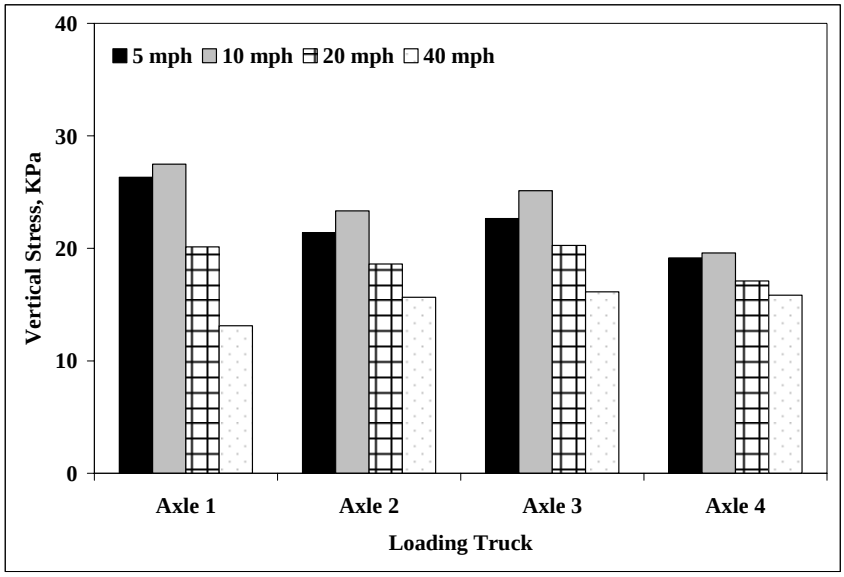

(a) vertical stress at the top of subbase layer

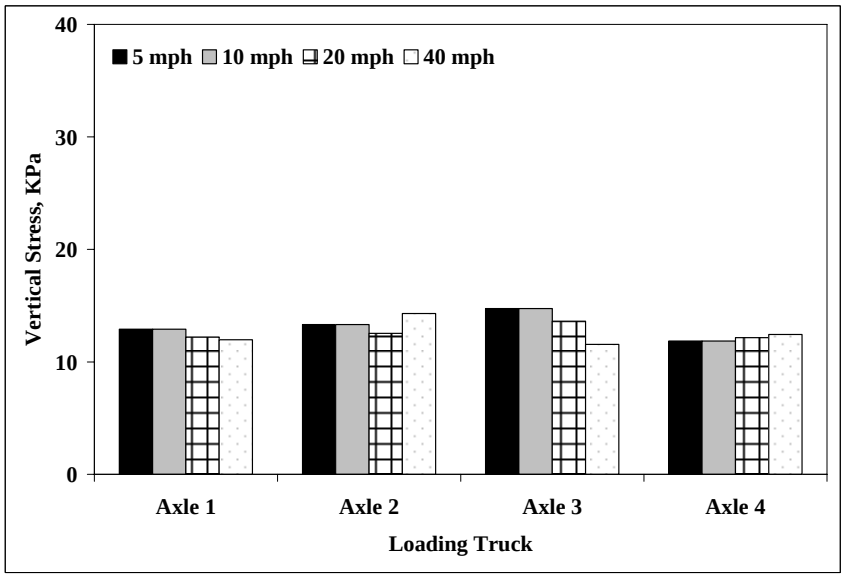

(b) vertical stress at the top of subgrade layer

Figure 13. Stress response of pavement layers at Blair location 2 (measured on 06/24/2008, front load configuration).

Deflection Data

During Phase II, falling weight deflectometer testing was conducted at the Blair site. The Blair site was selected for a number of reasons, including its age and condition. The primary reason was that backcalculation efforts using the Phase I data were only marginally successful; therefore, it was desirable to collect data at additional load levels and to collect the load-deflection history data during testing. Finally, it provided an opportunity to collect simultaneous data from the embedded instrumentation and the FWD. During Phase II, the falling weight deflectometer testing was performed by the Pennsylvania Department of Transportation (PennDOT) with their Dynatest falling weight deflectometer.

Backcalculation of modulus using FWD data was conducted through the MODCOM program. The backcalculated AC, subbase, and subgrade moduli were found to be fairly consistent throughout the measurement field. The subbase moduli appeared very low. During Phase I, FWD testing at three load levels, and without load-deflection histories being recorded, was performed on five different dates in different seasons after construction. Linear elastic backcalculations on all of those data sets also indicated very low subbase moduli.

Comparisons of elastic moduli obtained from the laboratory and the FWD backcalculations for the upper and lower AC layers are provided in Figures 14a and 14b, respectively. The backcalculated moduli are always higher than the laboratory-determined values. The observation is in general agreement with the 1993 AASHTO design guide (Stolle and Hein 1989), which says that the FWD backcalculated moduli are typically higher than the laboratory-determined moduli.

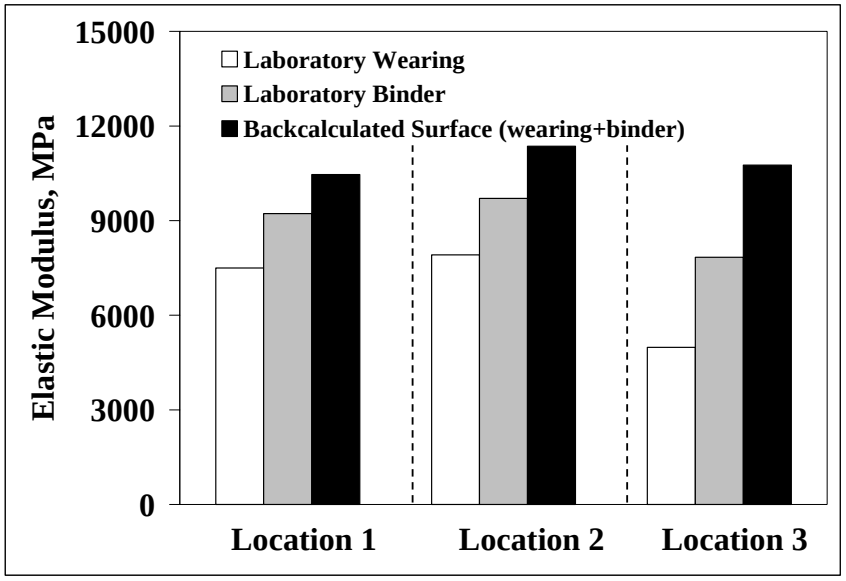

(a) wearing and binder combined layer

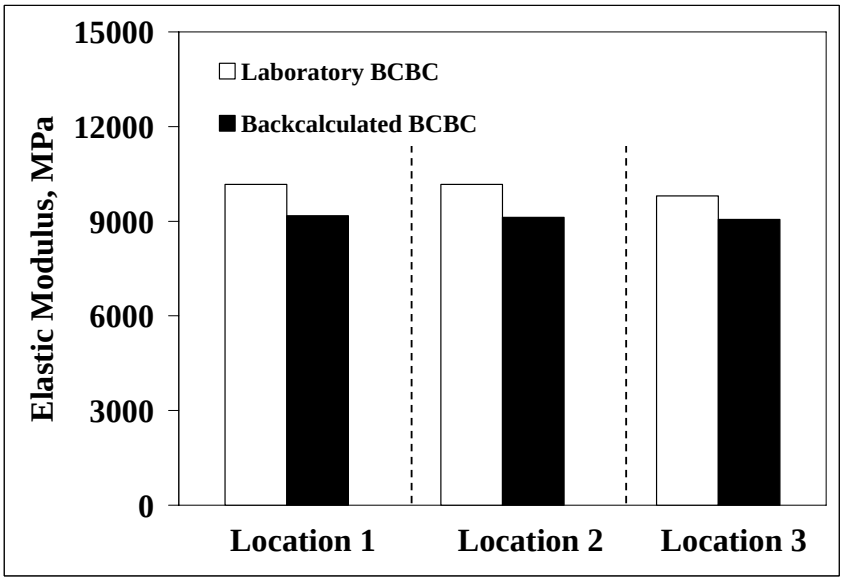

(b) BCBC layer

Figure 14. Comparison of layer elastic moduli.

Traffic Data

The Phase II traffic data were collected, processed, and analyzed for the period from January 2006 through May 2008. A full 12 months of data were analyzed for the years 2006 and 2007, whereas only five months of data were analyzed in 2008. Four sites were selected for analysis. The selected sites were Tioga (site 501), Mercer (site 502), Perry (site 505), and Blair (site 506). The other sites, Warren, Delaware, and Somerset, were not considered because of either pavement reconstruction or instrument maintenance problems at these locations.

The data collected at the selected sites were downloaded remotely every month from an FTP site posted by the PennDOT Bureau of Planning and Statistics. Once downloaded, the raw data files were pre-processed using PAT Reporter software to obtain readable ASCII files. The daily and monthly records of vehicle counts, classification, and weights were generated and analyzed. These summaries can be used to evaluate trends over time. A detailed report of SISSI phase-II traffic data is provided elsewhere. The following parameters were analyzed and presented in that report:

- Traffic volume
- Traffic variation over time
- Vehicle class distribution
- Axle load distribution factors

Environmental Data

Collection of environmental data continued during Phase II. The most successful data were on temperature and solar radiation. The largest variability in temperature was observed for the layers closer to the surface, obviously due to the effect of variations in solar radiation and the air temperature. For the most part, reliable frost and moisture data could not be collected during Phase II because of loss or malfunctioning of the gages. Details of temperature and solar data collection are provided in the volume 3 report of SISSI Phase II. Included in that report are also discussion and analysis of rate and depth of frost penetration and the freezing index for Pennsylvania conditions using environmental data collected during Phase I and the early part of Phase II.

Magnitude and Rate of Frost Penetration at SISSI Sites

There are several reasons that determination and control of depth of frost penetration is important for pavement design and construction. Knowledge of frost depth helps in determining proper depth for installation of drainage systems and underground facilities, such as sewer and pipelines. The magnitude of frost depth also affects the pavement potential for frost heave as well as pavement thawing, with the final effect on the period during which spring load limitations must be enforced.

Frost data from the Blair site were analyzed to determine the depth and rate of frost penetration. Data indicate that as the freezing period lasts longer, frost severity increases at various depths. Moreover, for the given temperature and site conditions, frost sensors closer to the pavement surface showed greater and sharper peak responses, implying faster rate of frost formation and penetration. Overall, at deeper pavement layers, more time is required to reach a specific freezing condition. It is observed that the upper portion of the subbase at the site studied experienced a higher rate of frost penetration compared to the lower portion. For the upper subbase, from about 330 to 400 mm in depth, the average freezing rate was 2 mm/hr, whereas for the lower section of the subbase, the rate was 13 mm/hr. Some time delay was observed between peak frost voltages measured at different depths. This was the basis for determination of the rate of frost penetration.

Frost Depth Evaluation Considering Freeze-Thaw Cycles at SISSI Sites

Freezing index has been the main factor for estimating pavement frost depth in cold regions. Many studies and researchers have investigated the relationship between freezing index and frost depth, such as those published by Hass and Bovid (1981), Chisholm and Phang (1983), McKeown et al. (1988), and Drumm and Meir (2003). Based on these studies, and using analytical models and principals of thermal conductivity, it has been shown that frost depth has a linear relationship with the square root of the freezing index. Empirical models developed from observed data of frost penetration in these studies also involve the square root of the freezing index as the main contributing factor.

In addition to the freezing index, characteristics of freeze-thaw cycles affect the depth of frost penetration. Sometimes, several low-intensity freeze-thaw cycles can result in the same freezing index numerically but with a less significant impact on frost depth. This is true for some areas of the Northeast region of the United States, where there are freezing cycles with relatively low temperature intensity that does not seem to significantly influence frost depth penetration. Summarized freezing index through winter season in these regions might be considerably different from the net freezing index that predominantly contributes to frost penetration. Recent work by Jackson and Puccinelli (2006) focused on evaluating the effect of freeze-thaw cycles on pavement performances for ‘moderate-frost’ climatic conditions.

In analytical frost models, freezing index is evaluated for a single freeze-thaw cycle. On the other hand, the empirical models are practically derived by adopting summarized freezing index from multiple freezing cycles through the whole period of the cold season. Thus, developing the proper relationship between the freeze-thaw cycles and the freezing index is an important step toward developing appropriate models to predict frost depth.

Using SISSI data, frost characteristics of the instrumented pavements were examined. The effects of a high-intensity freezing cycle and multiple low-intensity freezing cycles on the freezing index were evaluated. In the sites with summarized freezing indices of 250 to 450 °C-days, as the freeze-thaw cycle increased, the freezing index for a major cycle decreased, but the summarized freezing index from multiple cycles did not exhibit any relationship to freeze-thaw cycles. It was also observed that there is rarely a freeze-thaw cycle that is over 40 days in Pennsylvania. Most freeze-thaw cycles have periods less than 10 days. The study indicated that the freezing index difference due to number of freeze-thaw cycles is significantly large, and it is

in the range of 100 to 250 °C-days of a major cycle freezing index. Within this range, freezing index differences are mostly 200 to 300 °C-days, with the highest difference being around 445 °C-days. Thus, it was concluded that the summarized freezing index in the regions with this range of freezing index for a major cycle might be overestimated. Accordingly, frost depth that was too conservative could be obtained.

Based on the modified Berggren model with assumed thermal properties, for deeper frost penetration than about 0.8 meters, it was found that computed values are underestimated, whereas they are overestimated for frost depth less than about 0.8 meters. For actual frost penetrations less than 0.8 meters, it was observed that the freezing index for a major cycle is more in accordance with measured values than the freezing index for multiple cycles.

Freezing index within approximately 300 to 450 °C-days for multiple cycles seems not to have a significant relationship to measured frost depth. On the other hand, the freezing index for a major cycle has a relatively strong positive relationship to measured frost depth in the same range.

For a freezing index difference less than 150 °C-days, variation of computed frost depth, in most cases, does not exceed 0.20 meters. However, for a freezing index difference of approximately 200 °C-days, computed values vary from 0.15 to 0.25 meters.

MATERIAL CHARACTERIZATION

During Phase II of the SISSI project, indirect tensile tests (IDT) and repeated shear at constant height (RSCH) were conducted on laboratory-compacted specimens. Furthermore, the SISSI binders underwent bending test at a low temperature using Bending Beam Rheometer for validation of the equivalence principle used in the Superpave system. Details of material characterization are provided in two separate reports (Solaimanian et al., 2006 and 2008).

Creep Compliance D(t) and Tensile Strength of SISSI mixtures

Figure 15 presents the master curve of creep compliance [D(t)] for all SISSI mixtures at a reference temperature of -10°C. The difference in creep compliance between replicates for all SISSI sites was observed to be within 30 percent, which follows the values reported by Christensen and Bonaquist (2005). The average tensile strength data for all the SISSI sites is shown in Figure 16.

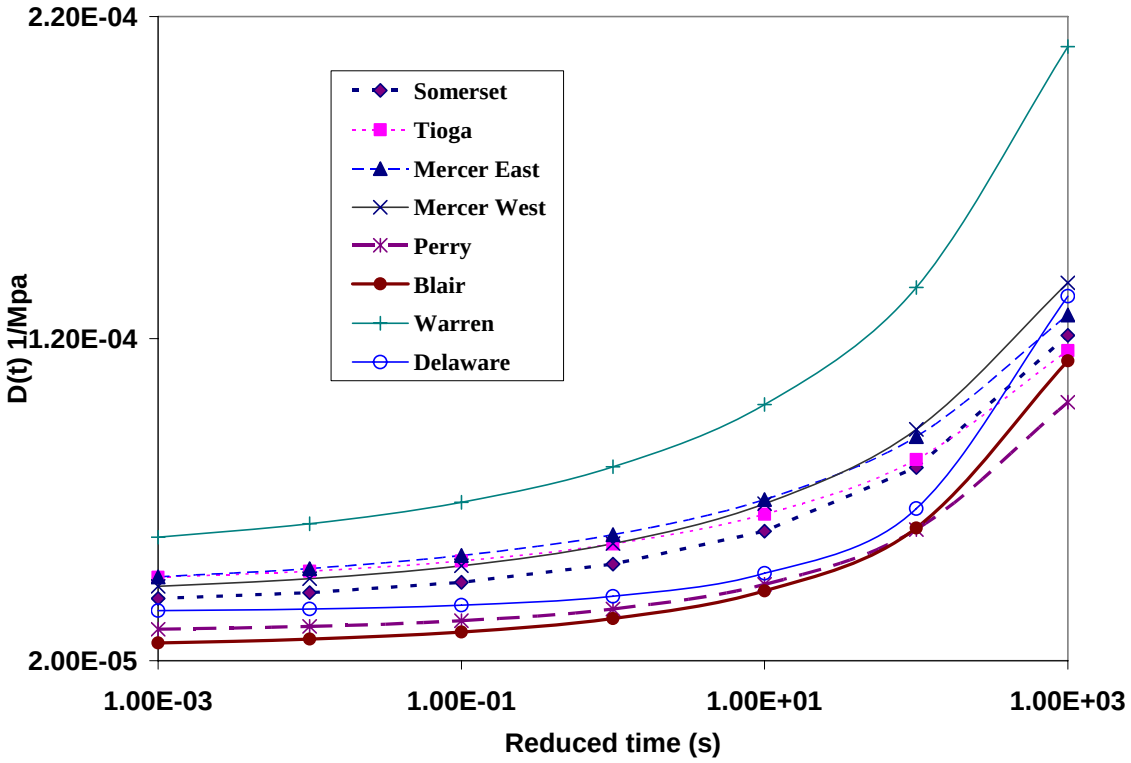

Figure 15. Compliance master curves for all SISSI sites at reference temperature of -10°C.

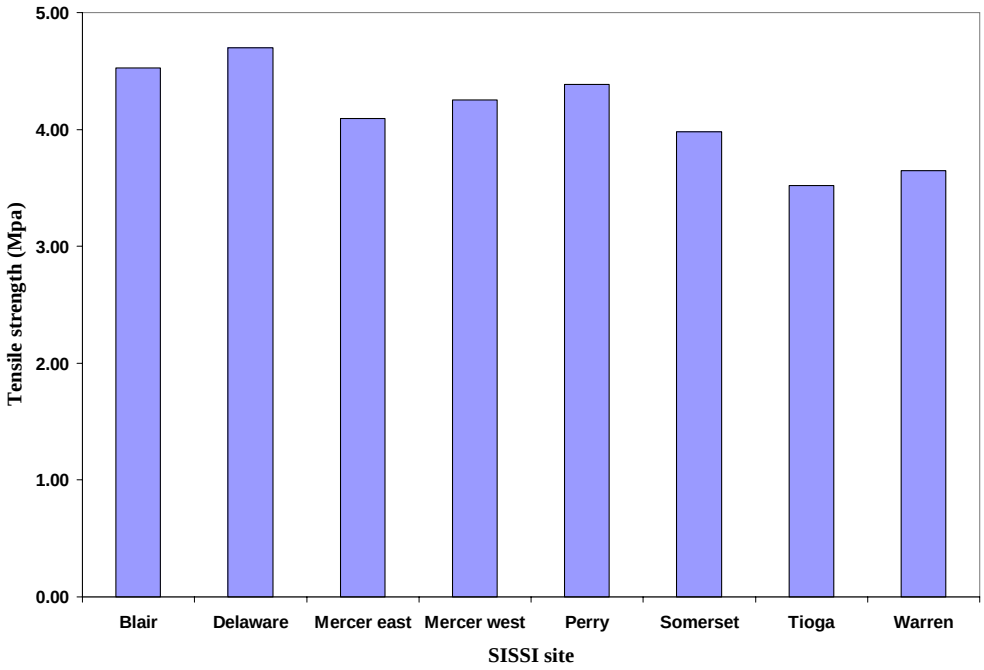

Figure 16. Average tensile strength values for all SISSI sites.

Poisson's Ratio

As for the IDT test, Poisson's ratio can be directly obtained from measured vertical and horizontal deformations, assuming AC specimens are isotropic. From linear viscoelasticity, Kim and Wen (2002) developed the following equation to calculate time-dependent Poisson's ratio, $\upsilon(t)$:

$$\upsilon(t) = -\frac{c * U(t) + d * V(t)}{e * U(t) + f * V(t)} \quad (1)$$

For the SISSI specimens, values of 3.358, 1.081, 1.000, and 3.122 were obtained for *c*, *d*, *e*, and *f*, respectively. Similar to the creep compliance, master curves of Poisson's ratio were generated using Equation 27 as shown in Figure 17. Since time-dependent $\upsilon(t)$ is needed to infer shear and bulk relaxation moduli, as discussed later in this paper, $\upsilon(t)$ values are reported to four significant digits (Lu et al. 1997).

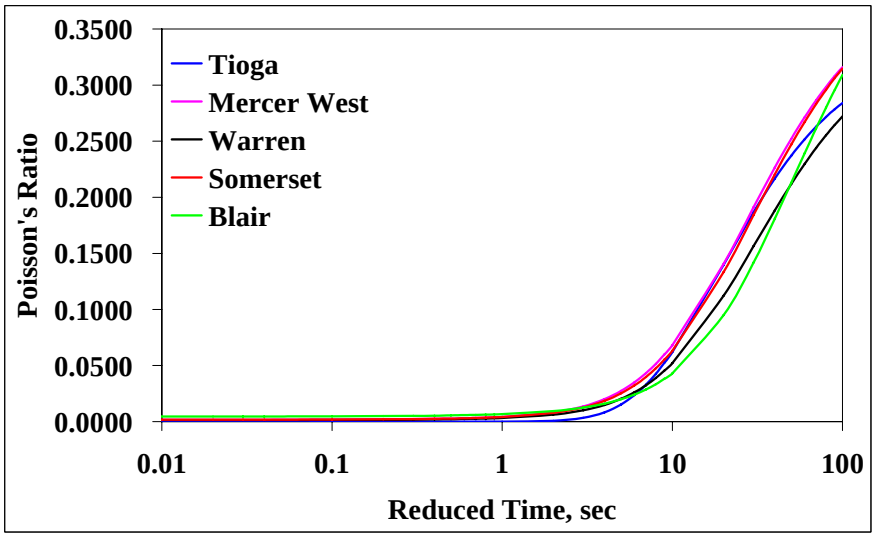

Figure 17. Poisson's ratio master curves at -10°C.

Fracture Analysis of Asphalt Concrete at Low Temperatures

Specific assumptions were made in conducting fracture analysis of the SISSI asphalt mixtures at low temperatures. The asphalt mix was assumed to be homogeneous, linear viscoelastic, and isotropic. Both experiment and numerical analysis were employed to study the fracture of AC mixtures at low temperatures. Viscoelastic material properties, obtained from the creep tests at -20°C, -10°C, and 0°C, were fed into a three-dimensional (3-D) finite element model. Simulated horizontal strains at the center of the specimen were then compared to an analytical solution. At the end, finite element analysis (FEA) was performed to simulate the fracture of SISSI mixtures during the strength test at -10°C. A far field solution by means of energy release rate (*J*-integral) was used to study the crack initiation. The *J*-integral allows an

approximate treatment without the need of a precise modeling of the nonlinear behavior at the crack tip (Schapery 1984, 1988). The crack opening displacement (COD) during the crack propagation was also investigated through ABAQUS FE simulations.

In ABAQUS, key material properties required for the viscoelastic model is the relaxation modulus [E(t)]. This modulus for SISSI mixtures was calculated from fitted D(t) and is presented in Figure 18.

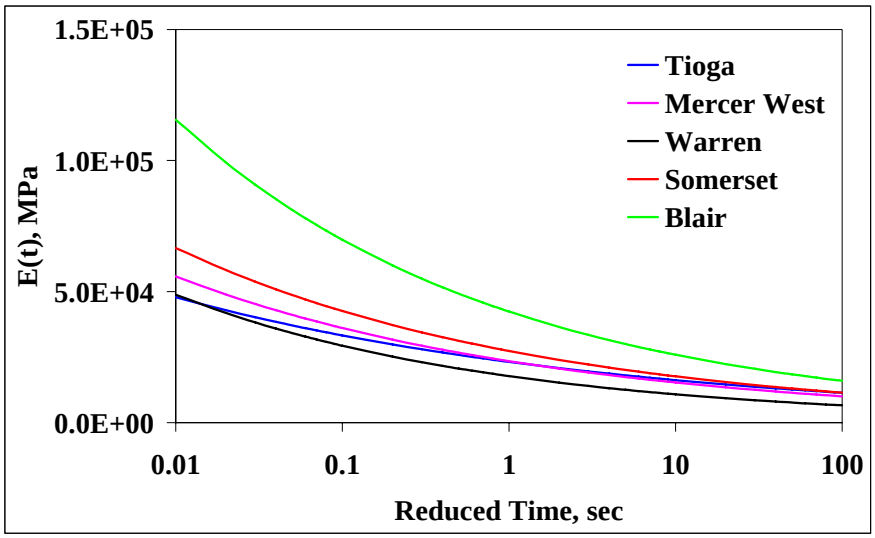

Figure 18. Relaxation modulus master curves at -10°C.

Model Validation

To evaluate the effectiveness of the developed FE model in simulating materials' responses, the center tensile strains of the specimen predicted from FE models were compared to the values calculated from the analytical solution derived by (Kim and Wen 2002):

$$\varepsilon(t) = U(t) * \frac{g + h * \upsilon(t)}{i + j * \upsilon(t)} \tag{2}$$

For the specimens and LVDTs used in this study, values of 12.4, 37.7, 0.291, and 0.908 were obtained for *g*, *h*, *i*, and *j*, respectively. Overall, the FE solution predicts comparable center tensile strains to the analytical solution. Two sets of center tensile strains are given in Figure 19.

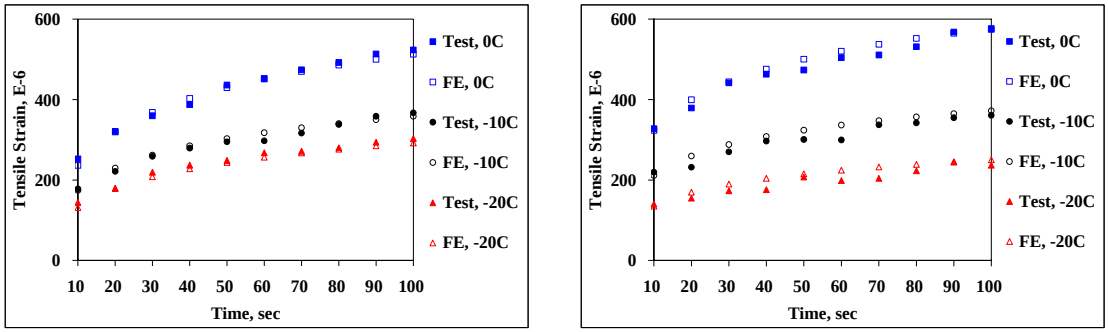

(a) Mercer West **(b) Blair**

Figure 19. Comparison of center tensile strains from analytical and FE solutions.

Finite Element Analysis

The finite element analysis (FEA) was carried out in two stages. The first stage simulated the creep test (Figure 20a). In the IDT test, a crack began and propagated toward the loading strips along the vertical direction due to the tensile stress. Therefore, the location of the crack initiation under the IDT mode was of interest. No crack growth was specified during this analysis stage. In the second stage, the crack was allowed to propagate from the location of crack initiation identified in the first stage while the top loading strip moved downward at a constant rate of 12.5 mm/min. The second stage simulated the tensile strength test. To simulate the crack propagation, a single crack was allowed to propagate from a single crack tip where two surfaces were initially partially bonded (Figure 20b). After debonding, the traction between two surfaces was initially carried as equal and opposite forces at the node on one surface and the corresponding point on the other. This force was then slowly and linearly reduced to zero after debonding started at a particular node on the bonded surface to improve convergence. This process continued at each element node along the direction of the crack propagation (Figure 20b). Finally, the crack stopped propagating at the edges of the specimen, which were in contact with the load strips.

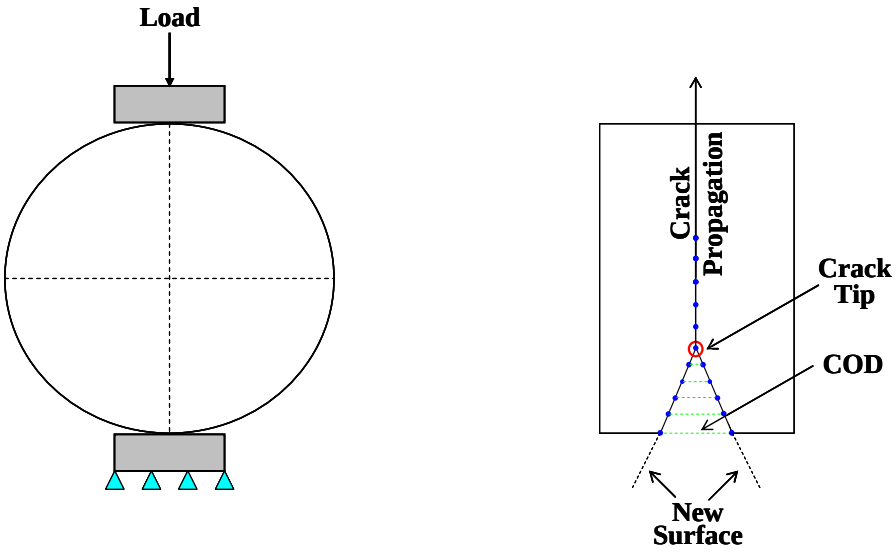

(a) Creep test **(b) Strength test**

Figure 20. Finite element simulation.

Stress Analysis

Knowing the location of the maximum tensile stress along the horizontal axis (Figure 21a) is vital for modeling the crack initiation. Figures 21b, 21c, and 21d show the distribution of tensile stresses at a 1.9-mm interval along the horizontal axis. Clearly, the maximum tensile stresses always occur at the edge of the specimen. This observation agrees with the finding from Roque and Buttlar (1992). The difference between the edge and the center becomes more significant at lower temperatures. It can be concluded that the crack initiates from the edge of the specimen during the IDT test. It is noted that the maximum tensile stress does not vary among mixtures, which means this tensile stress is independent of material properties.

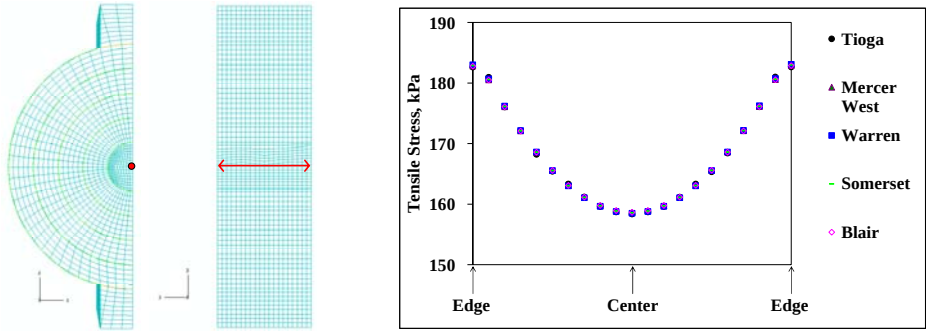

(a) Analysis location **(b) 0°C**

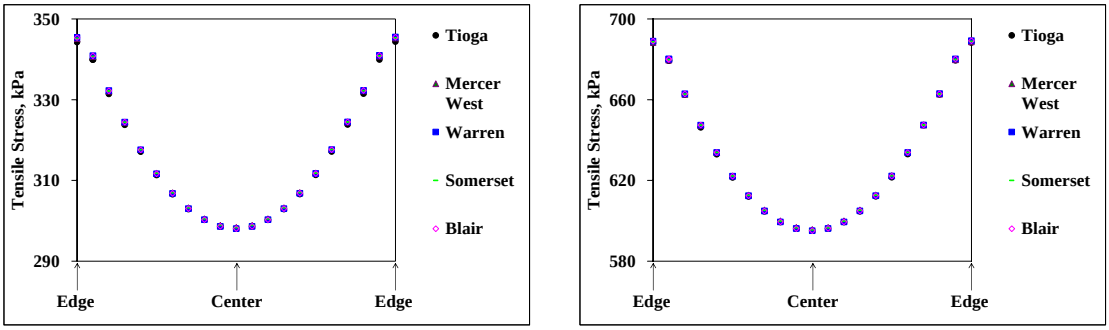

(c) -10°C **(d) -20°C**

Figure 21. Tensile stresses along the horizontal axis.

Crack Initiation

By placing the initial crack on the edge of the IDT specimen, the energy release rate (*J*-integral) during the strength test can be calculated. Before presenting analysis results, a new term, fracture life, is introduced here. Since SISSI mixtures failed at different times during the strength test, for comparison purposes, these times were first normalized to a unit time, called fracture life, and then evenly divided into 10 time regimes (e.g., 10, 20, and 30 percents).

The average quantities reported in this section exclude the first contour as shown Figure 22a. Results from two sets of simulations are presented in this section. The first set was conducted using linear viscoelastic material properties (Figure 22b), while the second one was conducted with linear elastic (LE) material properties (Figure 22c). The *J*-integral from both sets of simulations gradually increases during the fracture life. However, the magnitudes of the *J*-integral from the LVE and LE solutions are very different. Figure 22d presents the ratio of the *J*-integral from LVE over LE solution. The *J*-integral from the LVE solution was found to be always larger than that of the LE solution during the fracture life except for Tioga and Blair mixtures at shorter time regimes (i.e., 10 and 20 percents). This observation suggests that the use of linear elastic material properties would result in considerable deviations in the calculation of the *J*-integral. Therefore, if an elastic solution is available, satisfying appropriate traction and displacement boundary conditions, the application of the elastic material properties to a viscoelastic material cannot be used to approximate the solution for a quasi-static problem as in the strength test. Second, this ratio exhibits a much stronger dependence on the mixture during the first 50 percent of the fracture life (Figure 22d). After that, the ratio slowly converges to a value around 1.4 at the end of the fracture life. The J-integral ratio for the Mercer West and Warren mixtures decreases with time, while the ratio of the Tioga, Somerset, and Blair mixtures increases with time. It is expected that the Warren mixture has a superior cracking resistance to the others because of its higher value of the energy release rate.

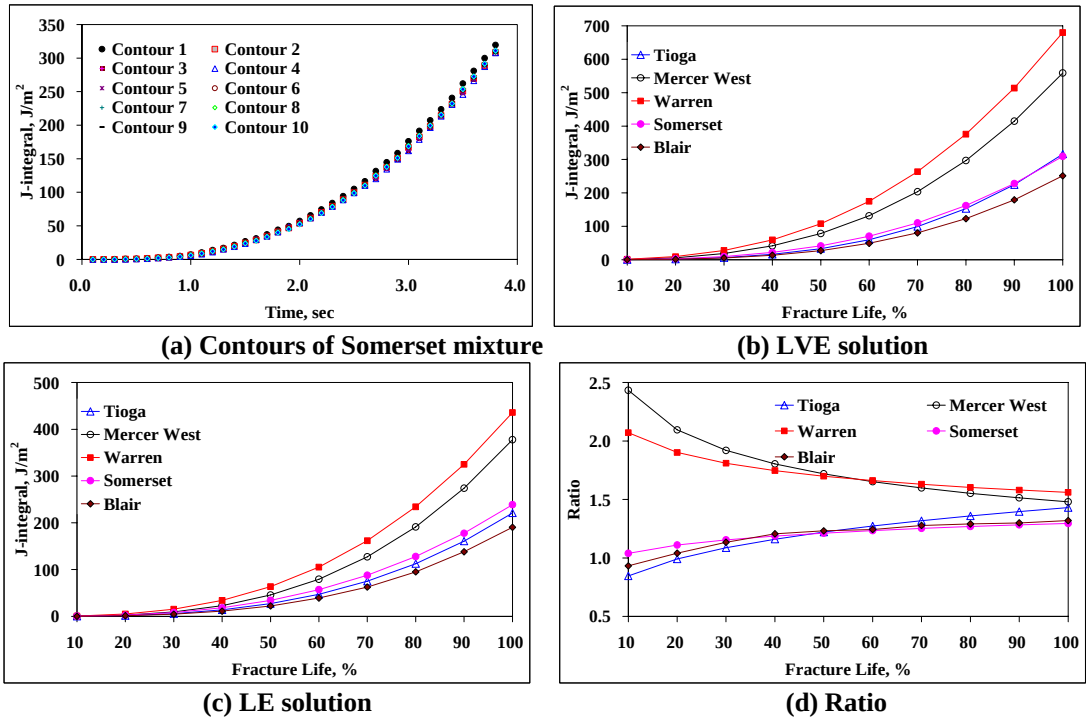

(a) Contours of Somerset mixture **(b) LVE solution**

(c) LE solution **(d) Ratio**

Figure 22. Energy release rate.

Crack Propagation

Figure 23 illustrates the final deformed shape and crack path from the experiment and FE simulations. Figure 23a shows that some portion of the propagated crack deviated from the center line of the specimen. This deviation was not observed in the FE-simulated crack propagation (Figures 23b through 23d) because in the developed FE model, AC was assumed to be homogeneous, and the existence of particles (i.e., aggregates) was not considered.

Accumulated crack opening displacement (COD) from FE simulations are given in Table 7. A graphic illustration is also provided in Figure 24a. The Warren mix has the smallest value of COD at failure, 2.10 mm. Together with the observation on the energy release rate from the preceding section, it can be concluded that the Warren mix exhibits the best low temperature performance among the five mixtures included in this study.

Monitoring crack propagation during the strength test requires sophisticated instrumentations, such as the COD gage; however, the measurement of COD at failure is rather simple. Through such measurement, it would become possible to correlate the energy release rate and COD. Once such correlation is established, the crack propagation at any time (time regime) can be predicted from the energy release rate. Of course, such a prediction is only valid for the material and testing conditions (e.g., load and temperature) used in the FE model development.

A nonlinear regression model in a Pure Power Law form was proposed to model the relationship between normalized crack opening displacement (*NCOD*) and normalized fracture energy (*NFE*):

$$NFE = a * (NCOD)^b + e \tag{3}$$

where a and b are nonlinear model coefficients, and e is random normal error with mean 0 and variance σ^2. Two constraints were applied to Equation 3:

- *NFE* = 0 when *NCOD* = 0
- *NFE* = 1 when *NCOD* = 1.

Through the nonlinear optimization, values of 0.9859 and 2.1719 were obtained for coefficients a and b, respectively. A R^2 value of 0.95 indicates the appropriateness of the selected model form for the AC mixtures and the strength test conditions (load and temperature) considered in this study as shown in Figure 24b.

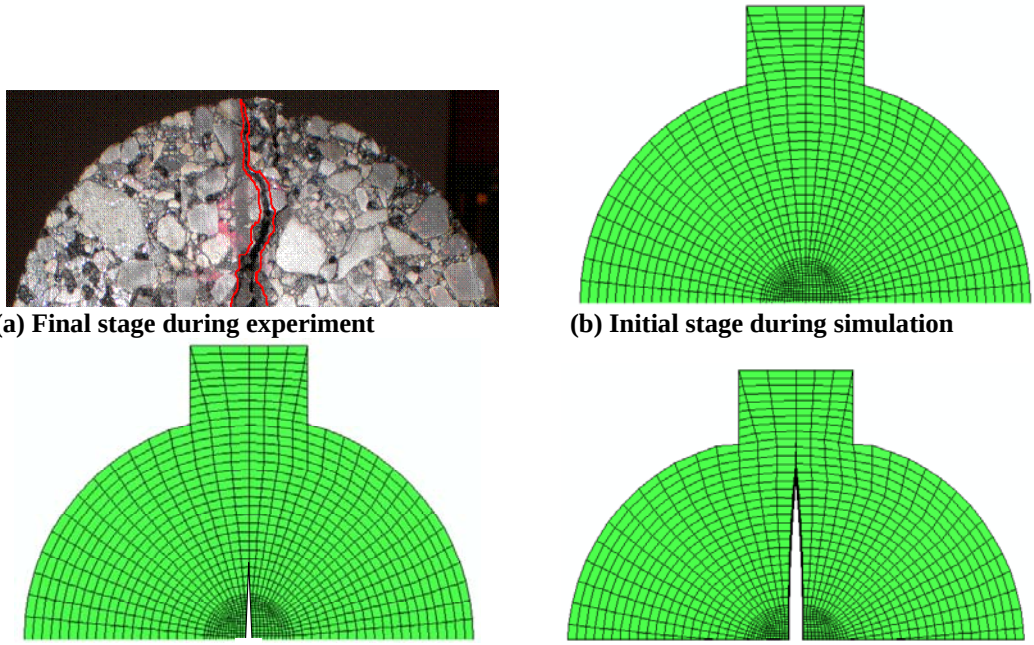

(a) Final stage during experiment **(b) Initial stage during simulation**

(c) Intermediate stage during simulation **(d) Final stage during simulation**

Figure 23. Crack propagation.

Table 7. Accumulated crack opening displacement, mm.

Fracture Life, %	Crack Opening Displacement, mm				
	Tioga	Mercer West	Warren	Somerset	Blair
10	0.07	0.10	0.08	0.12	0.13
20	0.22	0.33	0.24	0.33	0.46
30	0.41	0.71	0.46	0.56	1.17
40	0.70	0.97	0.66	0.95	1.80
50	1.11	1.30	0.86	1.33	2.42
60	1.45	1.65	1.06	1.76	3.02
70	1.82	2.01	1.34	2.22	3.74
80	2.21	2.43	1.56	2.59	4.65
90	2.76	2.79	1.88	3.07	5.41
100	3.17	3.12	2.10	3.56	6.11

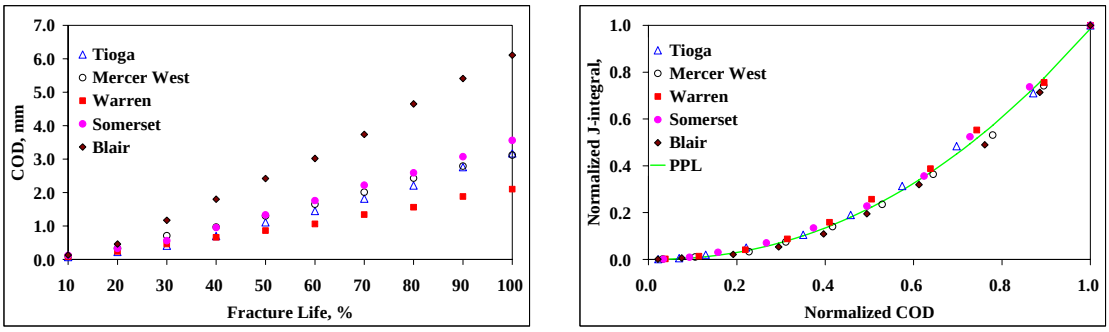

(a) COD (b) *NCOD* vs. *NFE*

Figure 24. Crack propagation analysis.

Flexural Creep Stiffness and M-Values of SISSI Binders

BBR tests were conducted on PAV-aged asphalt binders for seven of the eight SISSI sites to validate the criteria established in AASHTO Superpave binder specification M320. Tests were not conducted for the Tioga site, for which sufficient binder was not available. Two replicates from each site were tested for S(t) at 240-second and 2-hour durations. The average D(t) and m-values at 60-second loading and at the T_1+10ºC temperature are shown in Figures 25 and 26, respectively. Both the S(t) and m-value criteria are not satisfied for both Perry and Delaware. The results show that the modified asphalt binders, with the exception of Perry, have higher S(t) values compared to the unmodified asphalt binder.

For the SISSI asphalt binders tested, the equivalence principle is not satisfied, i.e., the stiffness at 60-second loading at a temperature of T_1+10ºC was different from the stiffness at 7,200-second loading at the temperature T_1. Figure 27 shows the percent difference between S(60) at T_1+10ºC and S(7200) at T_1. The difference ranges from 41 percent to 52 percent and appears to be consistent. It should be noted that the equivalence principle for all the SISSI asphalt binders is evaluated based only on data obtained from the 2-hour testing.

To satisfy the equivalence principle, it is necessary to adopt alternate testing times or temperatures for the SISSI asphalt binders as shown in Figures 28 and 29, respectively. Figure 28 represents the predicted test duration time for the SISSI binders at T_1+10ºC to satisfy the equivalence principle. As shown in the figure, this duration ranges from 240 seconds to 450 seconds.

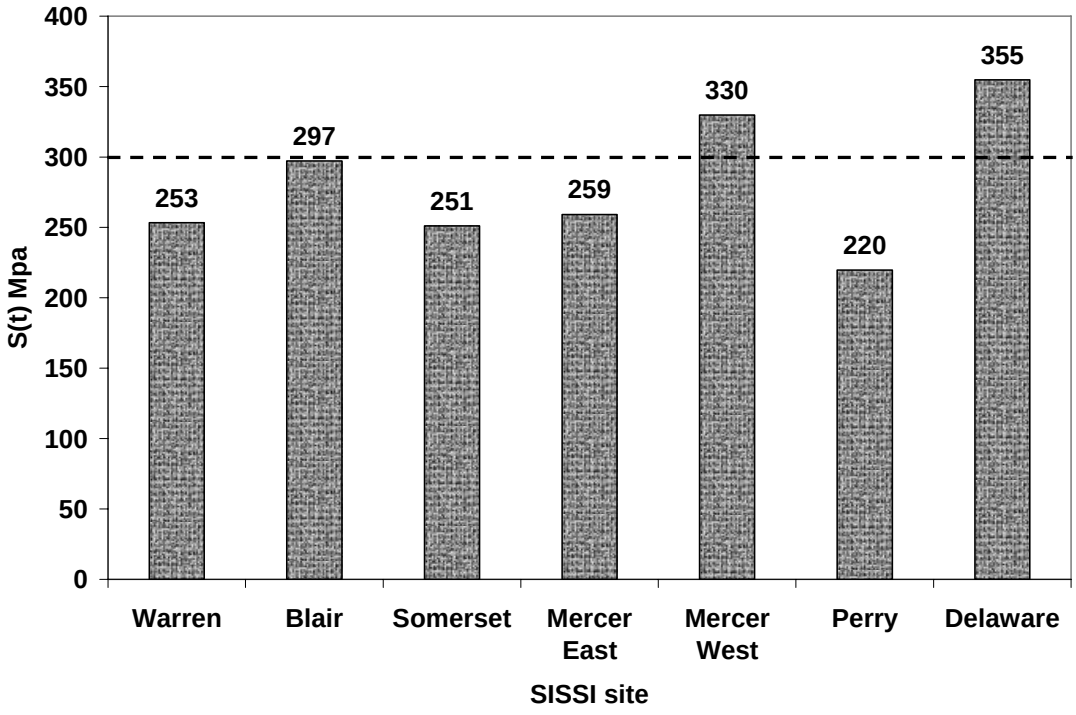

Figure 25. Comparison of average S(60) at T_1+10 for SISSI sites.

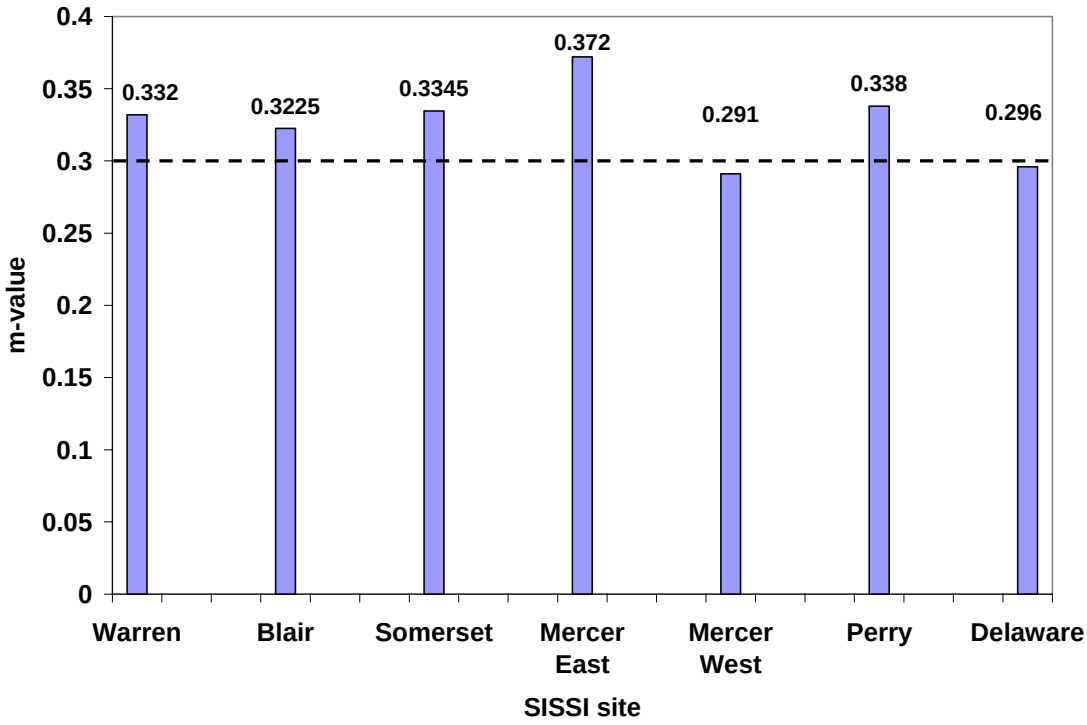

Figure 26. Comparison of m(60) at T_1+10 for SISSI sites.

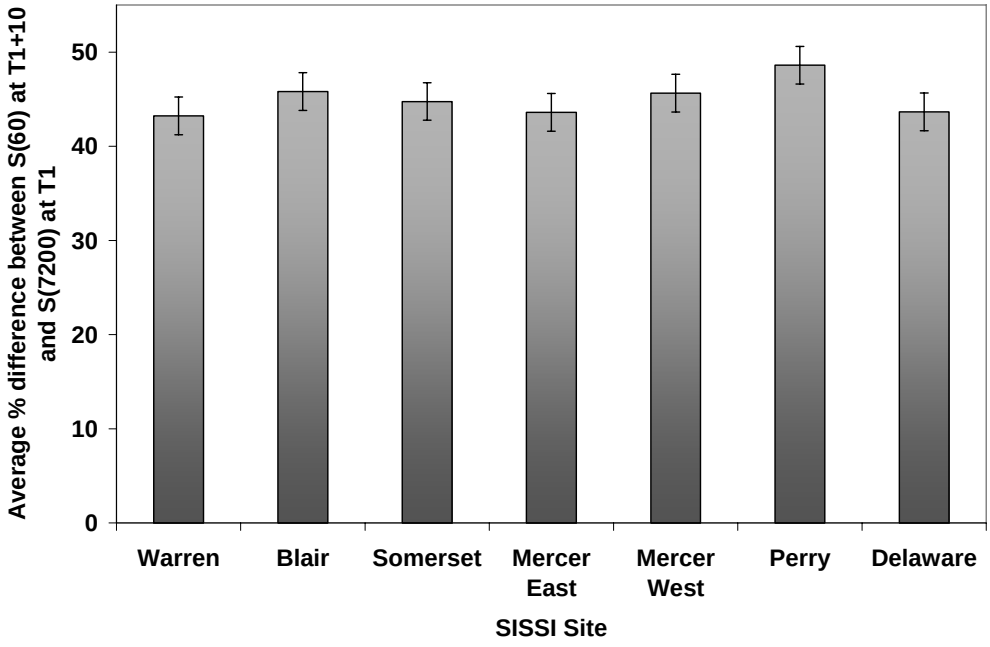

Figure 27. Average % differences between S(60) @ T_1 +10 and S(7200) @ T_2.

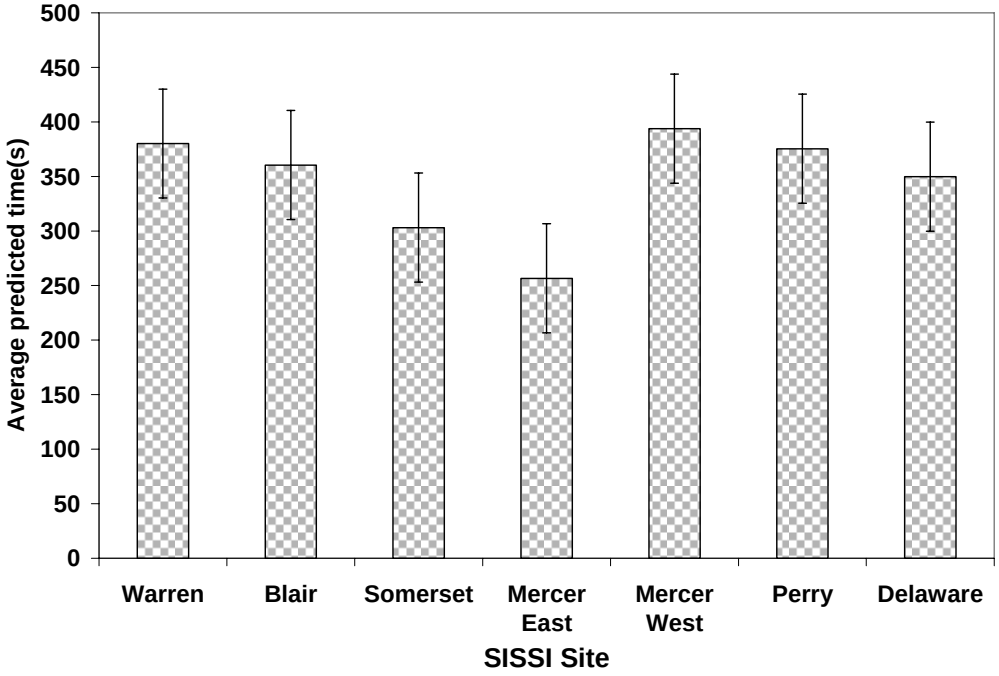

Figure 28. Average predicted time for S(60) @ T_1 +10 and S(7200) @ T_2 to be equivalent.

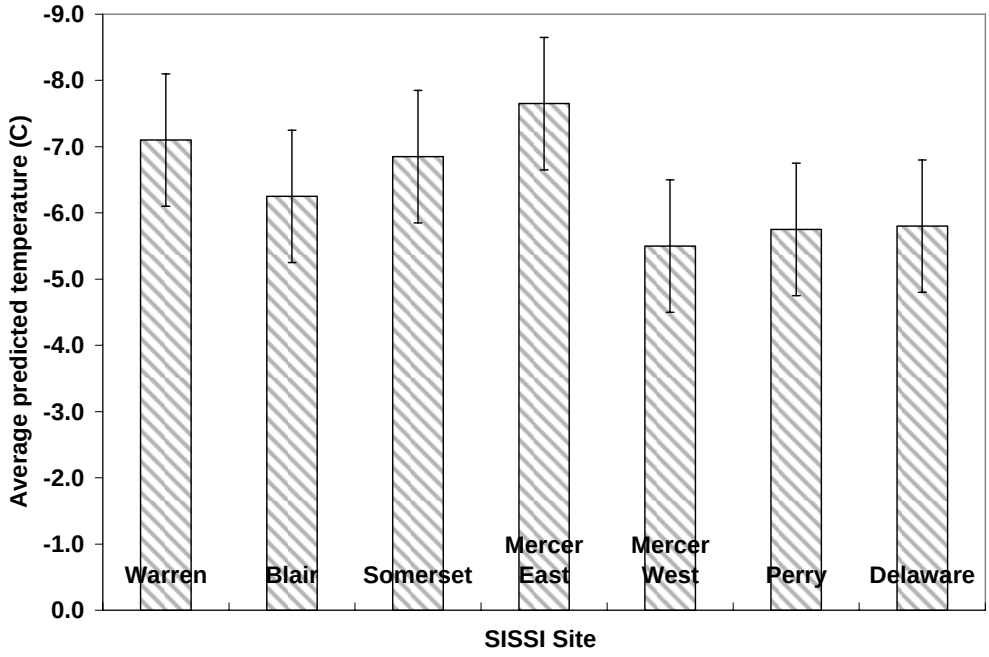

Figure 29. Predicted temperatures for S(60) @ T_1 +10 and S(7200) @ T_2 to be equivalent.

Relationship between Low Temperature Properties of SISSI Mixtures and Binders

Because thermal cracking is dependent on both the properties of the asphalt mixtures and binders, it is important to correlate their D(t) and/or S(t) and m-values. Figures 30 and 31 show the comparison of D(t) and/or S(t) and m-values, respectively, for the all SISSI sites, with the exception of Tioga. No definite correlation exists between the D(t) and S(t) data; however, Blair, Mercer West, Somerset, Tioga, and Warren tend to follow a linear pattern.

The m-values of the mixture are in the range of 0.2 to 0.49 compared to binder m-values with a range of 0.29 to 0.27. With the exception of Delaware, Blair, and Perry, the mixture m-values are lower than that of the asphalt binder. This is expected owing to the elastic nature of the aggregates, with an m-value of zero and a primary component of asphalt concrete mixtures. However, to better correlate the relationships between asphalt mixtures and binders, a detailed analysis incorporating other mixture properties such as air void content, gradation, and others must be performed, but that is beyond the scope of this study.

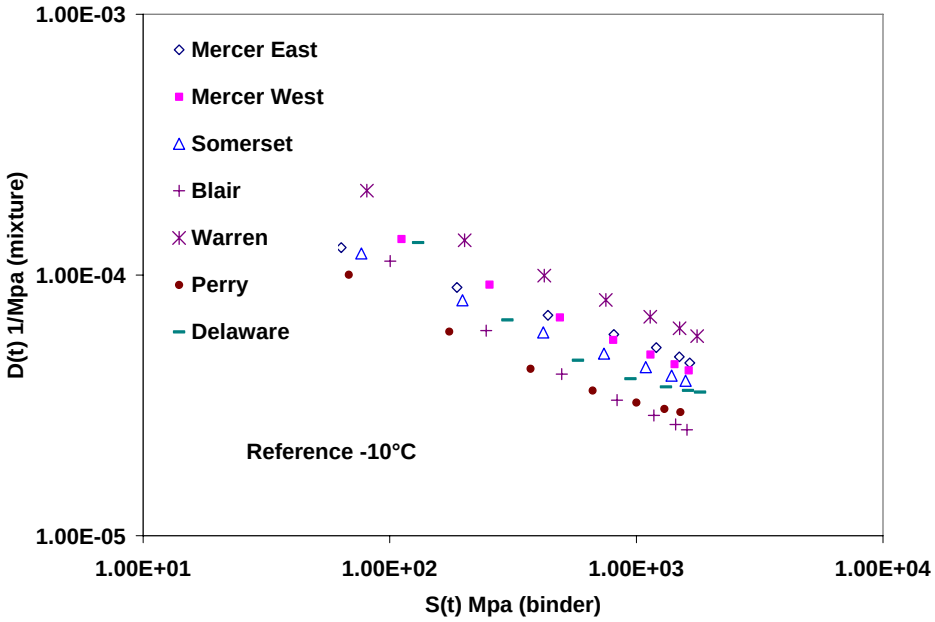

Figure 30. Comparison of average creep compliance/stiffness data for SISSI mixtures and binders.

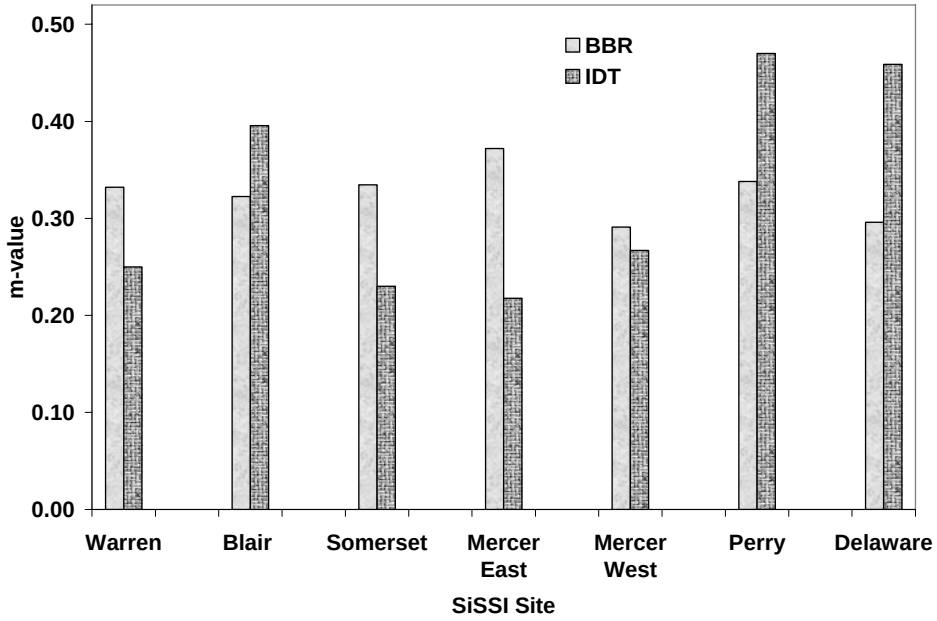

Figure 31. Comparison of average m-value for SISSI mixtures and binders.

Ranking of SISSI Sites Based on IDT and BBR Material Properties

All the SISSI sites, with exception of Tioga, are ranked for susceptibility of thermal cracking based on the IDT and BBR test results as shown in Table 8. The ranking of all SISSI sites based on mixture data is shown in Table 9. The sites are ranked from 1 to 8 based on their susceptibility to thermal cracking, i.e., 1 is least susceptible and 8 is the most susceptible. The ranking is based on the following observations and assumptions.

- S (t) (binder stiffness): It is assumed that the lower the binder stiffness, the less susceptible the mixture is to thermal cracking.
- Binder m-value: m-value of the binder represents the rate of stress relaxation and, hence, the ability to absorb more stresses developed in the pavement structure. Thus, binders with higher m-values are assumed to have the least susceptibility to thermal cracking.
- Mixture m-value: The same concept as that of the m-value for asphalt binders is adopted for ranking the SISSI sites.
- Tensile strength: Generally, if the strength of the mixture is high, it is less susceptible to thermal cracking. In this study, the sites were ranked based on tensile strength, i.e., high tensile strength leads to lower susceptibility to thermal cracking. The tensile strength and thermal stresses obtained from a typical BBR and DSR test is shown in Figure 32.

- D(t) [Creep compliance of the mixture]: The higher the creep compliance, the lower the complex modulus of the mixture, so sites with higher creep compliance are assumed to have lower susceptibility to thermal cracking.

The S(t) and m-values of asphalt binder are calculated at -12°C and time of 60 seconds. From Figure 38, it is observed that the m-value of the creep compliance curve varies with respect to time. It should be noted that the m-value of the asphalt mixture is calculated as the maximum slope of the D(t) master curve. The D(t) data at 60 seconds at -10°C and the strength data calculated at -10°C are considered for ranking the SISSI sites. The ranking of the sites with respect to D(t) of the mixture might vary if times greater than 100 seconds are considered because of overlapping of the curves, but for the sake of comparison, values at D(t) at 60 seconds are taken into account. The creep compliance master curve at -12°C will shift only along the time axis with the same creep compliance values, so the ranking of the sites at -10°C and -12°C will be the same at 60 seconds. The ranking of the sites varies with material property, so an overall ranking could not be derived.

From Table 8, with exception of tensile strength and m-value of the mixture, Delaware is most prone to thermal cracking of the SISSI sites. Cracking at this site is also evident from the field observations as shown in Figure 33 even though a definite conclusion cannot be drawn that observed cracking is purely the result of thermal stresses. Correlating the laboratory test data with field observations could provide an insight on the susceptibility to thermal cracking. Our study indicated that no single low temperature material property could be used for ranking the mixture for thermal cracking susceptibility. This finding is evident from the difference in rankings of the SISSI sites. Thus, developing a system by assigning weights for the low temperature material properties will be useful to achieve an overall ranking for the SISSI sites.

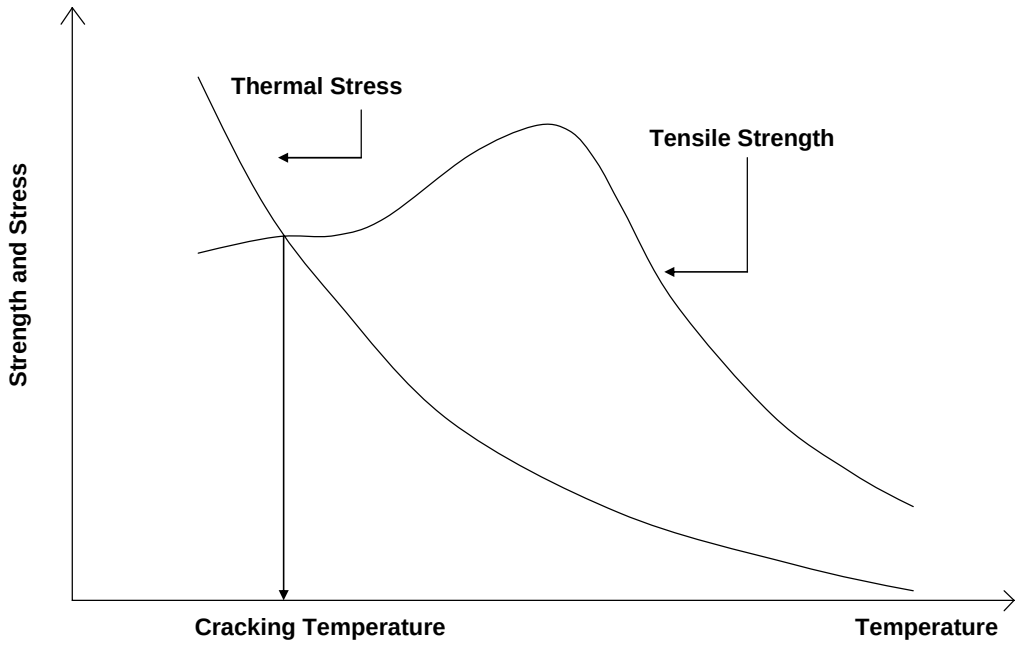

Figure 32. Tensile strength and thermal stress obtained from BBR and DSR testing.

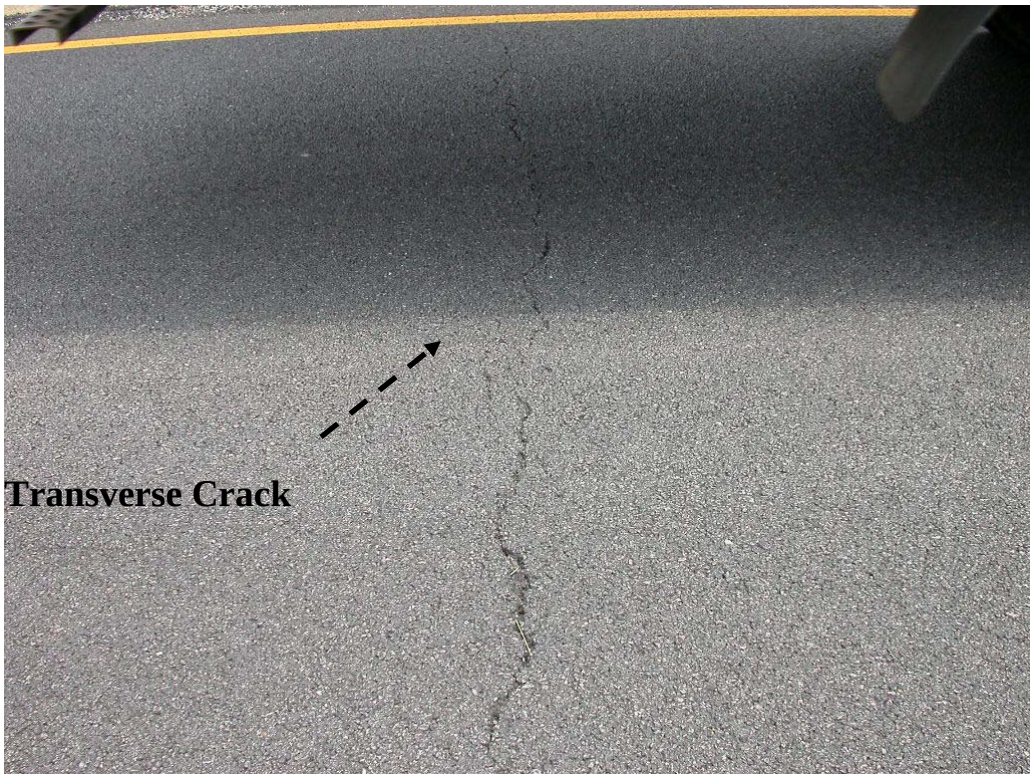

Figure 33. Transverse cracking in Delaware section (Stoffels and Solaimanian, 2006).

Table 8. Ranking of SISSI sites based on IDT and BBR test results.

SISSI site		Ranking based on				
		S(t)	Binder m-value	Mixture m-value	Tensile strength	D(t)
Blair		5	5	3	2	7
Delaware		7	6	2	1	5
Mercer East		4	1	7	5	2
Mercer West		6	7	4	4	3
Somerset		2	3	6	6	4
Perry		1	2	1	3	6
Warren		3	4	5	7	1

Table 9. Ranking of all SISSI sites based on IDT test results.

SISSI site		Ranking based on	
		Tensile strength	D(t)
Blair		2	8
Delaware		1	6
Mercer East		5	2
Mercer West		4	4
Somerset		6	5
Perry		3	7
Warren		7	1
Tioga		8	3

Shear Test Results and Analysis

Figures 34 and 35 represents the average shear deformation for wearing and binder layers of the SISSI sites. Results of repeated shear testing at maximum pavement temperature indicates performance of SISSI mixtures in the range of good to excellent because no excessive permanent deformation was observed from these laboratory tests. For the wearing layer, the permanent shear strain ranged between 0.3 and 1.7 percent, indicating an excellent-to-good rutting resistance. For the binder layer, the range was between 0.4 and 1.7 percent, indicating good rutting resistance. The exception was the binder layer of the Perry site, for which a permanent strain of 2.4 percent was obtained, indicating fair rutting resistance even though no excessive rutting was observed in the field for this site. Overall, the field-measured rutting, after 5 to 8 years of service, ranged between 2.5 and 8.5 millimeters, indicating excellent rut resistance of SISSI mixtures at all sites. This is, in general, consistent with laboratory-measured shear strains as discussed above.

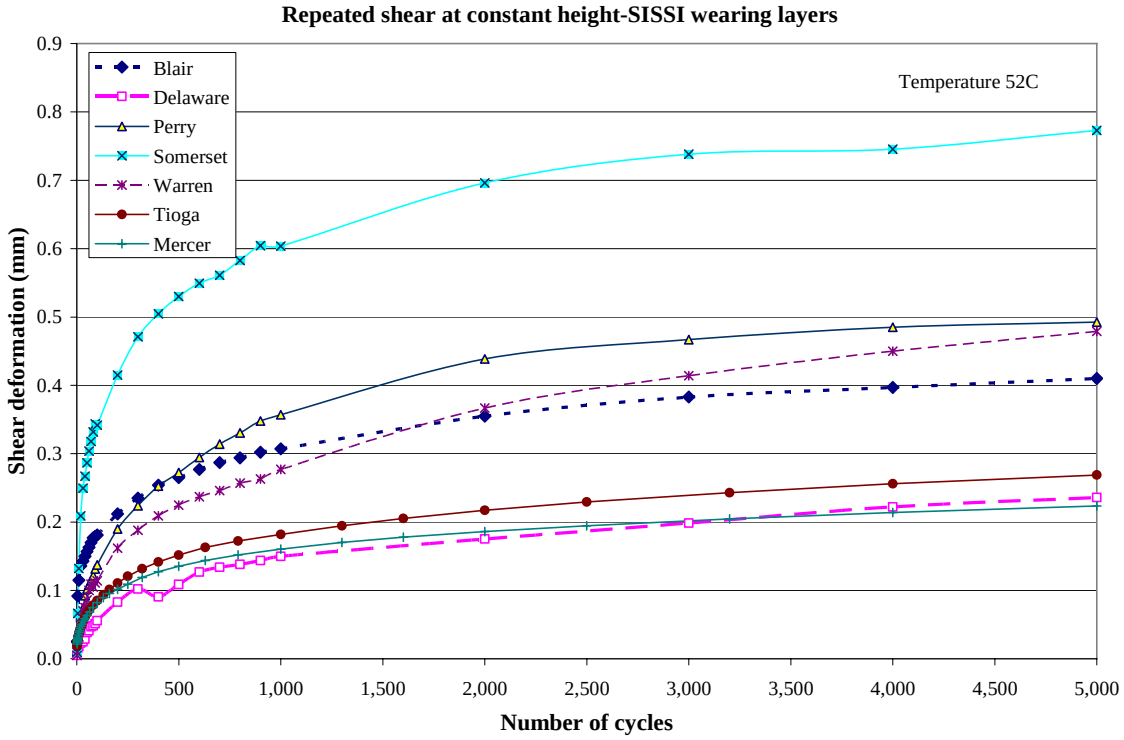

Figure 34. Shear deformation from RSCH Test for wearing layers of SISSI sites at 52°C.

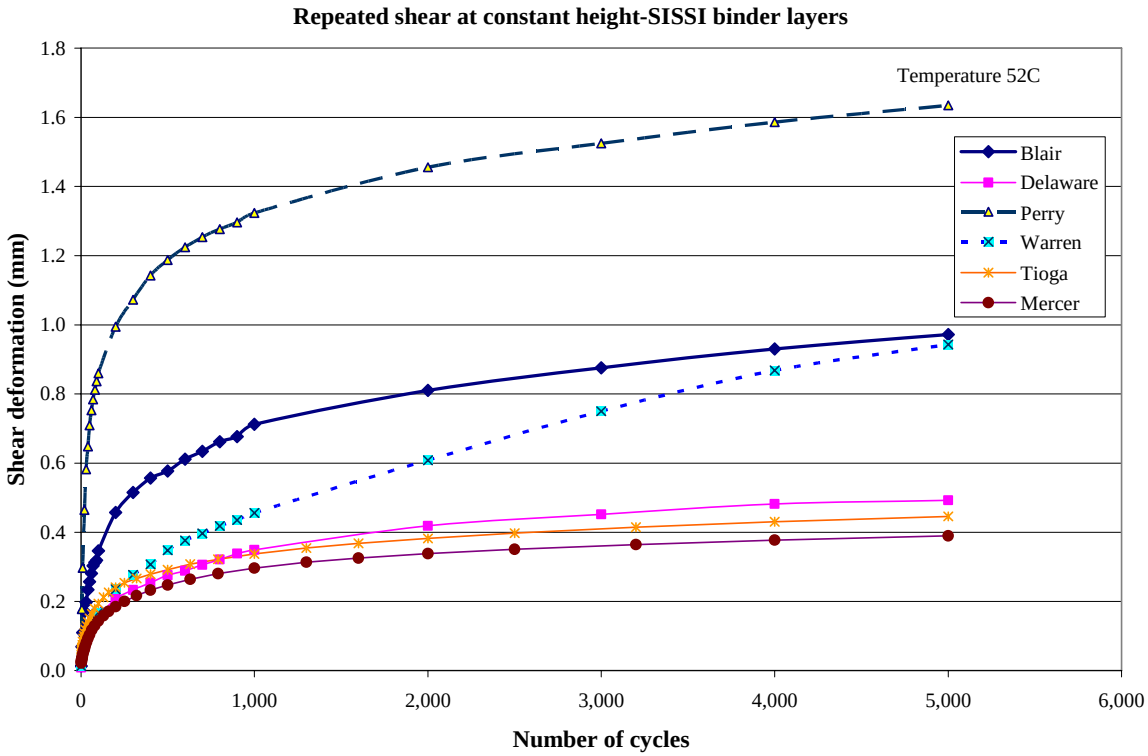

Figure 35. Shear deformation from RSCH Test for binder layers of SISSI sites at 52°C.

IMPLEMENTATION OF SISSI DATA WITH MEPDG

Overview of MEPDG

The MEPDG provides a state-of-the-practice tool for the design of new and rehabilitated pavement structures based on mechanistic-empirical principles. At present, the only comprehensive documentation for the MEPDG available to the general public is the Web-based version provided by the Transportation Research Board at http://www.trb.org/mepdg/. Version 1.0 of the MEPDG software is also available for downloading from this site. In this section, a brief review on some key considerations and features in the MEPDG, focusing on flexible pavements, is provided.

General Considerations

The MEPDG considers truck traffic loadings in terms of the full axle load spectra: single, tandem, tridem, and quad axles. The equivalent single axle load (ESAL) concept is no longer used as a direct design input. The MEPDG considers the number of heavy trucks as an overall indicator of the magnitude of truck traffic loadings (FHWA class 4 and above).

With available climate data from weather stations, the MEPDG uses the EICM to predict temperature and moisture within each pavement layer and the subgrade. The temperature and moisture predictions from the EICM are used to estimate material properties for the foundation and pavement layers on a semi-monthly or monthly basis throughout the design life. The frost depth is determined, and the proper moduli are estimated above and below this depth.

For the pavement structure, the surface AC layer is divided into sublayers to account for temperature and aging gradients. Asphalt aging is modeled only for the top sublayer. The largest change in stiffness due to aging occurs only in the top one half inch, and the aging gradient for layers other than the top layer is not significant. Irrespective of the thickness of the top AC layer, it is always divided in two sublayers (12.7 mm and the remaining thickness).

Hierarchical Input Level

One unique feature of the MEPDG is that pavement designers have a great deal of flexibility in obtaining the design input for a design project based on the critical nature of the project and the available resources through the Hierarchical Input Level (HIL). The HIL can be applied to various aspects: traffic, materials, and environmental input. In general, there are three HILs.

Level 1 input results in the highest level of accuracy and, thus, would have the lowest level of uncertainty or error. Input at this level would typically be used for designing heavily trafficked pavement or wherever there were safety concerns or serious economic consequences of early failure. Level 1 material input requires laboratory or field testing, such as the DSR

testing of asphalt binder, the complex modulus testing of AC, and site-specific axle load spectra. Consequently, obtaining Level 1 input requires more resources and time.

Level 2 input results in an intermediate level of accuracy. This level could be used when resources and testing equipment are not available for tests required for Level 1. Level 2 input typically would be user selected, possibly from an agency database, could be derived from a limited testing program, or could be estimated through correlations. Examples would be estimating the dynamic modulus of AC mixtures from binder, aggregate, and mixture properties or using site-specific traffic volume and traffic classification data in conjunction with agency-specific axle load spectra.

Level 3 input results in the lowest level of accuracy. This level might be used for design where there are minimal consequences of early failure (e.g., lower volume roads). Input typically would be user selected values or typical averages for the region. Examples include default unbound materials resilient modulus values or default AC mixture properties estimated from aggregate gradation and binder grade.

For the SISSI sites, all input was obtained using a mix of three HILs although comprehensive data had been collected for the SISSI project. Available HILs for the SISSI data are given in Table 10.

Performance Models

Details on MEPDG performance prediction models are provided in SISSI Phase II volume 4 report. A brief explanation of the models is provided here for clarification when discussing the predicted results.

Fatigue Cracking

The MEPDG approach first calculates the fatigue damage at critical locations that may be either at the surface and result in longitudinal (top-down) cracking or at the bottom of the AC layer and result in alligator (bottom-up) cracking. The fatigue damage is then correlated using a calibration factor to the fatigue cracking. Estimation of fatigue damage is based on Miner's Law, which states that damage is given by the following relationship:

$$D = \sum_{i=1}^{T} \frac{n_i}{N_i} \tag{5}$$

where D is damage, T is the total number of analysis periods, n_i is actual traffic for analysis period i, and N_i is traffic allowed under conditions prevailing in i. The relationship used for the prediction of the number of repetitions to fatigue cracking is expressed as:

$$N_f = 0.00432 * k'_1 * (10^{[V_b/(V_a+V_b)-0.69]}) * (\frac{1}{\varepsilon_t})^{3.9492} * (\frac{1}{E})^{1.281} \tag{6}$$

where V_b is the effective binder content, V_a is the air voids, and k_1 is introduced to provide a correction for different asphalt layer thickness (h_{AC}) effects.

Table 10. Available hierarchical input levels of SISSI data.

Category	Input	Availability	Hierarchical Input Level
Traffic	Initial AADTT	Y	1
	Monthly Adjustment Factor	Y	1
	Vehicle Class Distribution	Y	1
	Hourly Truck Distribution	Y	1
	Traffic Growth Factor	Y	1
	Axle Load Distribution Factor	Y	1
	Lateral Traffic Wander	N	3
	Number of Axles for Each Vehicle Class	Y	1
	Axle Configuration	N	3
	Axle Spacing	Y	1
	Wheelbase	N	3
Climate	Weather Data	Y	1
	Ground Water Table Depth	N	3
Structure	Layer Thickness	Y	1
Material	AC Mixture	Y	1
	Binder	Y	1
	AC General	Y	1*
	PCC	N	3
	Granular	N	3
Thermal Cracking	Creep Compliance	Y	1
	Tensile Strength	Y	1
	Coefficient of Thermal Contraction	N	3

* Except for Poisson's ratio, unit weight, and thermal properties

Rutting

In the MEPDG, for each sublayer of asphalt concrete, rutting is calculated as

$$RD_{AC} = \sum_{i=1}^{n} [(\varepsilon_r * k_1 * 10^{-3.4488} T^{1.5606} N^{0.479244})_i * h_{ACi}] \quad (7)$$

where RD_{AC} is rut depth in the AC layer, n is number of sublayers, ε_r is vertical resilient strain at the middle of the sublayer i for a given load, k_1 is depth correction factor, T is temperature, N is number of repetitions for a given load, and h_{ACi} is the thickness of sublayer i.

$$k1 = C * 0.328196^{D} \tag{8}$$

where D is depth to the point of strain calculation, and C is calculated as:

$$C = (-0.1039 * h^{2}{}_{AC} + 2.4868 * h_{AC} - 17.342) + (0.0172 * h^{2}{}_{AC} - 1.7331 * h_{AC} + 27.428) * D \tag{9}$$

The MEPDG also divides all unbound granular materials into sublayers, and the total rutting for each layer is the summation of the rut depth of all sublayers.

Thermal Cracking

The thermal cracking model (TCMODEL) incorporated in the MEPDG converts data directly from the Superpave Indirect Tensile Test (IDT) into viscoelastic properties, specifically the creep compliance function that is further converted to the relaxation modulus through Laplace Transformation. The relaxation modulus is then coupled with the temperature data from the Enhanced Integrated Climatic Model (EICM) to predict thermal stresses through the convolution integral, assuming AC to be LVE and thermorheologically simple:

$$\sigma(\xi) = \int_{0}^{\xi} E(\xi - \xi') \frac{d\varepsilon}{d\xi'} d\xi' \tag{10}$$

where $\sigma(\xi)$ = stress at reduced time, ξ; ξ' = integration variable; $E(\xi - \xi')$ = relaxation modulus at reduced time, $\xi - \xi'$; ε = strain at reduced time; $\xi = \alpha(T(\xi') - T_0)$; α = linear coefficient of thermal contraction of AC mixtures; $T(\xi')$ = pavement temperature at reduced time, ξ'; and T_0 = initial pavement temperature.

Smoothness

The models for predicting International Roughness Index (IRI) of flexible pavements with a granular base are a function of the base type as described below:

$$IRI = IRI_0 + 0.0463 * [SF * (e^{\frac{age}{20}} - 1)] + 0.00119 * TC_{LT} + 0.1834 * COV_{RD} + 0.00384 * FC_T \tag{11}$$

where IRI is IRI at any given time, m/km, IRI_0 is initial IRI, m/km, SF is the site factor, $e^{\frac{age}{20}} - 1$ is age term (where age is expressed in years), COV_{RD} is the coefficient of variation of the rut depths, percent, TC_{LT} is the total length of transverse cracks at all severity levels, m, and FC_T is fatigue cracking (alligator plus longitudinal) in the wheel path, percent of total lane area.

Evaluating Sensitivity of MEPDG Predictions Using SISSI Data

The objective of the sensitivity study was to evaluate the input parameters related to AC material properties, traffic, and climate that significantly or insignificantly influenced the

predicted performance for two specific SISSI flexible pavements: Warren and Blair. To achieve this objective, the sensitivity analysis of five MEPDG performance measures (longitudinal cracking, alligator cracking, AC rutting, subgrade rutting, and smoothness) was conducted by either varying the magnitudes or the distribution of a single input parameter. Although reflection cracking is arguably the most important distress in rehabilitated flexible and composite pavements, it is not included in the present study because the reflection cracking model in the current MEPDG is intended only as a very rough placeholder until a more accurate, reliable reflection cracking model can be developed; this work is currently under way in NCHRP Project 1-41.

Analysis Results

Longitudinal Cracking

As demonstrated in Figure 36, the MEPDG predictions for longitudinal cracking were found to be very sensitive to the effective binder content of upper AC layers. This observation is reasonable because the effective binder content is an important source of variability in construction and among the most influential parameters determining the mixture stiffness and, hence, performance measures. Longitudinal cracks may be also caused by high tensile strains at the top of the surface AC layer due to load-related effects and the effects of age-hardening of AC materials. However, the binder layer thickness for both Warren and Blair exhibited some sensitivity on longitudinal cracking predictions. Part of this observation could be due to the immature nature of the MEPDG model; an enhanced top-down cracking model is the expected product from NCHRP Project 1-42A, which is currently under way.

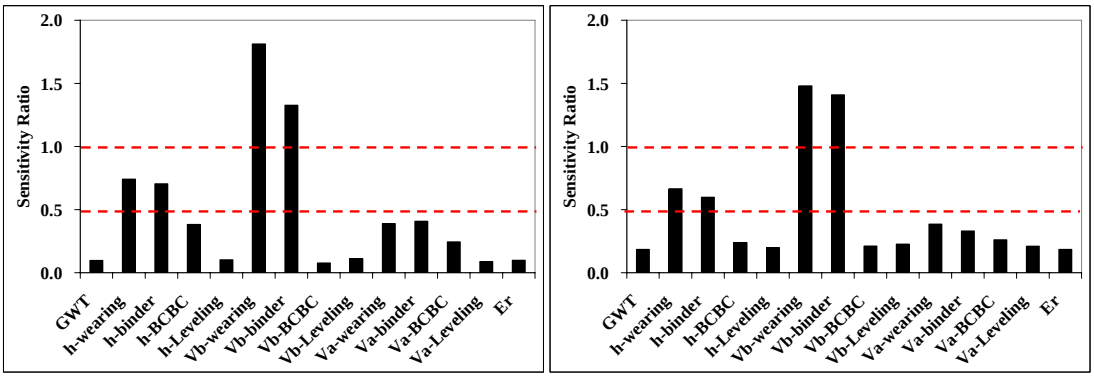

(a) Warren (b) Blair

Figure 36. Sensitivity of longitudinal cracking to analysis parameters.

Alligator Cracking

It can be concluded from Figure 37 that the MEPDG predictions for alligator cracking are very sensitive to the layer thickness and effective binder content, particularly for upper AC layers. The total AC layer thickness not only influences strain and stress magnitude but is directly linked to the location where fatigue cracks initiate, as well as under the specific mode of loading (constant stress or strain) under which fracture occurs. Increasing the AC thickness reduces the tensile strains at the bottom of the AC layer and consequently mitigates alligator (bottom-up) cracking. This feature is evident for both the Warren and Blair sites. Effective binder content also has a pronounced impact on top-down cracking. Mixtures rich in binder generally have better tensile strength and better cracking resistance.

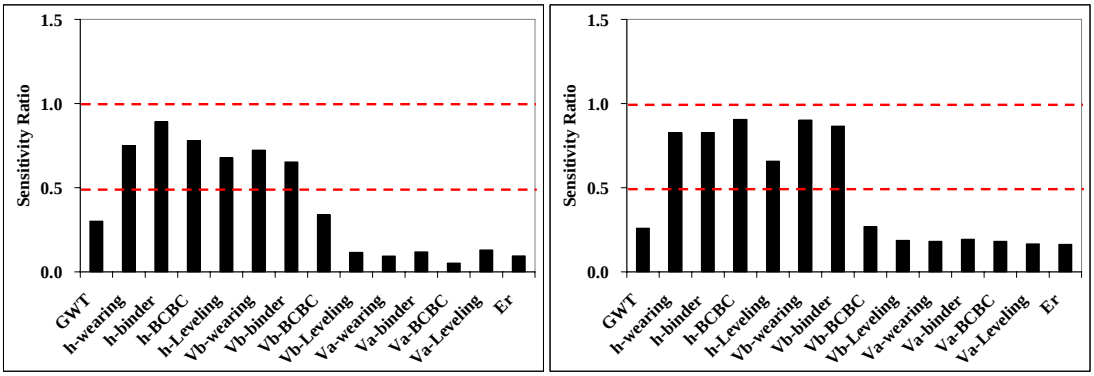

(a) Warren (b) Blair

Figure 37. Sensitivity of alligator cracking to analysis parameters.

AC Rutting

Rutting was found to be sensitive or very sensitive to most of the analysis parameters. Figure 38 suggests that air voids have a more significant impact on rut depth than other parameters. Lack of adequate field compaction results in high air voids, which generates premature permanent deformations as the mixture is densified by traffic. The MEPDG computes the total AC rutting depth from the permanent deformation of individual AC layers; therefore, it is expected that the layer thickness would play an important role in rutting predictions. Nevertheless, this feature is not very clear in the two pavement structures considered in this study.

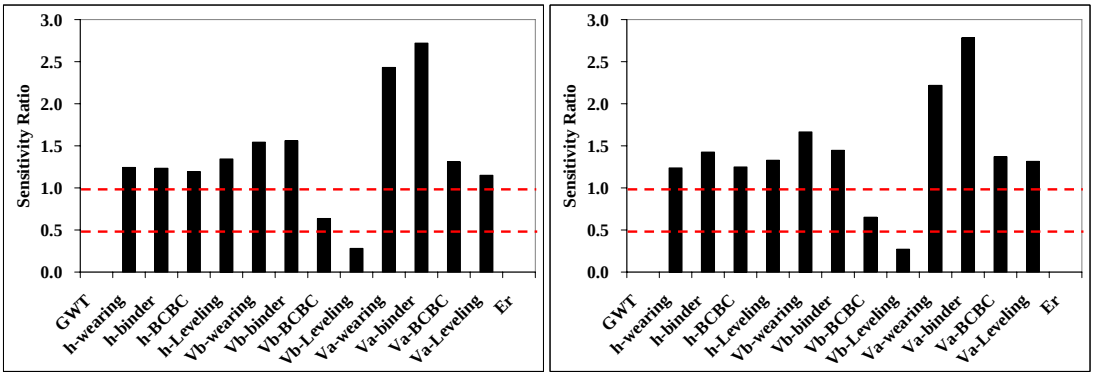

(a) Warren (b) Blair

Figure 38. Sensitivity of AC rutting to analysis parameters.

Subgrade Rutting

Figure 39 reveals the sensitivity of subgrade rutting to unbound material-related analysis parameters, ground water table depth, and resilient modulus, which is what was expected. Compared to low resilient modulus, ground water table depth seems to weaken the subgrade more and, accordingly, causes a poorer subgrade rutting performance.

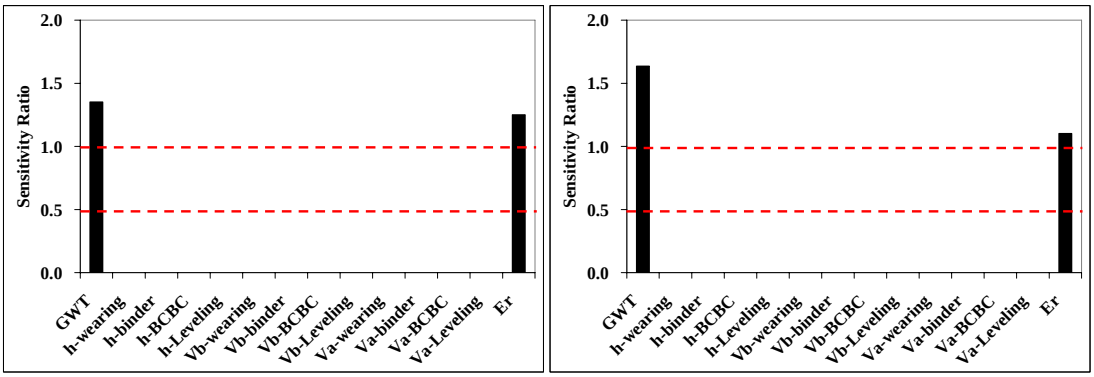

(a) Warren (b) Blair

Figure 39. Sensitivity of subgrade rutting to analysis parameters.

Smoothness

Interestingly, there is no input parameter that has an *SR* above 1.0 for either Warren or Blair. This examination indicates that a pavement designer using the MEPDG for flexible pavement design should recognize the interactive effects among input parameters to obtain the predicted functional performance for satisfying the design criteria. Among all analysis parameters selected for the sensitivity study, only resilient modulus of unbound materials shows a discrepancy in terms of sensitivity classifications in the projected smoothness (Figure 40) for

Warren and Blair. This discrepancy might be attributed to the variations in traffic, climate, and the material components in the structures of the two investigated flexible pavements.

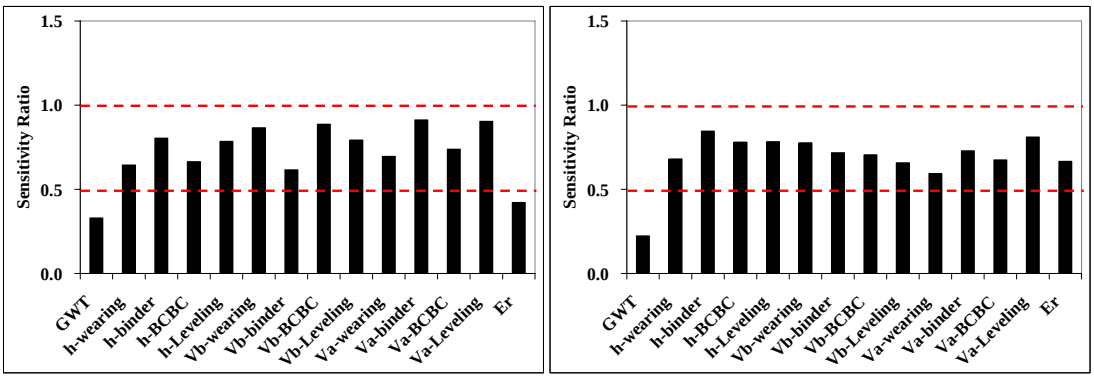

(a) Warren (b) Blair

Figure 40. Sensitivity of smoothness to analysis parameters.

From the sensitivity study, it may be concluded that a small amount of change in some design parameters will result in a large difference in the predicted pavement performance. Consequently, if the predicted performance results are used in a design procedure, different budget planning and rehabilitation activities would be needed. This means that uncertainties in estimating these parameters as design input variables introduce a dilemma for a pavement designer in deciding which prediction is accurate and which preservation actions should be taken in a given year. Therefore, accurate prediction of pavement performance is one of the most important tasks in having a reasonable road network system for pavement maintenance/rehabilitation alternative strategies. In other words, the efficiency of the budget plan and the expected pavement service life depend mainly on the accuracy of the pavement performance prediction. Therefore, each of the sensitive and very sensitive parameters, such as AC layer thickness, should be considered as a random variable following a certain probability distribution. In turn, it is appropriate to develop a probabilistic-based approach for pavement performance predictions.

MEPDG Applications to the SISSI Sites

The sensitivity analysis in the previous section was conducted using version 0.9 because that was the version available at the time of conducting the analysis. However, the application of SISSI data with MEPDG for performance prediction was applied using version 0.9, as well as version 1.0, which had later become available. It is not anticipated that significant differences in the key sensitive parameters occurred between the two versions. Explained here is performance prediction results using version 1.0.

Description of MEPDG Input

A 20-year design life was assumed for all SISSI sites. Dates of pavement construction and traffic opening were obtained from previous SISSI reports, and initial IRI values were input as measured during the first profiling activity. A default reliability level of 90 percent was

assumed for all performance criteria. It is further assumed that the pavement distress levels are limited to the following.

- an IRI of 2.7 m/km,
- longitudinal cracking of 190 m/km,
- alligator cracking of 25 percent,
- AC thermal fracture (transverse cracking) of 190 m/km
- 19 mm rut depth in the total pavement.

These criteria were kept the same for all SISSI sites. The MEPDG input is grouped under separate modules: traffic, climate, and structure. Some of the input is highlighted in the following sections.

Traffic Module

MEPDG-required traffic input was determined from SISSI WIM data. This input included general traffic information (initial two-way annual average daily truck traffic (AADTT), percent of trucks in design direction, percent of trucks in design lane, and operational speed), traffic volume adjustment (monthly adjustment factors, AADTT distribution by vehicle class, hourly AADTT distribution), axle load distribution factors, number of axles per truck, lateral traffic wander, axle spacing, and wheelbase. Table 11 summarizes general traffic information for all SISSI sites. No traffic growth was observed for the SISSI sites based on the historical traffic data after the base year. Figure 41 shows the operational speed variation at the Tioga site as an example.

Table 11. Summary of general traffic information.

SISSI Site	Initial AADTT	Trucks in design direction, %	Trucks in design lane, %	Operational speed, kph
Tioga	866	53	89	106
Mercer*	4724	48	81	108
Warren	400	50	89	93
Perry	1281	44	84	107
Delaware	905	41	79	77
Somerset	1994	40	98	100
Blair	175	48	81	68

*Mercer East and Mercer West share the same traffic condition

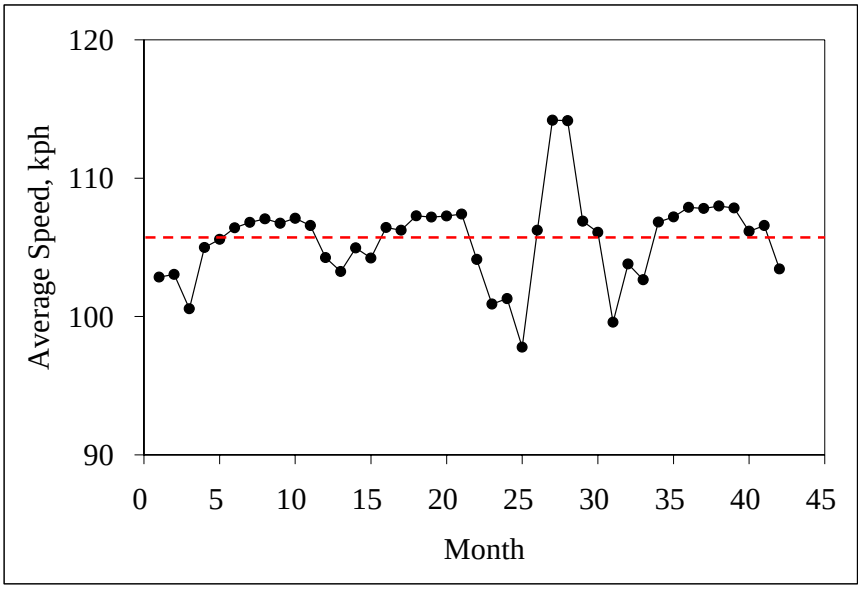

Figure 41. Operational speed at Tioga site.

Climate Module

For the SISSI project, a new climate data file was generated for each site. By specifying latitude and longitude, the software lists the six closest weather stations in the climate database within a radius of 160 km to the site and the amount of climate data (i.e., 60 months) stored at each weather station. A groundwater table depth (*GWT*) of 3 m was assumed, and all six weather stations were selected to interpolate climate data. The software created a climate data file that contained the sunrise time, sunset time, and radiation for each day of the design life period.

Structure Module

The structure module includes structural and materials input. The subgrade layer was automatically divided into two sublayers by the software as required by the EICM. The MEPDG software calls for different input for different HILs. All material properties of AC layers were input as Level 1, while fractured JPCP and granular materials were input as Level 3. The structure module also asks the user to provide the tensile strength, creep compliance, and coefficient of thermal contraction of AC mixtures to predict thermal cracking.

Evaluation of MEPDG Predictions

After all input is provided, the MEPDG software begins the analysis process to predict the performance over the design life of the pavement. The software then creates a summary file and other output files. The summary file contains an input summary sheet, computed material modulus values, and distress summaries for all predicted distresses in a tabular format. Further, the predicted distresses and IRI over time are reported. During Phase II of the SISSI project, final distress surveys were scheduled for all sites except Somerset. The condition data collected from the most recent distress surveys were considered in this study. Results of MEPDG predictions and field measurements are summarized in Table 12 and Figures 42 through 48.

Table 12. Summary of performance predictions and field conditions.

SISSI site	Distress	MEPDG Prediction	Field Condition (avg. of both locations for rutting except Perry and Delaware sites)	
Tioga (Nov 2007)	Longitudinal Cracking (m/km)	0	0	
	Alligator Cracking (%)	0	0	
	Transverse Cracking (m/km)	0.2	0	
	Rutting (mm)	2.9	Left Wheelpath	Right Wheelpath
			4.7	6.5
	Terminal IRI (mm/km)	1.967	N/A	
Mercer East (Oct 2007)	Longitudinal Cracking (m/km)	0	0	
	Alligator Cracking (%)	0	0	
	Transverse Cracking (m/km)	0.2	0	
	Rutting (mm)	3.0	Left Wheelpath	Right Wheelpath
			4.2	3.7
	Terminal IRI (mm/km)	0.982	N/A	
Mercer West (Oct 2007)	Longitudinal Cracking (m/km)	0	0	
	Alligator Cracking (%)	0	0	
	Transverse Cracking (m/km)	0.2	0	
	Rutting (mm)	2.8	Left Wheelpath	Right Wheelpath
			4.2	3.2
	Terminal IRI (mm/km)	1.184	N/A	
Warren (Mar 2007)	Longitudinal Cracking (m/km)	0	2340	
	Alligator Cracking (%)	0	0.2	
	Transverse Cracking (m/km)	0.2	103.3	
	Rutting (mm)	2.8	Left Wheelpath	Right Wheelpath
			5.2	3.5
	Terminal IRI (mm/km)	1.304	N/A	
Perry (Jul 2008)	Longitudinal Cracking (m/km)	0	0	
	Alligator Cracking (%)	0	0	
	Transverse Cracking (m/km)	0.2	0	
	Rutting (mm)	1.0	Left Wheelpath	Right Wheelpath
			5.5	2.9
	Terminal IRI (mm/km)	1.551	N/A	
Delaware (Oct 2008)	Longitudinal Cracking (m/km)	0	213	
	Alligator Cracking (%)	0	10	
	Transverse Cracking (m/km)	0.2	240.4	
	Rutting (mm)	0.8	Left Wheelpath	Right Wheelpath
			2.4	8.6
	Terminal IRI (mm/km)	1.671	N/A	
Somerset	Longitudinal Cracking (m/km)	0	N/A	
	Alligator Cracking (%)	0	N/A	
	Transverse Cracking (m/km)	185	N/A	
	Rutting (mm)	5.3	Left Wheelpath	Right Wheelpath
			N/A	N/A
	Terminal IRI (mm/km)	1.766	N/A	
Blair (Apr 2008)	Longitudinal Cracking (m/km)	0	0	
	Alligator Cracking (%)	0	0	
	Transverse Cracking (m/km)	0	0	
			Left Wheelpath	Right Wheelpath
	Rutting (mm)	3.6	3.8	5.6
	Terminal IRI (mm/km)	1.853	N/A	

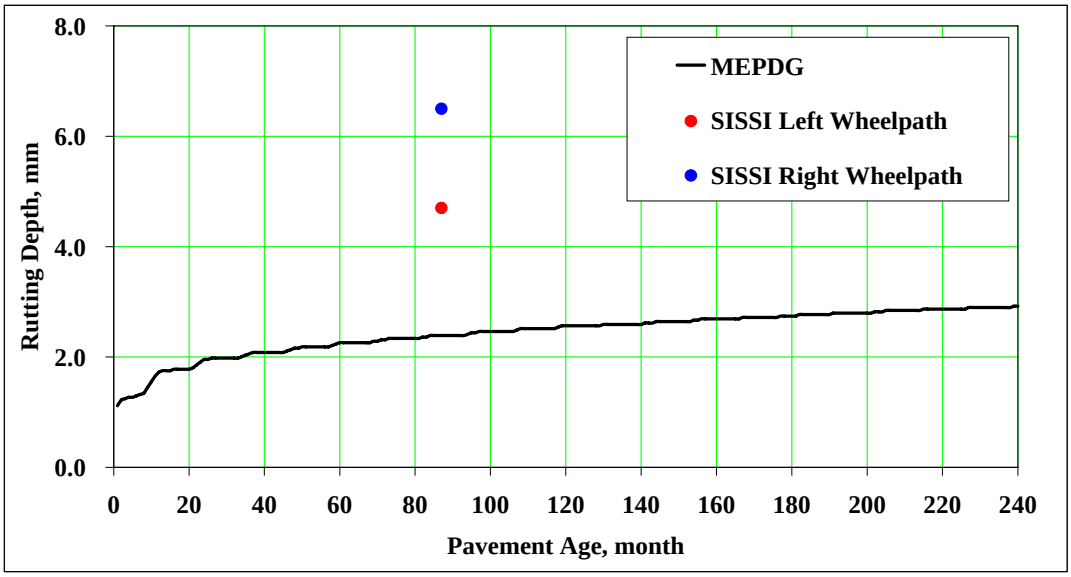

Figure 42. Comparison between predicted and observed rut depth at Tioga site.

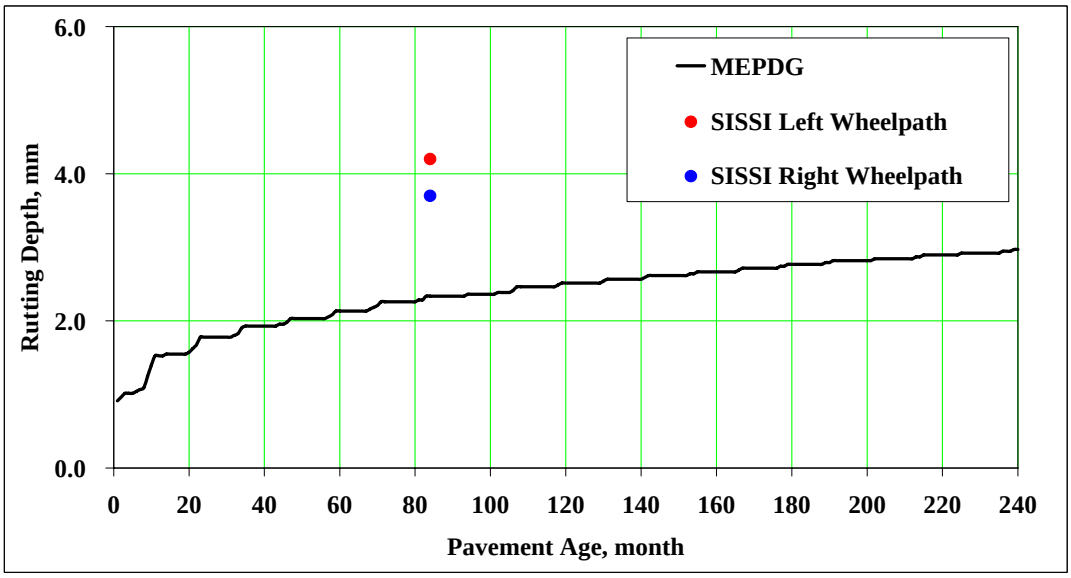

Figure 43. Comparison between predicted and observed rut depth at Mercer East site.

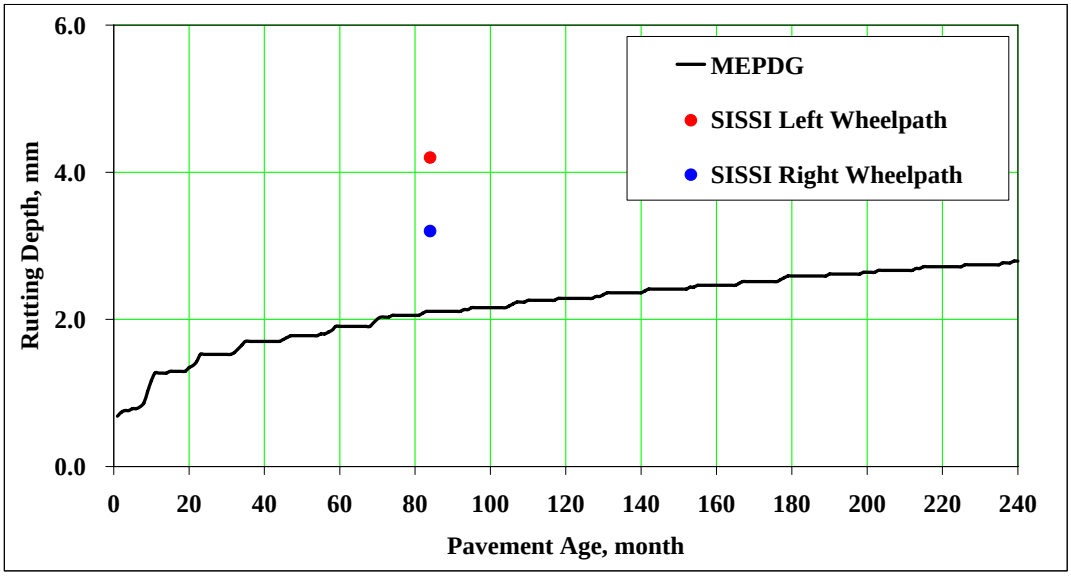

Figure 44. Comparison between predicted and observed rut depth at Mercer West site.

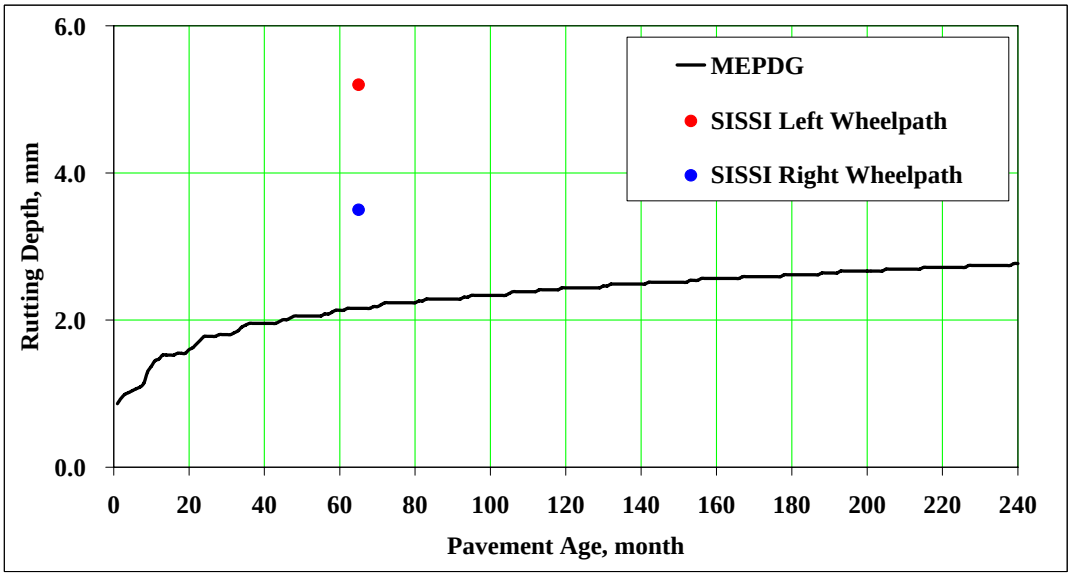

Figure 45. Comparison between predicted and observed rut depth at Warren site.

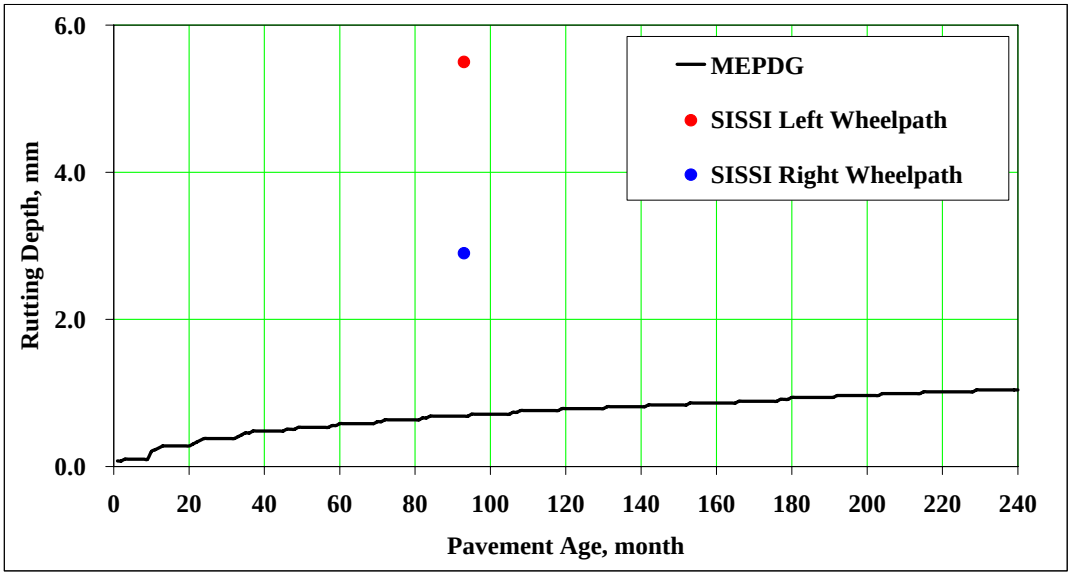

Figure 46. Comparison between predicted and observed rut depth at Perry site.

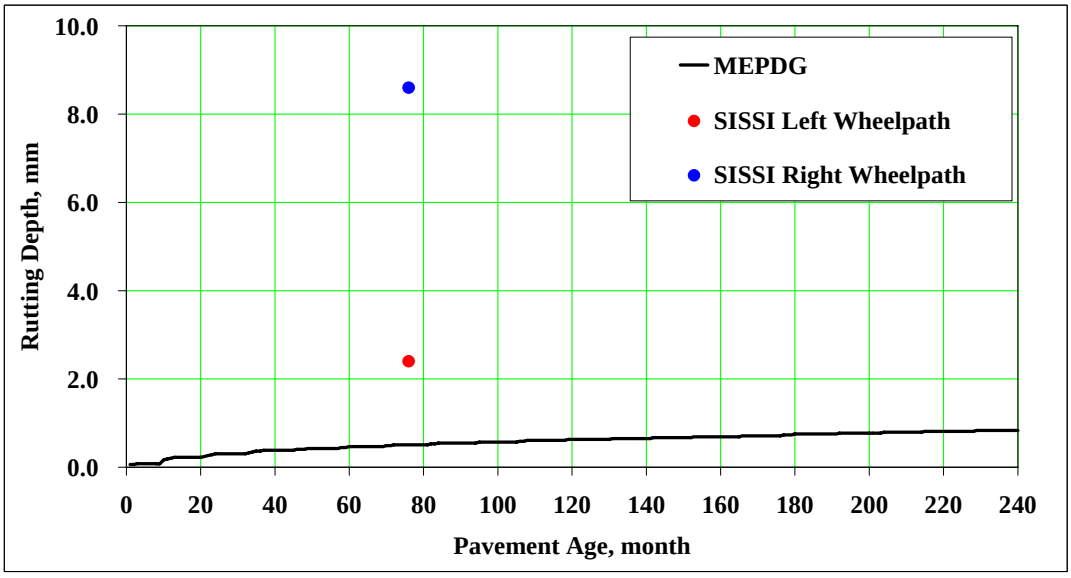

Figure 47. Comparison between predicted and observed rut depth at Delaware site.

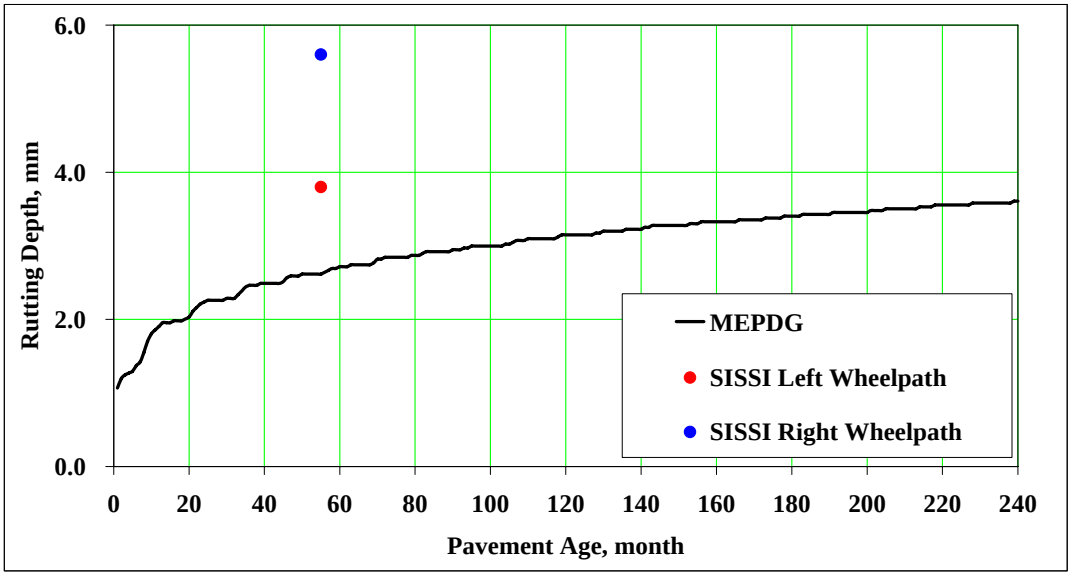

Figure 48. Comparison between predicted and observed rut depth at Blair site.

Our general conclusions from Level 1 analysis using MEPDG was that no significant amount of fatigue or thermal cracking was predicted by MEPDG models, and this is consistent with field observations for most of the sites except the sites at Delaware and Warren counties, where transverse cracking was dominant. At the Warren site, the pavement is built on a cracked and seated old rigid pavement, and there is possibility that observed transverse cracks are reflective cracks even though this could not be determined with certainty. For the Delaware site, the pavement is built over old concrete in some places and on old flexible pavements in others. As a result, it cannot be determined with certainty that the observed transverse cracking at this site was thermally induced.

In regard to pavement permanent deformation, overall MEPDG under-predicted rutting compared to field measurements. The magnitude of this under-prediction varied significantly in the range of 5 to 90 percent depending on the site. Average under-prediction was approximately 40 percent. The discrepancy observed between the predictions and field conditions was perhaps due to the national calibration coefficients in the empirical performance models. It is believed that with the availability of large amounts of field condition data, the MEPDG models could be more accurately calibrated locally.

Simulation of Pavement Response Using 3-D Finite Element Modeling

The effectiveness of any mechanistic-based pavement design depends on the accuracy of employed mechanistic parameters, such as stress and strain. There are three common approaches that can be used to compute the stresses and strains in pavement structures: layered elastic analysis, two-dimensional (2-D) finite element (FE) modeling, and three-dimensional (3-D) finite element modeling.

The general purpose finite element software ABAQUS (version 6.6, 2006) was used for finite element analysis using SISSI data because of its capability in reducing the computation time through the use of 3-D reduced integration elements. ABAQUS also includes various material models, such as linear elastic, viscoelastic, and elastoplastic models. The following section presents the validation study using SISSI field measurements.

Modeling Strategy

Details of the modeling strategy are reported elsewhere. In summary, two stages were considered in constructing the finite element mesh. In the first stage (global level) of the G-L approach, the pavement section subjected to loading and boundary conditions was analyzed using a relatively coarse mesh. In the second stage (local level), a more refined mesh was used to model a local part of the pavement section based on interpolation of the solution from the initial, relatively coarse, global model. A very fine mesh was applied to the area of interest and to some depth under the pavement surface. The results of the global model were interpolated on the cutting edge of the local model corresponding to different calculation steps, and the interpolation results were applied as boundary conditions to the local model.

Because of symmetry in the transverse direction, only the half width of the truck axle (915 mm) was modeled. In the vertical direction, the thickness of the global model was predetermined by the pavement structure (3000 mm). In the longitudinal direction, the finite domain from the infinitely long AC pavement was properly selected to deliver accurate predictions for stresses and strains in the field.

The bottom of the model was prevented from axial movements in the three directions to represent the bedrock (rigid layer) beneath the pavement structure. All sides of the model were also fixed in all directions except the one at the centerline of the truck axle. This symmetry line was fixed in the *y* direction, which is perpendicular to the longitudinal direction. All layers were considered perfectly bonded to one another so that the nodes at the interface of two layers had the same displacement in all three (*x*, *y*, and *z*) directions. These boundary conditions are applicable to the FE models for both Blair and Warren.

Material Properties

Among the most important parameters needed as input for mechanistic-empirical pavement design models are the properties of materials used in different pavement layers. In order to obtain properties, the materials were considered in two general categories: bound materials (AC) and unbound materials (fractured PCC at Warren, granular subbase, and subgrade). For bound materials, shear relaxation modulus and bulk relaxation modulus master curves were developed.

The properties of unbound materials such as fractured PCC, subbase and subgrade soils are often not as well characterized as those of AC. For the SISSI project, this difficulty was overcome by backcalculating effective layer moduli from Falling Weight Deflectometer (FWD) data so that the FE model reasonably predicted the response of the unbound materials.

Simulation of Moving Load

To accurately simulate pavement response to vehicular loading, the contact pressure distribution and dimensions of the contact area between the tire and pavement are required. A uniform contact pressure over a rectangular tire print area on the pavement surface was considered.

Contact pressures of the NECEPT truck under different load configurations were calculated from the axle weight and tire print area as summarized in Table 13. Although different contact pressures may result in different contact areas, for simplicity, averaged dimensions (330 mm by 216 mm) were assumed for all tractor/trailer tires as shown in Figure 49a. These dimensions correspond to a circular loaded area that has a radius of 150 mm. Uniform contact pressure was then applied on these tire prints.

Table 13. Summary of contact pressure under different load configurations.

Axle	Axle Spacing, m			Tire	Contact Pressure, kPa	
					Front Load Configuration	Back Load Configuration
1	4.5			single	454	441
2		1.3		dual	580	384
3			5.8	dual	550	408
4				dual	559	799

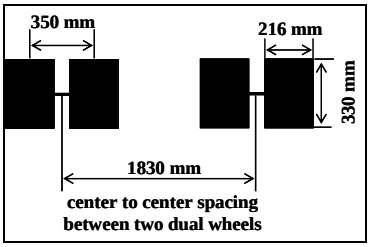

(a) Tire print of the NECEPT truck

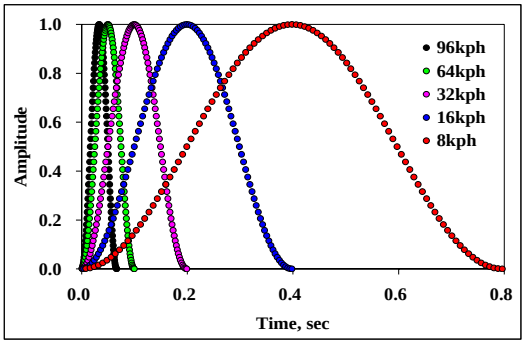

(b) Load amplitude as a function of time

Figure 49. Simulation of moving load.

The effect of a moving load on a point in the pavement can be simulated by noting that a time function of the stress can be used to approximate the stress experienced by the point. The relationship between the duration of the moving load and the load amplitude was approximated through a sine function presented by Huang (1993):

$$L(t) = q * \sin^2(\frac{\pi}{2} + \frac{\pi}{d}) \quad (12)$$

where t is the time of loading, d is the load duration, and q is the load amplitude. When the load is at a considerable distance from a given point, or $t = \pm d/2$, the load above the point is zero, or $L(t) = 0$. When the load is directly above the given point, or $t = 0$, the load $L(t) = q$. The duration of the load depends on the vehicle speed V and the tire contact radius a. A reasonable assumption is that the load has practically no effect when it is at a distance of $6a$ from the point under consideration. As a result, the load duration d can be computed as $d = (12*a)/V$.

Element Type and Size

The accuracy of FE solutions depends strongly on the element type used to mesh FE models. In view of the geometric size of the pavement section and preferred accuracy of FE solutions, unbound materials were meshed with eight-node linear brick elements (C3D8R) with reduced integration. The optimum element size was determined through a mesh refinement analysis that evaluates the merits of the FE model's performance in accurately predicting pavement response at multiple depths under a single tire load. The mesh refinement analysis was performed for Blair and Warren pavement structures separately. Details of such analysis are reported elsewhere. The same FE models used in the mesh refinement analyses were employed with a length of 6 m.

Pavement Response Computation

AC layers were modeled as viscoelastic materials. A lower speed produces a larger duration of loading and subsequently larger dimensions of the stress influence zone. A tire load with 8-kph vehicle speed was applied on the pavement surface. This was the lowest target speed for SISSI-filed measurements. Horizontal strain in longitudinal direction and vertical strains were predicted at various spatial locations. As an example, predictions of response parameters from the Blair FE model are shown in Figure 50. It is clear from Figure 50 that the FE model provides an acceptable description of longitudinal strain response observed in the field—the compression-tension-compression pattern. Both longitudinal and vertical strain curves follow the same trend, i.e., the strain magnitude decreases at deeper locations. This trend was also detected in the field response data. Because the tire load has almost no influence on both strain curves at longitudinal distances more than 2 m from the center of the loading area, the longitudinal dimension was set at 4 m for both the Blair and Warren FE global models. All layers were modeled with the same shape to preserve the continuity of nodes at the interface of adjacent layers.

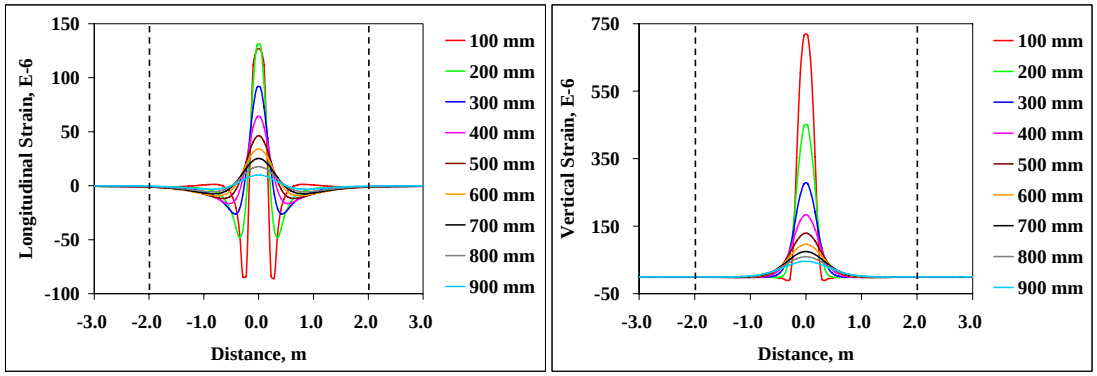

(a) Longitudinal Strain (b) Vertical Strain

Figure 50. Determination of the longitudinal dimension of the global models.

Model Validation

Although an effort was made to approach real pavement conditions in the developed FE models based on the available laboratory results and modeling techniques, some approximations were inevitable. Therefore, model validation is an essential step for pavement performance predictions using FE-simulated stress and strain responses. Based on all dynamic measurements collected during the SISSI project, various sets of pavement responses were selected to validate the developed FE models. These data sets cover various seasons, vehicle speeds, and load configurations. Although strain gages were also installed at the bottom of the wearing layer at Warren, they stopped responding in 2004. Since other researchers found that the effect of tire wander (between the center of the tire and the instrument) was very significant (Chatti et al. 1996), tire wander was considered in the model validation. An average of two lateral offsets recorded at 7.3 m before and after the centerline of instrumentation was applied in each FE simulation. Both target and actual speeds are reported, but only actual speeds were used to simulate moving loads.

A layered elastic analysis (LEA) program, KENLAYER, was used to compute horizontal strains at the bottom of the wearing and leveling layers at the Warren site. KENLAYER was also used to determine vertical strains in both bound and unbound layers where measured responses were not available. KENLAYER was selected because it is widely accessible and is included with the textbook *Pavement Analysis and Design* (Huang 1993). With time-temperature superposition, for a specific temperature and actual vehicle speed in the field at the time of pavement response measurement, the elastic modulus was obtained from dynamic modulus master curves. These elastic moduli were input in KENLAYER. The effectiveness of developed FE models in simulating pavement response is evaluated in terms of the prediction error at peak strains or stresses, e:

$$e = \frac{R_{FE} - R_{m(KEN)}}{R_{m(KEN)}} * 100 \qquad (13)$$

where R_{FE} is the peak response simulated from FE models, R_m is the peak response measured in the field, and R_{KEN} is the peak response calculated from KENLAYER. A positive value of e indicates an over-prediction from FE simulations, while a negative value of e suggests an under-prediction.

Comparison of FEA and Measured Responses

Blair FE Model

In general, the Blair FE model seems to under-predict pavement responses in AC materials. The main conclusions of strain predictions can be made as follows:

- FE model is capable of simulating pavement responses under different load configurations.
- FE model results in a slightly larger prediction error at the bottom of the wearing layer. This is possibly due to the simplification of contact pressure distribution at the pavement surface.

The FE model predicts smaller strains (a larger prediction error) during warm seasons. Since AC materials are modeled in viscoelastic mode, tests other than the complex modulus test, such as the creep-recovery test, are needed to capture the viscoplastic behavior of AC such that the accuracy of strain predictions at high temperatures can be improved.

On the other hand, the Blair FE model always over-predicts response in granular materials. The main conclusions of stress predictions can be made as follows: No obvious dependency of prediction error on load configuration, axle, and vehicle speed has been observed.

The prediction error decreases as deeper points in the pavement are considered. Prediction errors are quite large in the summer. This is probably due to the low subbase modulus backcalculated from FWD data. Further improvements on the accuracy of stress response prediction require soil characterization tests, such as the resilient modulus test.

For all the selected response data sets, the FE model accuracy is acceptable, with an overall error of -11.2 percent in predicting longitudinal strains and 14.3 percent in predicting vertical stresses. Hence, the assessment is that the Blair FE model provides a satisfactory prediction of pavement response to vehicular loading.

Warren FE Model

Similar to the Blair FE model, the Warren FE model seems to under-predict pavement responses in AC materials. However, an overall prediction error of -7.8 percent suggests a better

agreement between measured and predicted longitudinal strains. Several conclusions of strain predictions can be made as follows:

- Load configuration (front vs. back) has no impact on strain predictions.
- The trend that the prediction error is smaller at a deeper location is not clear.
- The inability to simulate strain responses at high temperature is apparent due to the viscoelastic mode included in the FE model.

Comparison of FEA and KENLAYER

Horizontal strains at deeper locations of bound layers and vertical strains in unbound layers were not captured by field instrumentation at the SISSI sites. To further verify the developed FE models, the responses at these locations from FE solutions were compared to LEA solutions. Comparisons were only made with strain responses under the fourth axle of the NECEPT truck. A radius of 150 mm was chosen for the circular contact area in KENLAYER. This radius corresponds to an equivalent contact area as measured for the NECEPT truck. It was found that FE models had poor agreement with KENLAYER. In general, FE models seemed to under-predict both vertical strains and horizontal strains regardless of load configurations. An overall prediction error is about 22 percent for vertical strains and 35 percent for horizontal strains.

Linearity of Pavement Response

As discussed in previous sections, linear viscoelastic and elastic behaviors were assumed for bound and unbound materials. These assumptions imply that the response (stress or strain) is linearly proportional to the applied load. That is, as the load increases or decreases on the pavement surface, the response at a given point will increase or decrease linearly. In order to verify the above assumption of linearity, two sets of analysis were conducted using the developed Blair and Warren FE models separately. To exclude the tire wander effect, three runs were first selected from each site, Blair (runs #4, 8, and 12) and Warren (runs #3, 13, and 21). These runs cover all three seasons in which dynamic data were collected in the field. Then, for each run, the contact pressure was increased at a 100-kPa interval while vehicle speed and pavement temperature were kept constant. FE-simulated strain responses at various load levels are shown in Figures 51 and 52. Figure 51 shows the tensile strains at the bottom of the BCBC layer, whereas Figure 52 shows the compressive strains at the top of the subgrade as a function of load level. Responses at these two locations are critical for the determination of distresses, such as fatigue cracking and permanent deformation in the respective layers. The linear relationship between the contact pressure and the response clearly validates the assumption of linearity. For both Blair and Warren FE models, as the load increases, the response also increases proportionally. As expected, this trend is pronounced at higher temperatures, which results in lower stiffness of AC materials.

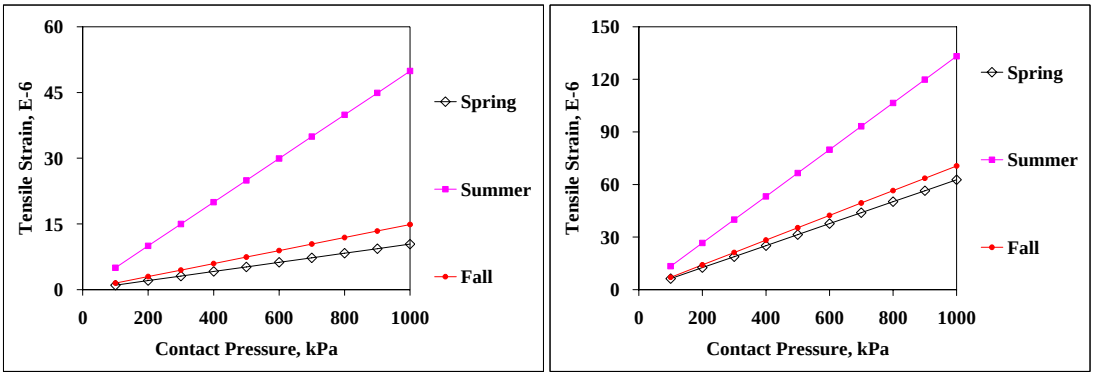

(a) Blair, BCBC (b) Warren, Leveling

Figure 51. Tensile strains at the bottom of the last AC layer.

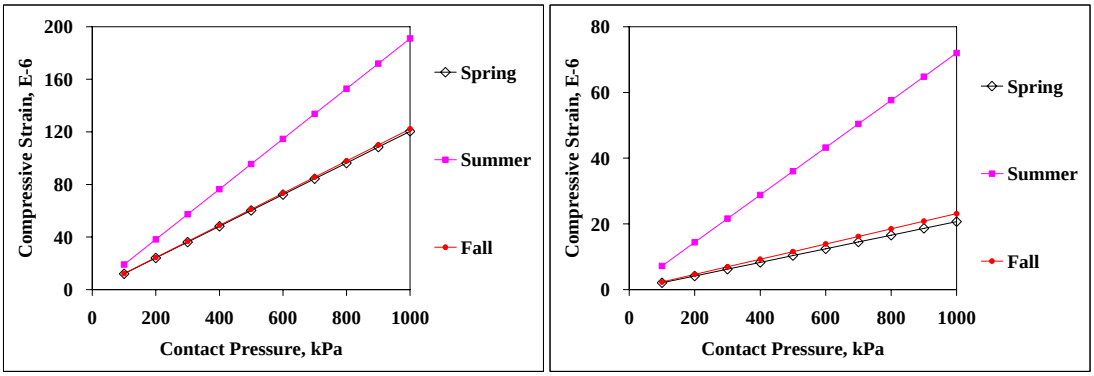

(a) Blair (b) Warren

Figure 52. Compressive strains at the top of subgrade.

SIMULATING FLEXIBLE PAVEMENT RESPONSE TO FWD LOADS: A MECHANISTIC APPROACH

One of the most important parameters required by the response models of MEPDG software is the modulus of each pavement layer. Two basic means of obtaining layer material properties are laboratory and in-situ testing. The use of in-situ layer moduli has become an integral part of structural evaluation and rehabilitation design for pavements. The in-situ layer moduli are typically obtained by falling weight deflectometer (FWD) testing and backcalculation analysis. Most of the backcalculation analyses in use today are based on layered elastic theory for calculating the modulus of elasticity for each pavement layer such that the difference between the measured and predicted deflection basins is minimal. Some backcalculation programs also account for the viscoelastic and/or nonlinear material behavior. There are some uncertainties related to the backcalculation because only one single modulus value per pavement layer can be obtained with no sufficient discrimination of the near-surface AC moduli. Furthermore, various studies reported that backcalculated moduli usually differ significantly from those obtained

through laboratory testing; no consensus exists as to which procedure provides the most appropriate moduli values for pavement design.

One of the goals pursued during Phase II of the SISSI project was to integrate in-situ tests, laboratory material characterization, backcalculation, and FEA in a rational manner such that flexible pavements' responses to FWD loads could be numerically simulated. At this stage, only one instrumented full-depth AC pavement was studied, and the laboratory characterization was focused on the bituminous layers. To achieve the research goal, a three-phase mechanistic approach was taken, which is illustrated in Figure 53.

Pavement Response Predictions

The general purpose finite element software ABAQUS was used to compute surface deflections, horizontal strains in the AC layers, and vertical stresses in the subbase and subgrade. Both backcalculated and laboratory-derived AC moduli were used in FE simulations such that broad conclusions can be drawn.

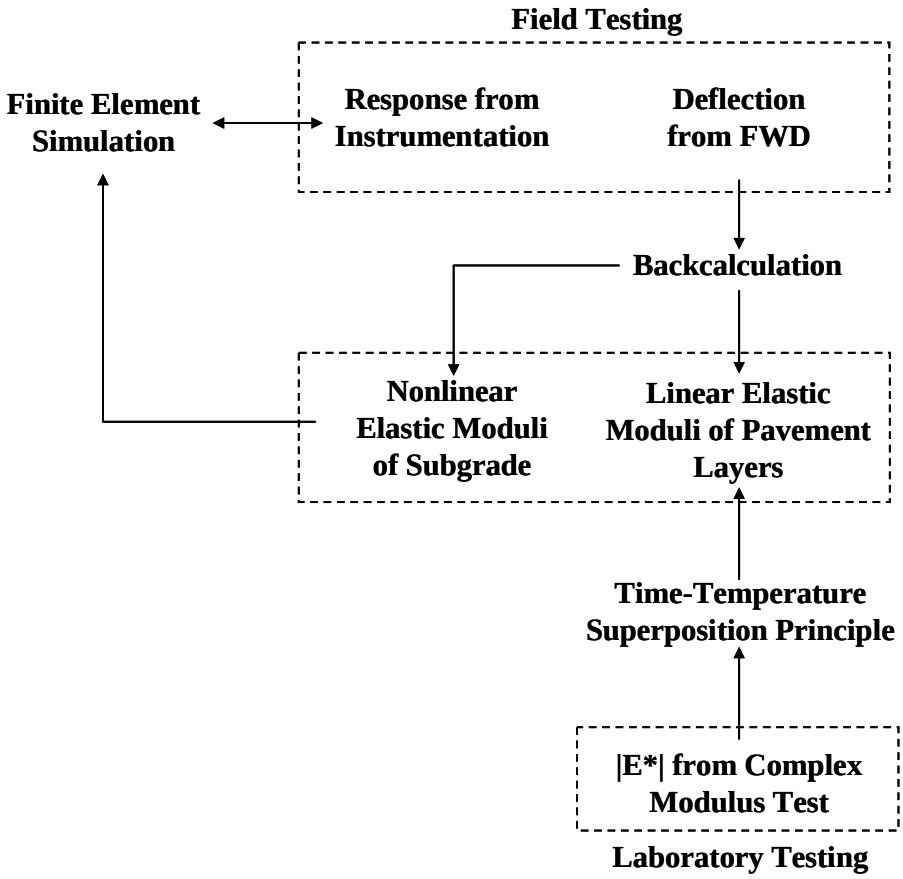

Figure 53. Analysis approach.

The effectiveness of developed FE models in simulating pavement response is evaluated in terms of the prediction error at each load level, *e*:

$$e = \left(\frac{\varepsilon_M - \varepsilon_{FE}}{\varepsilon_M}\right) * 100 \qquad (14)$$

where ε_{FE} is the simulated response, and ε_M is the measured response. A positive value of *e* indicates an under-prediction from FE simulations, while a negative value of *e* suggests an over-prediction.

A corresponding graphic illustration is given in Figure 54a. A general observation of the deflection prediction is that the prediction error drops as the FWD load level increases regardless of the source of AC moduli. Prediction errors are also much higher at greater distances from the load. At 60 inches (1524 mm) from the FWD load, the maximum prediction errors are -55.1 percent and 58.3 percent for backcalculated and laboratory-derived AC moduli, respectively. As indicated by the average prediction errors (-9 percent and -12 percent), both sources of AC moduli result in over-prediction of surface deflections.

The FE model always over-predicted strain and stress responses directly under the FWD load in all pavement layers regardless of the FWD levels. On the other hand, the response location had a considerable impact on the magnitude of the prediction error. For all load levels, the prediction errors in the wearing HMA layer and subbase layer were constantly higher than those in other pavement layers. There are possibly several reasons for this observation, such as treating wearing and binder layers as a single surface layer in the backcalculations and FE simulations and the considerably higher temperature of the wearing layer compared to the binder layer. One possible solution to reduce the prediction error in the subbase would be laboratory material characterization (e.g., the resilient modulus test) such that the model constants (K_1 and K_2) in Equation (1) can be more accurately determined.

Although the predicted responses exceed the measured responses, it would be valuable if a relationship between predictions using backcalculated and laboratory-derived AC moduli could be established. In some new pavement designs in which laboratory-derived properties are not available, backcalculated AC moduli from FWD deflections could be used. The opposite is also true: When FWD tests are not yet available for rehabilitation design, laboratory results could be employed. Linear regression analyses were conducted using the predicted responses, and as shown in Figure 55, strong correlations were observed for the surface deflections, horizontal strains in AC layers, and vertical stresses in the subbase and subgrade.

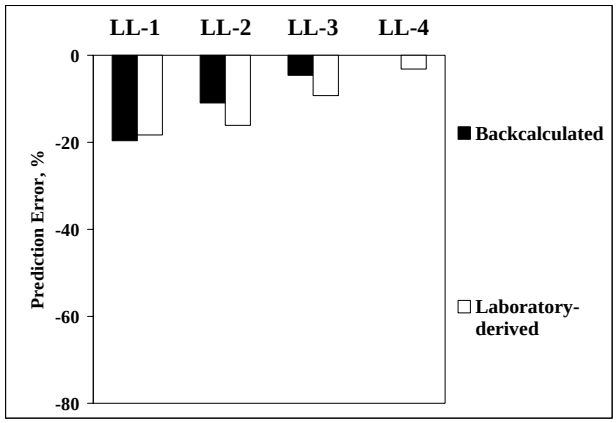

(a) Surface deflections

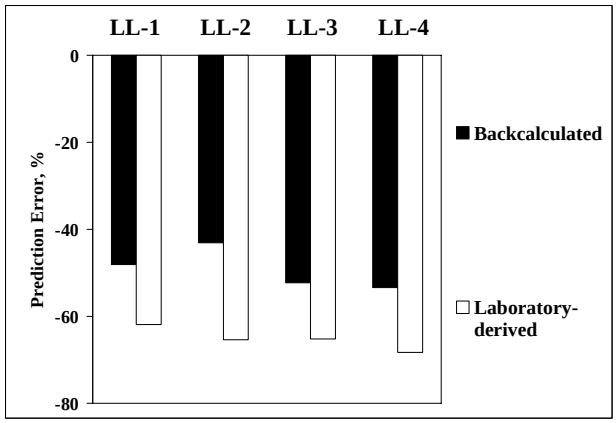

(b) Strains at the bottom of wearing layer

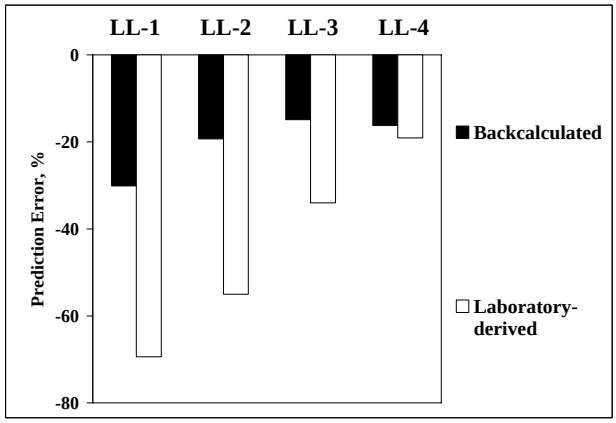

(c) Strains at the bottom of binder layer

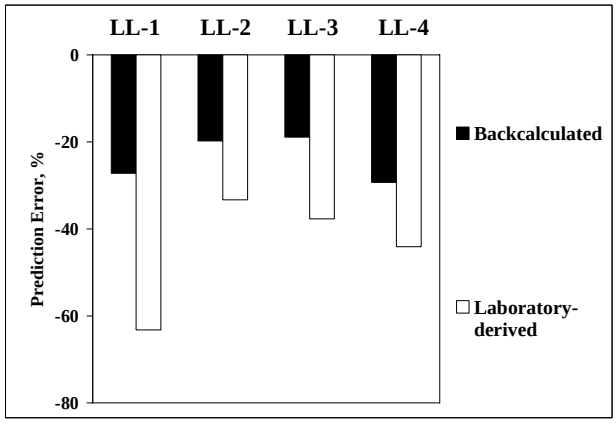

(d) Strains at the bottom of BCBC layer

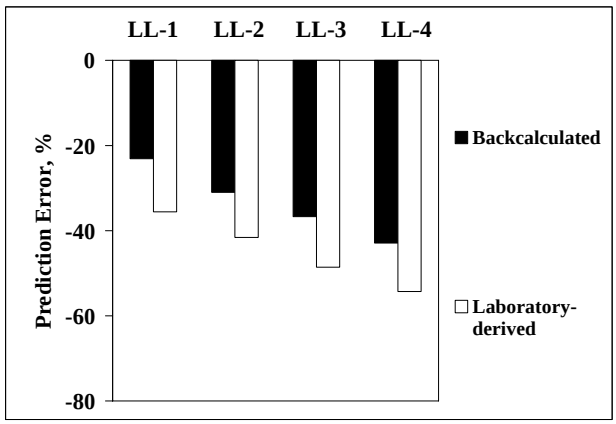

(e) Stresses at the top of subbase

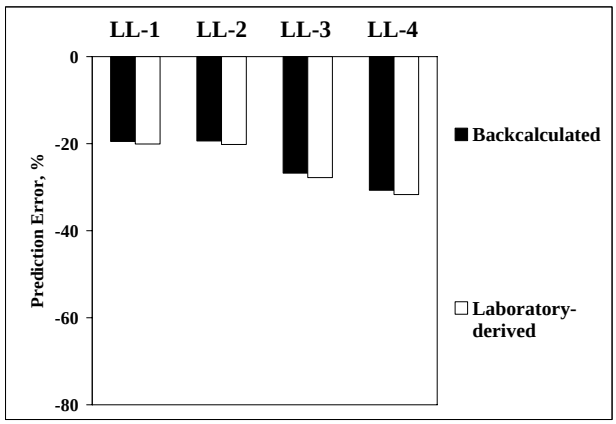

(f) Stresses at the top of subgrade

Figure 54. Comparison of measured and predicted pavement responses.

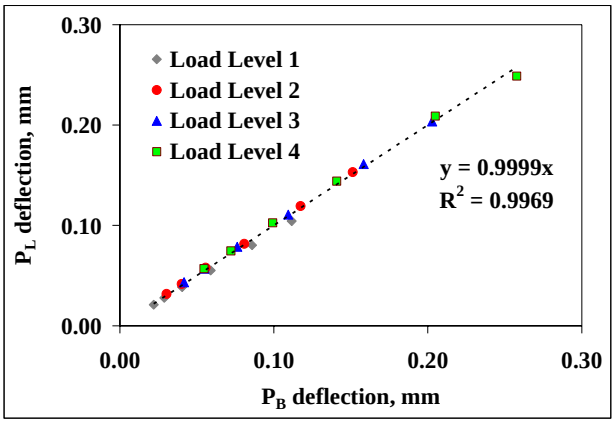

(a) Surface deflections

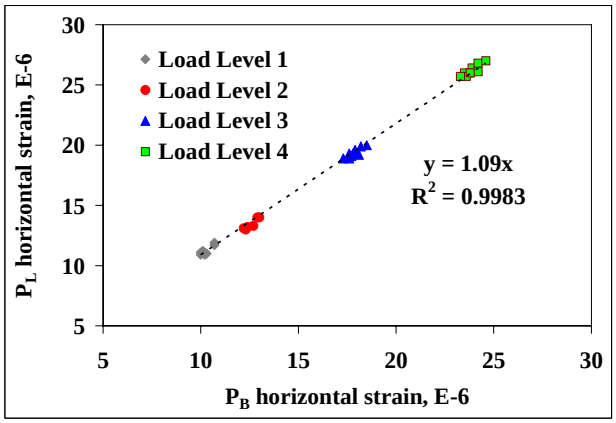

(b) Strains at the bottom of wearing layer

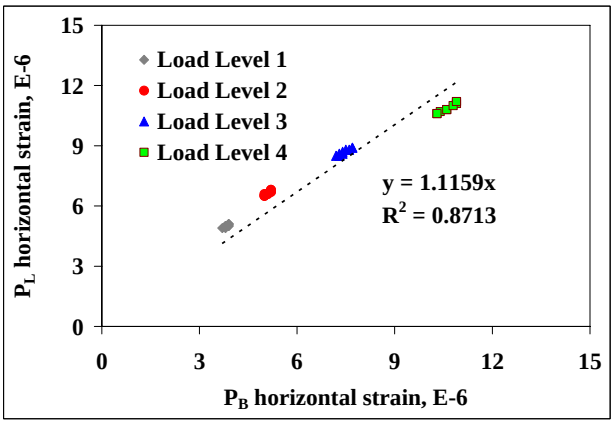

(c) Strains at the bottom of binder layer

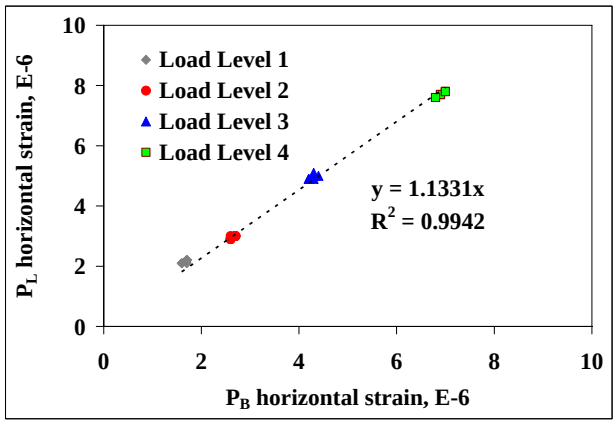

(d) Strains at the bottom of BCBC layer

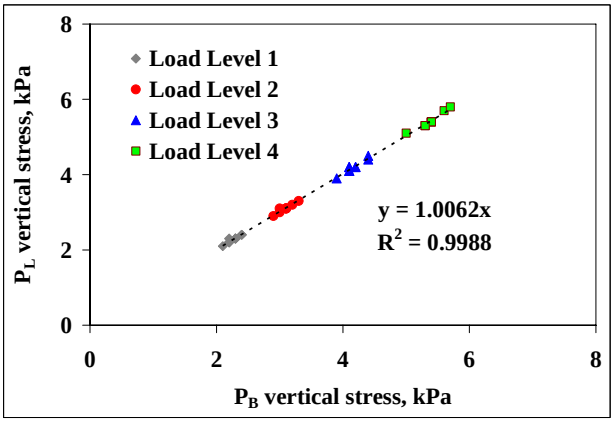

(e) Stresses at the top of subbase

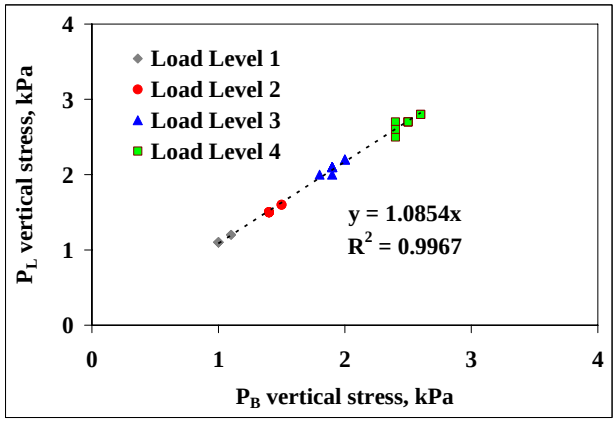

(f) Stresses at the top of subgrade

Figure 55. Relationship between predicted pavement responses using backcalculated and laboratory-derived AC moduli.

PREDICTING STTRAIN RESPONSE OF FLEXIBLE PAVEMENT USING INSTRUMENTATION AND SIMULATION DATA

A major application of instrumentation data is in validating existing or novel design and analysis approaches. This is accomplished by verifying field-measured parameters with theoretically calculated parameters from pavement response models. This type of work is well documented in the literature. As previously discussed, it is possible to perform theoretically rigorous 3-D FEA, incorporating a rich set of sophisticated modeling features, to estimate strains and stresses within a pavement structure. However, computational practicality (e.g., the ability to perform the calculations in an acceptable amount of time) nonetheless remains a major discouragement against using 3-D FEA (MEPDG 2004). The damage accumulation scheme incorporated in the Mechanistic Empirical Pavement Design Guide (MEPDG) would require thousands of FE simulations for a single case of performance prediction. Thus, it is desirable to develop a procedure that can accurately and rapidly predict strain response with known traffic and environment information, particularly axle load and configuration, vehicle speed, and pavement temperature.

Simulation of Pavement Response

The effectiveness of any mechanistic-based pavement design depends on the accuracy of employed mechanistic parameters, such as stress and strain. The general purpose finite element software ABAQUS (version 6.6) was used in this study to simulate strain responses in the field. Key features of the developed FE model, such as model dimensions, boundary conditions, material properties, and element type, were presented in earlier sections of this report.

Prediction of Pavement Response

In previous sections, a comprehensive validation study on the developed FE model suggested good agreement between measured and FE-simulated tensile strains for the two load configurations, front and back. Verification analysis on the linearity of strain response also suggested that as the axle load (contact pressure over a rectangular contact area) increases, the strain response increases proportionally. These two conclusions reveal that at the same vehicle speed and pavement temperature, pavement response under one load configuration can be estimated from another. Therefore, only response data under one load configuration are needed for strain predictions.

The following sections present an analytical procedure developed to predict pavement response using a mix of measured and FE-simulated response data. Nine sets of field response data were used to establish a response database such that the compiled response data are representative of a wide range of vehicle speeds and pavement temperatures.

Exploratory Data Analysis

Exploratory data analysis is an approach to data analysis that postpones the usual assumptions about what kind of model the data follow with the more direct approach of allowing

the data itself to reveal its underlying structure and model. Response data in the analysis database were first divided into different groups corresponding to all combinations of analysis locations and pavement temperatures. One set of response data at the bottom of the wearing layer is plotted in Figure 56. These graphs show that for a certain load configuration and analysis location, strain response in AC layers is highly dependent on the vehicle speed and pavement temperature. EDA suggests a nonlinear function to describe the dependency of the strain response on the vehicle speed and pavement temperature.

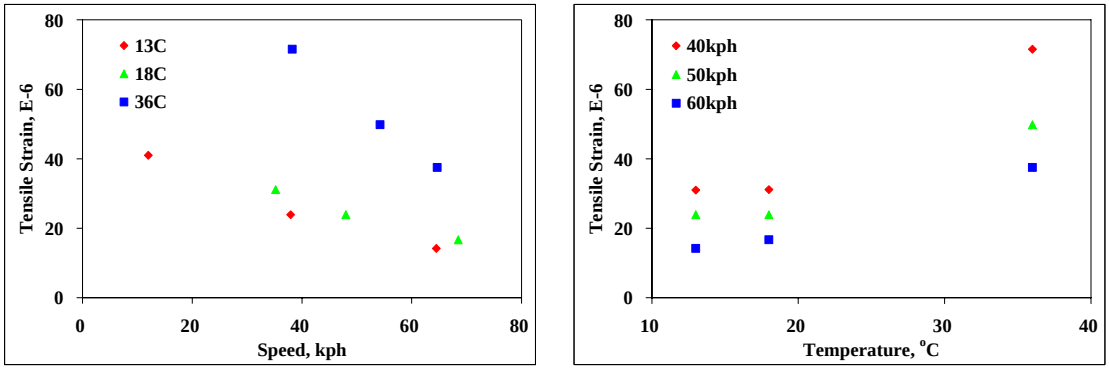

(a) Speed effect (b) Temperature effect

Figure 56. Speed and temperature dependence of tensile strains.

Nonlinear Regression Analysis

Speed Effect on Strain Response

Based on the conclusion from exploratory data analysis, a nonlinear regression model was used to model the relationship between the strain response and vehicle speed:

$$\varepsilon = a * EXP(b * S) + e \qquad (15)$$

where ε is tensile strain, S is vehicle speed, a and b are nonlinear model coefficients, and e is random normal error with mean 0 and variance σ^2. Estimates of Eq. (15) are summarized in Table 14. Opposite signs of model coefficients a and b suggest that the strain response decreases with the increase in speed, the reason being that when speed increases, there is a decrease in the time of contact between the tire and the pavement surface. Excellent R^2 values indicate the appropriateness of the selected model form. Before proceeding with further prediction on strain response, for each combination of analysis location and pavement temperature, strain responses were extrapolated to a wide range of vehicle speeds at a 5-kph interval. This range covers the vehicle operational speeds at the Blair site. One such example is graphically shown in Figure 57.

Table 14. Nonlinear tensile strain-speed model coefficients.

Analysis Location	Temperature, °C	Model Coefficient		R^2
		a	*B*	
Bottom of Wearing	13	51.97	-0.0202	1.000
	36	182.70	-0.0243	0.997
	18*	59.42	-0.0186	0.998
Bottom of Binder	15	21.96	-0.0121	0.952
	33	80.96	-0.0216	0.971
	13*	20.98	-0.0207	0.999
Bottom of BCBC	12	20.17	-0.0059	0.997
	29	30.92	-0.0114	0.959
	5*	12.33	-0.0119	0.994

*NOTE: from FE simulations

Temperature Effect on Strain Response

To account for the effect of pavement temperature on strain response, strain response at a field temperature was shifted to the reference temperature:

$$\varepsilon_T = \varepsilon_0 * SF \qquad (16)$$

where ε_0 is the tensile strain at the reference temperature, and ε_T is the tensile strain at a field temperature. For a particular vehicle speed (e.g., 70 kph), the duration of mechanical loading was assumed constant throughout pavement depths. The lowest temperature was arbitrarily chosen as the reference temperature for each combination in the analysis database. For the sake of brevity, one set of shift factors is plotted in Figure 57b. It can be seen that *SF* is always larger than unity because the strain response increases as the temperature increases.

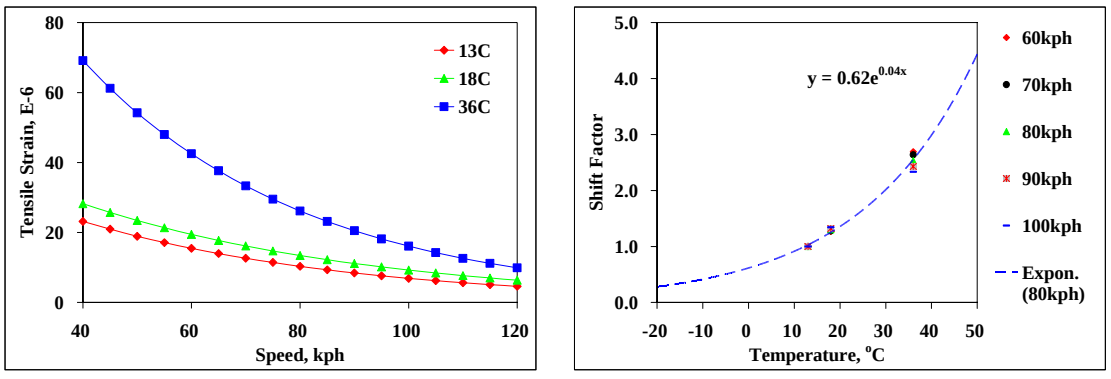

(a) Strain extrapolation (b) Temperature vs. shift factor

Figure 57. Strain prediction (bottom of wearing layer).

Finally, a nonlinear regression model was used to model the relationship between the shift factor and pavement temperature for each vehicle speed:

$$SF = c * EXP(d * T) + e \quad (17)$$

where T is pavement temperature, c and d are nonlinear model coefficients, and e is random normal error with mean 0 and variance σ^2. An average R^2 value of 0.95 was observed for all combinations in the analysis database.

Evaluation of Response Prediction

Figure 58 presents a comparison of predicted tensile strains to the measured values for the bottom of wearing, binder, and BCBC layers, respectively. Overall, the developed analytical procedure predicts tensile strains reasonably well, and the analytical procedure tends to under-predict strain response. There is a fair amount of deviation between predictions and measurements at high strain magnitudes, especially for the upper layers (Figure 58a and 58b).

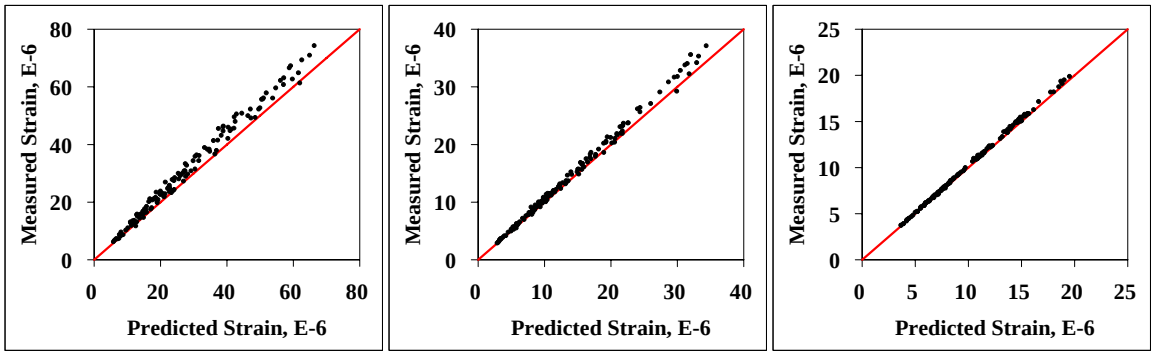

(a) Bottom of wearing layer (b) Bottom of binder layer (c) Bottom of BCBC layer

Figure 58. Predicted vs. measured strain responses.

To further investigate this phenomenon, response differences (predictions-measurements) were plotted for individual axles at various vehicle speeds and pavement temperatures. As illustrated in Figures 59 through 61, a better concurrence at lower strain magnitudes implies that the effect of extremely low vehicle speeds, high pavement temperatures, and heavy axle loads on the strain response is not accounted for precisely. These conditions result in a difference between predicted and measured strain of approximately 9 microstrain, suggesting a still reasonable prediction. At high strain magnitudes, it can be seen that under-prediction of tensile strains occurs at the bottom of the AC layers. One possible source of this response difference is from the inability of the developed FE model to properly capture the viscoplastic behavior of AC at high temperatures and slow loading rates.

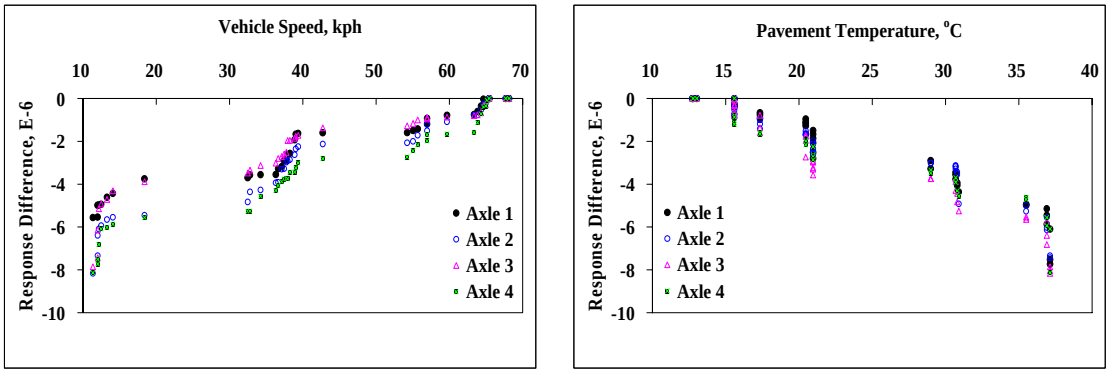

(a) Speed effect (b) Temperature effect

Figure 59. Speed and temperature dependency of response differences, bottom of wearing layer.

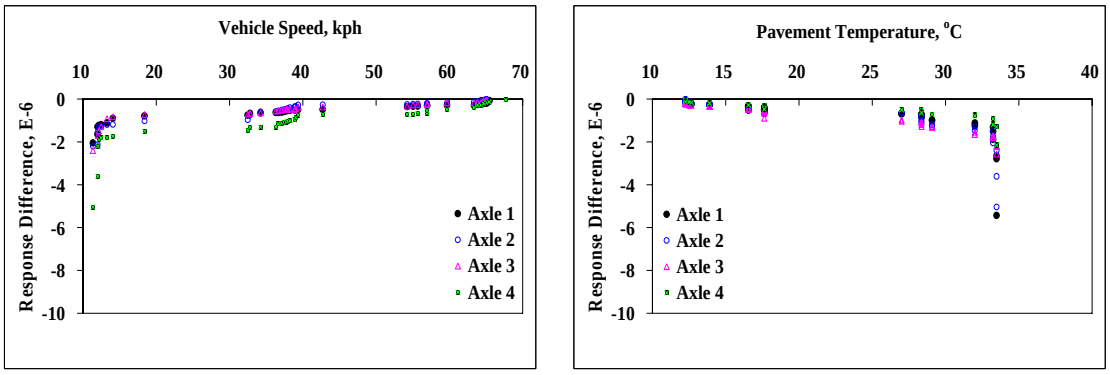

(a) Speed effect (b) Temperature effect

Figure 60. Speed and temperature dependency of response differences, bottom of binder layer.

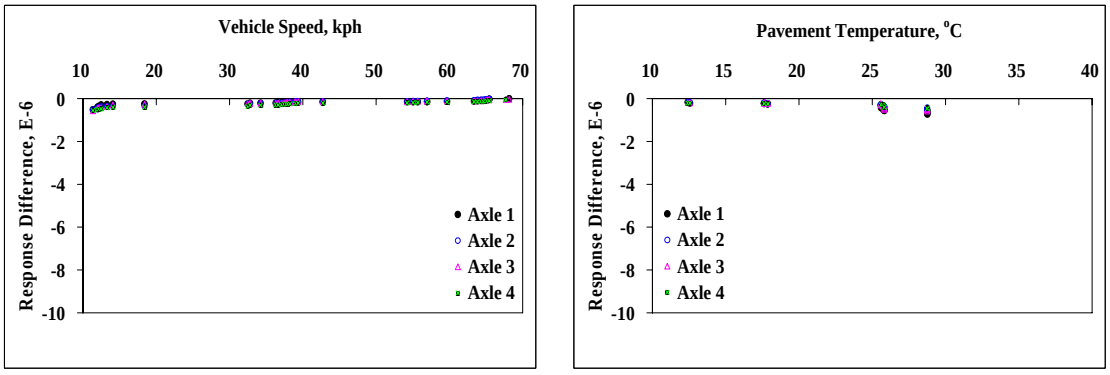

(a) Speed effect (b) Temperature effect

Figure 61. Speed and temperature dependency of response differences, bottom of BCBC layer.

THE IMPACT OF STRAIN GAGE INSTRUMENTATION ON LOCALIZED STRAIN RESPONSES

As discussed before, partial validation analyses indicated a prediction error varying from 20 to 30 percent from FE simulations as compared to response data collected from strain gages installed in asphalt concrete (AC) layers. A vital assumption in the previous FE model was that AC layers were homogenous continuum media. Here, we present the effect of strain gage instrumentation on localized strain responses in AC layers. The materials characterization and pavement structure are those used at the Blair SR 1001 site.

Strain Gages in AC Pavements

The Dynatest PAST II strain gages used in the SISSI project are characteristic of typical H-type AC strain gages (Figure 62). The gage produces a strain measurement when the midsection is compressed or elongated. Therefore, when the AC is subjected to a force, the midsection follows any deformation in the material and gives a measurement of strain.

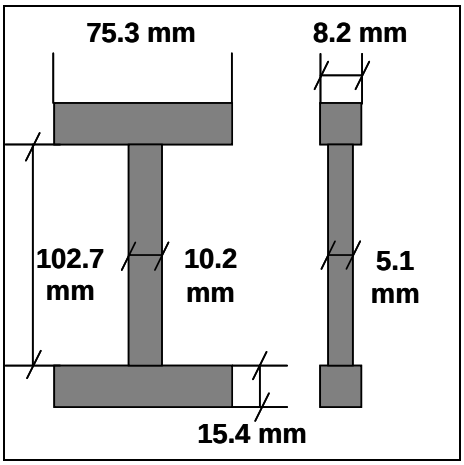

Figure 62. Dimensions of modeled AC strain gage, characteristic of the Dynatest PAST II.

Finite Element Model

The finite element model previously described and validated was used for this investigation. To improve the rate of convergence and the compatibility at the AC material-strain gage (SG) interface, 10-node quadratic tetrahedron elements were used (Figure 63). Considering the temperature dependency of AC materials, coupled temperature-displacement features that have both displacement and temperature degrees of freedom were also added into the elements.

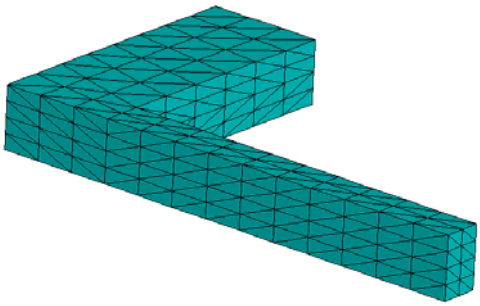

Figure 63. Modeling a quarter strain gage.

Resulting Typical Pavement Dynamic Responses

Compared to the FE model without strain gage, inclusion of a strain gage always results in predicting smaller strain responses. The time retardation of the viscoelastic behavior of AC materials is not present in Figure 64. The longitudinal and transverse strains reach their peak values at the same time. Finally, the longitudinal strain does not show the compression-tension-compression pattern, and the transverse strain does not preserve unrecovered strain at the end of loading time. All of these dissimilarities may result from the elastic behavior of the strain gage.

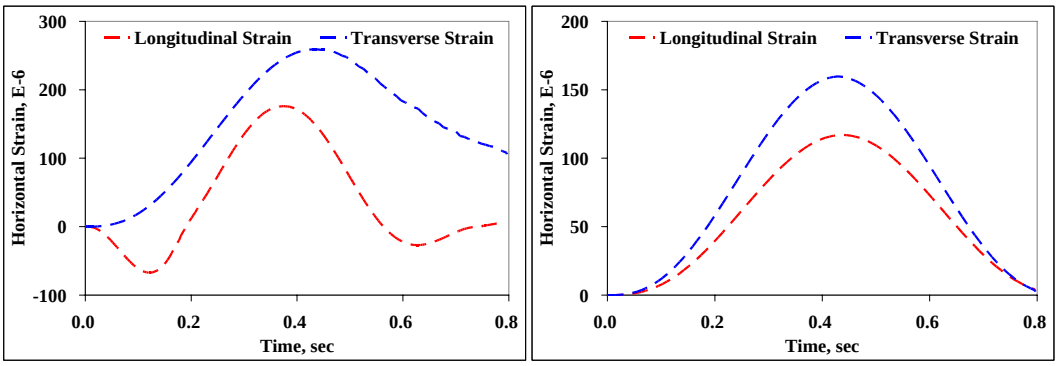

(a) without strain gage (b) with strain gage

Figure 64. Typical pavement responses at 50-mm depth (mix 2, pavement temperature=40°C, vehicle speed = 8 kph, contact pressure = 800 kPa).

The Effect of Loading Time on Flexible Pavement Dynamic Response

To predict pavement response, the MEPDG uses both pavement temperature and loading time in layered elastic analyses. The results from SISSI measurements were used in Phase II to develop a single factor that represents both temperature and time dependency of AC materials. This single factor is referred to as "effective temperature." With only one factor (effective

temperature) instead of two (temperature and time), more advanced theoretical analysis tools, such as the finite element method, can be readily utilized.

Duration of Loading Time

In determining the magnitude of load duration at a specific point within the pavement structure, the speed of the moving load and the depth of that point must be known. In this work, vertical stresses due to a circular moving load at various vehicle speeds (16, 32, 64, and 96 kph) were first computed at different times and spatial locations. This circular load was assumed to have a radius '*a*' of 150 mm and a uniform contact pressure *q* of 0.5 MPa. Further, the calculated vertical stresses were normalized to obtain the load amplitude at different times. An example is given in Figure 65.

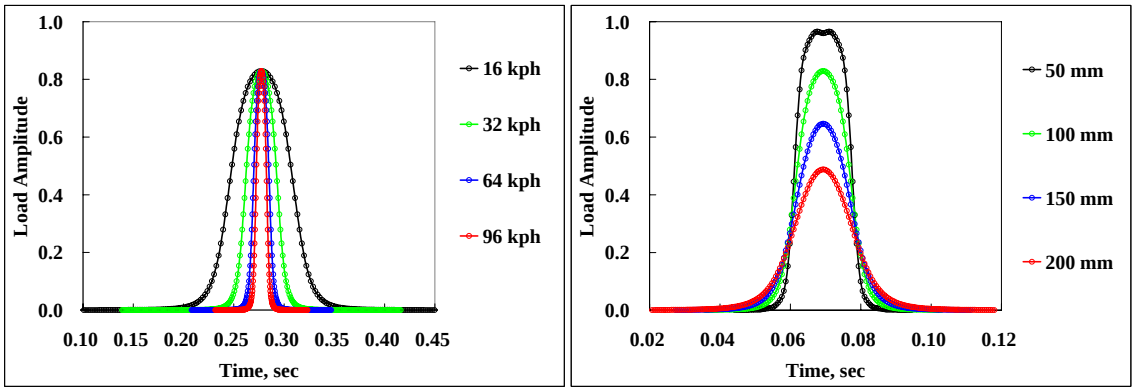

(a) 100 mm depth (b) 64 kph

Figure 65. Dependency of the duration of moving load on vehicle speed and depth.

An example showing calculated durations of moving load is included as Figure 66a.

Equation 12, explained previously, was used to simplify the process of simulating a moving load in FEA. The durations of moving load versus the load amplitude for different vehicle speeds are plotted in Figure 66b.

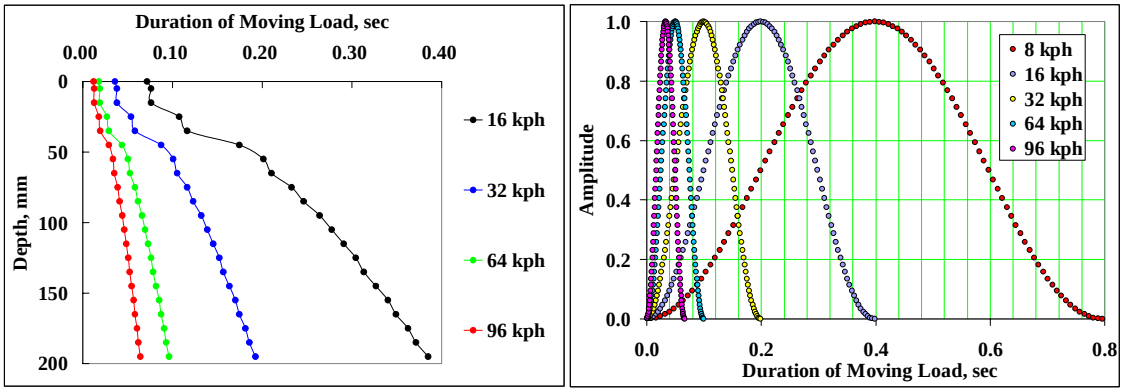

(a) At different pavement depths (b) At pavement surface

Figure 66. Duration of moving load.

Effective Temperature

The MEPDG uses the "effective length" and "effective depth" to determine the slope value and subsequent loading time at a given AC layer depth. Under Phase II of the SISSI project, a new analytical procedure was developed to account for the effect on pavement response of varying loading time across the depth. The developed method is based on the fact that in viscoelastic materials, the effect of time of mechanical loading can be transferred to the effect of temperature loading and vice versa. Consequently, the viscoelastic behavior of AC materials is incorporated systematically in the response analysis. The transfer factor, *T*, in time domain, at the depth of interest was first calculated from the duration of moving load:

$$T = \frac{t_0}{t_D} \tag{19}$$

where t_D is the duration of load application at the depth of interest, and t_0 is the duration of load application at the pavement surface. Transfer factor T is always smaller than unity because the duration of moving load increases as the depth increases. Different vehicle speeds result in different loading times at the pavement surface and at different depths; however, the transfer factor T remains the same.

Pavement Response from Finite Element Analyses

Horizontal and vertical strain responses were predicted using effective temperatures only at the middle of each AC layer. Some results from simulations of a moving load with a time period of 0.0358 seconds corresponding to a vehicle speed of 32 kph are presented. Figures 67 and 68 show tensile and compressive strain histories (as well as stresses) for different mixtures and seasons. Figures 67and 68 provide a description of the viscoelastic behavior of AC materials under applied vertical stresses. The strain response contains two parts: elastic strain (resilient

strain) and inelastic (residual) strain. The latter is only partly recoverable if the duration of moving load is short.

On Figures 67 and 68, the differences between strain responses from measured and effective temperatures represent the effect of loading time. In general, vertical compressive strain is much higher than horizontal tensile strain at the same depth. In the summer, the loading time has a considerable effect on both tensile and compressive strains. Consequently, a more pronounced time lag between the applied stress and the resulting strain is observed. In the spring, strain responses predicted from the effective temperature and measured temperature are almost identical. In other words, the pavement response during a cold season is barely influenced by the loading time. A possible reason is that the AC is stiffer in spring compared to summer, and therefore the effect of the loading time is less pronounced.

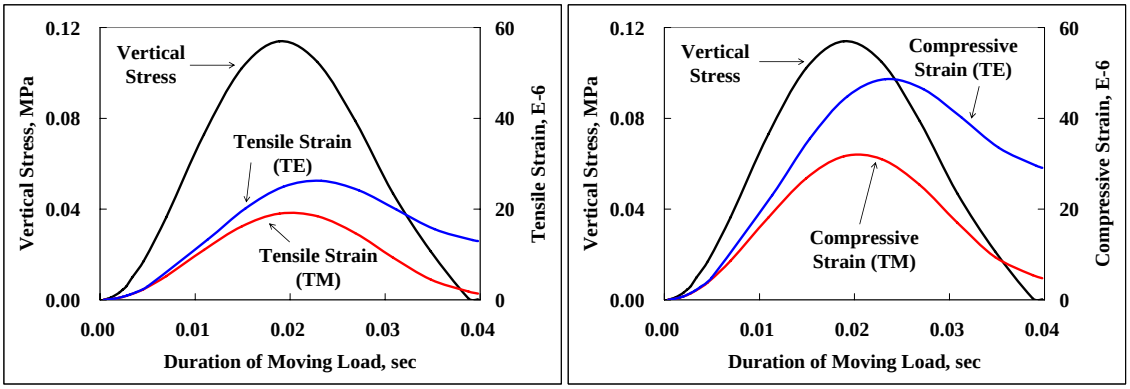

(a) Tensile Strain (b) Compressive Strain

Figure 67. Strain responses of mixture 1 at 145-mm depth in the summer.

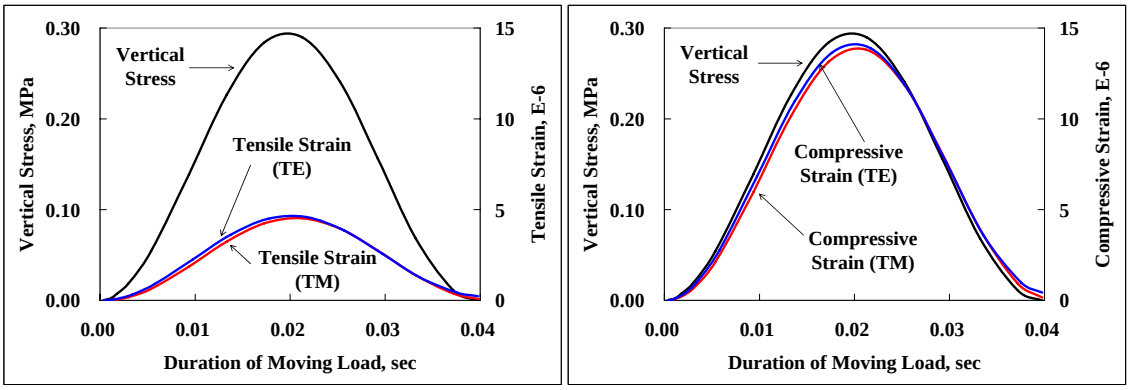

(a) Tensile Strain (b) Compressive Strain

Figure 68. Strain responses of mixture 2 at 95-mm depth in the spring.

CHAPTER 4
SUMMARY AND CONCLUSIONS

The Superpave mix design system was one of the major products of the Strategic Highway Research Program (SHRP). Implementation of this new technology began in the mid-1990's, soon after introduction to state highway agencies and industry. After several years of using this new system, a major question that remained to be addressed in regard to the Superpave system was whether constructed Superpave pavements would meet design expectations. Furthermore, with the emergence of improved mechanistic-empirical performance prediction models, actual pavement response and performance data were needed to calibrate and validate such models. Development of performance prediction models for hot-mix asphalt concrete pavements has been pursued aggressively since the beginning of the Strategic Highway Research Program (SHRP). The models of the system were developed to predict fatigue cracking, thermal cracking, and rutting and rely on detailed material properties, pavement structure, traffic, and detailed environmental data as input. While Superpave models underwent some validation during the 5-year research program of SHRP, modifications, improvements, and validations continued beyond 1993 with the goal of obtaining a thoroughly reliable model. The final product is what is today known as the AASHTO mechanistic empirical pavement design guide (MEPDG). The accuracy of performance prediction models depends on an effective process of calibration and subsequent validation with independent data sets. Current NCHRP projects 9-30A (Calibration of Rutting Models for HMA Structural and Mix Design) and 1-40B (User Manual and Local Calibration Guide for the Mechanistic-Empirical Pavement Design Guide and Software) are aimed at providing guidance for calibrating and validating these models at the local level.

To address the concerns with performance of Superpave mixes, and to provide an independent data set for calibration of performance prediction models, PennDOT initiated a major 5-year research program with Penn State titled "Superpave In-Situ Stress/Strain Investigation" (SISSI). Phase I of the project began in May 2001 and was completed in May 2006. The project was then extended under Phase II for an additional two and a half years and ended in November 2008.

Phase I of this project focused on instrumentation and data collection for validation of the Superpave mix design system, as well as pavement performance prediction models. The main objectives achieved under the SISSI project included instrumentation of several pavements through the Commonwealth of Pennsylvania, direct measurement of the response of Superpave asphalt pavement sections to vehicle loading and environment, direct evaluation of distresses developed in pavements using Superpave mixes, and collection of the data for verification of the mechanistic-empirical pavement design guide (MEPDG) and of the integrated climatic models for pavement design.

Phase II of SISSI focused on extensive analysis of the data collected during Phase I and implementation of the results from Phase I. The major objective achieved during Phase II of the program included use of SISSI data with MEPDG and comparing predicted performance versus

observed field measurements. Phase II also included continuation of the data collection efforts of Phase I.

Instrumentation of the planned eight pavement sites throughout the Commonwealth of Pennsylvania took place during pavement construction to minimize interference to common and normal paving operations. Four of the selected sites were full-depth new construction or reconstruction. These included sites in Tioga, Mercer (East), Somerset, and Blair counties. The remaining sites, in Mercer (West), Warren, Perry, and Delaware counties, are considered as overlay structures. Instrumentation included dynamic (load-associated) sensors and environmental (non-load) sensors. Upon completion of the instrumentation, a vast amount of effort was applied to testing, measurements, and data collection. In general, these efforts fell into two major categories: field activities and laboratory activities.

LABORATORY ACTIVITIES AND MATERIALS CHARACTERIZATION

An extensive laboratory testing program was followed during Phase I of the Superpave In-situ Stress Strain Investigation (SISSI) project to characterize SISSI binders and mixtures. The binder testing included Superpave grading tests: short- and long-term aging, rotational viscometer, dynamic shear rheometer (DSR), and bending beam rheometer (BBR). The mixture testing included the tests required for verification of mix design, as well as dynamic modulus testing at a range of temperatures and frequencies to capture properties required for input to performance prediction models.

To complement this material characterization, further laboratory testing was conducted during Phase II of the project. The second phase of this work concentrated on determination of the resistance of the SISSI mixtures to low-temperature cracking and permanent deformation. The tests were performed on mixes procured from the sites at the time of construction. Indirect tensile creep and strength tests were conducted at three temperatures to capture low temperature properties of SISSI mixtures. Constant height repeated shear tests were conducted at 52ºC to capture rutting resistance properties. The testing also included characterizing the behavior of SISSI binders at low temperatures under extended loading times to validate the Superpave low-temperature binder specification.

Of the eight SISSI sites, six were constructed using BCBC, binder, and wearing courses. Only a binder course and a wearing course were used for the remaining two. All surface mixes had a nominal maximum aggregate size (NMAS) of 12.5 mm, except one that was prepared as a 9.5-mm mix. The binder courses were either 19 mm or 25 mm, and the BCBC courses were 37.5 mm, except one that was a 25-mm mix. The hot-mix asphalt samples for all of these courses were procured behind the paver and were tested in the laboratories. AASHTO test procedures were followed for conducting relevant tests.

The validity of the Superpave binder specification in regard to the equivalence principle for the binder flexural creep stiffness was evaluated during Phase II. Based on this principle, the binder creep stiffness at a specified temperature under two hours of loading [S(7200)] is approximately equal to its creep stiffness at a temperature 10ºC warmer under 60 seconds of loading [S(60)]. This principle also assumes that all asphalt binders can be characterized by

similar shift factors. Our testing and analysis indicated that the S(60) at T_1+10 is significantly different from S(7,200) at T_1. The S(60) values are significantly higher than the S(7,200) values and the differences range between 40 and 52 percent. Alternate testing times and temperatures to satisfy the equivalence principle for the SISSI binders were developed and introduced as part of this work.

The SISSI sites were ranked based on their low-temperature material properties obtained from indirect tensile creep and strength tests. Based on measured properties, it seems that the SISSI mixture used at the wearing course of the Delaware site is the most susceptible to thermal cracking.

Results of repeated shear testing at maximum pavement temperature indicates expected performance of SISSI mixtures in the range of good to excellent since no excessive permanent deformation was observed from these laboratory tests. For the wearing layer, the permanent shear strain ranged between 0.3 and 1.7 percent, indicating excellent to good rutting resistance. For the binder layer, the range was between 0.4 and 1.7 percent, indicating good rutting resistance. The exception was the binder layer of the Perry site, for which a permanent strain of 2.4 percent was obtained, indicating fair rutting resistance; however, no excessive rutting was observed in the field for this site. Overall, the field-measured rutting after 5 to 8 years of service ranged from 2.5 to 8.5 millimeters, indicating excellent rut resistance of SISSI mixtures at all the sites. This is, in general, consistent with laboratory-measured shear strains.

FIELD ACTIVITIES

Part of the Phase II work included all field data collection activities as was conducted during Phase I, with the exception that pavement condition surveys and dynamic data collection were conducted at a significantly lower frequency. A major challenge during Phase II was the need for an extensive level of effort to maintain sensors and data acquisition systems in functional condition. Continuity of environmental data collection was not able to be maintained at all times, and this resulted in gaps and discontinuity in the collected data. Some of the sensors did not provide reasonable responses due to malfunction or damage, specifically the frost and moisture content gages. In regard to dynamic sensors, the best results were obtained from strain gages, and the most serious problems were noticed with multi-depth deflectometers (MDD). In spite of all data collection problems, the data collected at SISSI sites is extremely valuable considering that multiple sites were available and collection of data was continued for such an extended time period. It is a unique data set of particular value to Pennsylvania but also of value for analysis in a national context.

An additional field activity during Phase II included determination of in-situ modulus using Portable Seismic Pavement Analyzer (PSPA). In summary, field-focused efforts during Phase II consisted of collection of pavement condition data, dynamic data, falling weight deflectometer (FWD) data, traffic data, in-situ modulus data, and environmental data. The current report provides details of these data collection efforts and the corresponding analysis and interpretation of such data.

ASSESSMENT OF PAVEMENT CONDITION

All SISSI sites appeared to be in good shape except for the two overlaid pavement sections at the Warren and Delaware sites. At these two sites, a significant amount of the longitudinal cracks at the lane-lane and lane-shoulder joints were probably due to poor construction. Transverse cracks on the pavement surface might have been induced by underlying concrete slabs or may have been thermally induced. Durability of Superpave mixes was of concern at two of these sites, Warren and Mercer, based on observations of PennDOT personnel. The Warren site was finally milled and overlaid during spring 2007. For the Mercer site, only a small section of the road prior to the SISSI site was milled and overlaid. Our last pavement condition survey at this site, during November 2007, indicated no cracking of the pavement mat at the site even though minor to moderate raveling and loss of fine was evident at the vicinity of the longitudinal joint. The pavement had also experienced longitudinal cracking both at the joint between two lanes and at the joint between the travel lane and the shoulder. These cracks appeared to be construction related rather than mix related. However, the minor to moderate raveling observed at the Mercer site is probably an indication of insufficient binder content at this site. In general, some Superpave mixes have demonstrated being highly resistant to rutting, and this excellent rut resistance has come at the cost of lower durability in some cases. In general, the field-measured rutting after 5 to 8 years of service ranged between 2.5 and 8.5 millimeters, indicating excellent rut resistance of SISSI mixtures at all the sites. Rut depths continued to increase over the years although the magnitude of increase was small at most sites. The Blair site exhibited the greatest percentage increase in rutting between 2004 and 2008. At the time of the most recent distress surveys, the SISSI sites appeared to be in good shape except for those at Warren and Delaware.

DYNAMIC, FWD, AND PSPA DATA

Collection of dynamic data during Phase II was conducted at a significantly lower frequency compared to Phase I. During Phase II, dynamic data collection was conducted at specific sites to complement data collected during Phase I. More repeated measurements were conducted at the same speed, and lower speeds were included in Phase II. At a few sites, collection of such data did not become possible because of loss or corrosion of gages. Dynamic data collected during Phase II indicated significantly larger strain levels induced in the pavement during warmer times and lower speeds compared to colder seasons and higher speeds. Measurements at very slow speeds resulted in considerably higher strain levels; increases in speed above 20 mph do not produce further significant changes in response. The vertical stresses at the top of the subbase were significantly greater than those at the top of the subgrade. This demonstrates the protective role of the subbase layer. The overall magnitudes of the Phase II dynamic data measurements are consistent with those from Phase I for approximately the same conditions of environment and testing.

Backcalculated moduli of asphalt concrete from FWD measurements were compared with the laboratory-obtained elastic moduli. The comparisons indicated that the backcalculated moduli are always higher than the laboratory-determined values. The observation is in general agreement with the determination by the 1993 AASHTO Pavement Design Guide that the FWD

backcalculated moduli are typically higher than the laboratory-determined moduli. Additional FWD testing at the Blair site using additional load levels and collection of load deflection history indicated that the subgrade was behaving in a significantly nonlinear manner. Accounting for this nonlinearity explained much of the backcalculation difficulties encountered during Phase I for the Blair site.

The moduli of asphalt concrete determined from laboratory complex modulus tests were also compared to the moduli from in-situ nondestructive tests using PSPA. Statistical analysis indicated an excellent PSPA measurement repeatability. In the field, testing of cracked areas resulted in lower seismic moduli as anticipated. Comparison between field seismic moduli and dynamic moduli from laboratory tests indicated about 30 percent difference in these two moduli. The seismic moduli were consistently lower than the laboratory dynamic moduli; the laboratory complex modulus test always resulted in an elastic modulus about 4000 to 7000 MPa higher than the corresponding in-situ seismic modulus. When making such comparisons, it is important to consider the effect of air void content because the in-situ seismic modulus is very sensitive to the air void content of the asphalt concrete. For the SISSI project, pavement cores obtained one to two years after construction revealed air voids very similar to those of the laboratory specimens tested for dynamic modulus. The second important point in making such a comparison regards the aging of the asphalt binders. Aging increases binder stiffness and therefore results in a higher mixture modulus. In this study, no attempts were made to determine the aging level of binder and base layers; however, it is expected, since these layers are not exposed to solar radiation and also experience moderate temperatures considering the Pennsylvania climate, that there is not a significant aging effect for the binder and base layers. Significant aging is expected for the wearing course binder, but modulus of this layer is not measured by PSPA.

ENVIRONMENTAL DATA

Most of the successful environmental data during Phase II consists of pavement temperature and solar radiation. Frost and moisture content data were limited because of gage malfunction. Environmental data from Phase I and the first year of Phase II were analyzed in regard to frost depth and freezing index. Different approaches were used in determination of freezing index, and the effects of freezing index on the computed frost depth were evaluated as part of the Phase-II SISSI research. Freezing index was calculated based on a major freeze cycle and multiple freeze-thaw cycles. It was observed that there is rarely a freeze-thaw cycle that is over 40 days in Pennsylvania; in fact, most freeze-thaw cycles have periods less than 10 days. For freezing index differences less than 150 °C-days, variation of computed frost depth, in most cases, does not exceed 0.20 m. However, for freezing index differences of approximately 200 °C-days, computed values vary from 0.15 to 0.25 m. Frost data from the Blair site was analyzed to determine the depth and rate of frost penetration. Data indicate that as the freezing period lasts longer, frost severity increases at various depths. Overall, at deeper pavement layers, more time is required to reach a specific freezing condition.

In summary, a great deal of valuable data were collected from SISSI sites during Phases I and II of this project. The data were extensively used with the AASHTO mechanistic empirical pavement design guide (MEPDG), as well as for independent mechanistic analysis, documented in a separate report. The data were also analyzed to provide overall assessment of the condition

of SISSI pavements and Superpave mixtures and to provide information about the freezing conditions of Pennsylvania pavements. These data provide a very useful source for local calibration and verification of the MEPDG and the Enhanced Integrated Climatic Models (EICM) used in the MEPDG.

IMPLEMENTATION OF SISSI DATA WITH THE MEPDG

Mechanistic-empirical procedures take advantage of empirical models to fill in the gaps that exist between the theory of mechanics and the performance of pavement structures. The newly released MEPDG, based on NCHRP 1-37A (ARA 2004), has adopted a mechanistic-empirical pavement design procedure in which pavement distresses are calculated through calibrated distress prediction models based on material properties determined from laboratory tests and local traffic and climate conditions. The calibrated distress prediction models are based on the critical pavement responses mechanistically calculated by a structural model and coefficients determined through national calibration efforts using the LTPP database.

One major attempt made during Phase II of the SISSI project was to use data with the highest analysis level in MEPDG, i.e., Level 1. One general conclusion from Level 1 analysis was that no significant amount of fatigue or thermal cracking was predicted by the MEPDG models, and this is consistent with field observations for most of the sites, except the sites at Delaware and Warren counties, where cracking was dominant. At the Warren site, the pavement is built on a cracked and seated old rigid pavement with undercut and filled sections in some areas. There is the possibility that observed transverse cracks were caused by underlyting old pavement even though such a conclusion cannot be drawn with certainty. For the Delaware site, the pavement is similarly built on old Portland cement concrete and no definite conclusion can be drawn regarding the cause of observed transverse and edge longitudinal cracks, It cannot be concluded with certainty that the observed transverse cracking at this site was thermally induced.

In regard to pavement permanent deformation, overall the MEPDG under-predicted rutting compared to field measurements. The magnitude of this under-prediction varied significantly in the range of 5 to 90 percent depending on the site. The average under-prediction was approximately 40 percent. The discrepancy observed between the predictions and field conditions is perhaps due to the national calibration coefficients in the empirical performance models. It is believed that with the availability of large amounts of field condition data, the MEPDG models could be more accurately calibrated locally.

REFERENCES

ABAQUS/Standard Version 6.6. (2006). *Finite Element Computer Program*, Hibbitt, Karlsson, and Sorenson, Inc., Pawtucket, RI, USA.

American Association of State Highway and Transportation Officials (AASHTO) (1993). *Guide for Design of Pavement Structures, Vol. II,* Joint Task Force on Pavement, Highway Subcommittee on Design, Washington, D.C.

Anderson, D.A., Solaimanian, M., Hunter, D., and Soltani, A., (2003). "Superpave Validation Studies: SISSI Instrumentation, Operating Instructions and Baseline Measurements," Final Report. Pennsylvania Transportation Institute, University Park, PA.

Applied Research Associates (2003). "Guide for Mechanistic-Empirical Design of New and Rehabilitated Pavement Structure,". Transportation Research Board, National Research Council, Washington, D.C.

Chatti, K., Kim, H.B., Yun, K.K., Mahoney, J.P. and Monismith, C.L., (1996). "Field Investigation into Effects of Vehicle Speed and Tire Pressure on Asphalt Concrete Pavement Strains," *Transportation Research Record*, 1539, Transportation Research Board, National Research Council, Washington, D.C.

Chisholm, R. A. and Phang, W. A., (1983), "Measurement and prediction of frost penetration in highways," *Transportation Research Record*, 918, Transportation Research Board*,* 918, pp. 1-10.

Christensen, D. and Bonaquist, R. (2005). "Evaluation of Indirect Tensile Test (IDT) Procedures for Low-Temperature Performance of Hot Mix Asphalt," NCHRP Report 530, Phase III of Project 9-29, Washington, D.C.

Drumm, E. C., and Meier, R. (2003), "LTPP Data Analysis: Daily and Seasonal Variations in In-situ Material Properties," Final Report, Project No. NCHRP 20-50, pp. 7-12.

Hass, W. M. and Bovid, G. C., (1981), "Frost depth prediction for highway subgrade soils," *Northern community: A search for a quality environment.* pp. 719-733.

Huang, Y., (1993) *Pavement Analysis and Design,* Prentice Hall, NJ.

Kim, Y.R. and Wen, H. (2002). "Fracture Energy from Indirect Tension Testing," *Journal of Association of Asphalt Paving Technologists,* Vol. 71, pp. 779-793.

Jackson N. and Puccinelli, J., (2006), "Long-Term Pavement Performance (LTPP) Data Analysis Support, National Pooled Fund Study TPF-5(013): Effects of Multiple Freeze Cycles and Deep Frost Penetration on Pavement Performance and Cost" Publication FHWA-HRT-06-121, FHWA,

Lu, H., Zhang, X., and Knauss, W.G. (1997). "Uniaxial, shear, and Poisson relaxation and their conversion to bulk relaxation," *Journal of Polymer Engineering and Science.* Vol. 37, pp. 1053-1064.

McKeown, S., Clark J. I., and Matheson. D. (1988), "Frost Penetration and Thermal Regime in Dry Gravel." *Journal of Cold Regions Engineering,* Vol. 2, No. 3, pp. 111-123.

Roque, R. and Buttlar, W. G. (1992). "The Development of a Measurement and Analysis System to Accurately Determine Asphalt Concrete Properties Using the Indirect Tensile Mode," *Journal of The Association of Asphalt Paving Technologist,* Vol .l. 61, pp. 304-333.

Schapery, R. A. (1984). "Correspondence Principles and a Generalized J Integral for Large Deformation and Fracture Analysis of Viscoelastic Media," *International Journal of Fracture,* Vol. 25.

Schapery, R.A. (1988). "On some path independent integrals and their use in fracture of nonlinear viscoelastic media," *Proceedings, IUTAM Meeting on Advances in Nonlinear Fracture Mechanics*.

Solaimanian, M., D.A. Hunter, J. Shah, and S.M. Stoffels (2006). "Characterization of Materials for Superpave In-Situ/Stress Strain Investigation," Final Report, PennDOT Project No. 0R-02, Pennsylvania Transportation Institute.

Solaimanian, M., Stoffels, S. M., Hunter, D. A., Morian, D. A., and Sadasivam, S., (2006). "Superpave in-situ/stress strain investigation". Final Report, Publication FHWA-PA-2006-019-350R02, Pennsylvania Department of Transportation.

Stoffels, S.M., Solaimanian, M. (2006). "Pavement Condition Report: Superpave In-situ Stress/Strain Investigation," The Pennsylvania Transportation Institute. University Park, PA.

Solaimanian, M., Stoffels, S.M., Yin, H., Bae, A., and Sadasivam, S. (S.2008). "Field Data Collection and Summary," Final Report, The Pennsylvania Transportation Institute. University Park, PA.

Stolle, D., and Hein, D., (1989). "Parameter Estimates of Pavement Structure Layers and Uniqueness of the Solution in Nondestructive Testing of Pavements and Backcalculation of Moduli." *Special Technical Publication (STP) 1026*, ASTM, Philadelphia, PA.